

**ADVANCES IN THE SYNTHESIS OF INDAZOLES: REGIOSELECTIVE C-7
FUNCTIONALIZATION BY DIRECTED ORTHO METALATION AND
PROGRESS TOWARDS INDAZOLE BASED AZABORINE COMPOUNDS**

By

Fu Cullen

A thesis submitted to the Department of Chemistry

In conformity with the requirements for

the degree of Master of Science

Queen's University

Kingston, Ontario, Canada

(January, 2017)

Copyright © Fu Cullen, 2017

Abstract

As one of the fundamental heterocyclic building blocks, indazole and its derivatives have spurred significant research interest and patented applications. In particular, C-7 substituted indazole derivatives are of prime interest due to their significant bioactivities. Azaborine molecules incorporating the B-N structural motif are also of prime interest to chemists and material scientists stemming from their distinctive photophysical properties. The aim of this thesis is to construct new azaborine targets incorporating the indazole framework using Directed *ortho* Metalation (DoM) reactions as a key step, as well as devise new methods for C-7 functionalization of indazole heterocycles using DoM reactions.

Successful N-1 functionalization of indazoles enabled the subsequent Suzuki-Miyaura or Sonogashira cross coupling reactions to prepare C-3 substituted indazoles. Efforts in Directed *ortho* Metalation (DoM) reactions at the C-3 aryl groups of substituted indazoles towards azaborine targets were unsuccessful. Internal alkyne bearing substituted indazole was subjected to hydroboration conditions but without any conversion to the desired products. C-3 protected Indazoles bearing N-Directed Metalation Groups (DMGs) enabled their C-7 functionalization using DoM chemistry, and thereby led to the development of a new general route to these derivatives.

Acknowledgements

Aromatic and heteroaromatic molecules are arguably some of the most important chemical compounds to ever exist. Such is the way that nature had built the world, atom by atom, to form the stars, the planets, and life in the universe. By mastering these molecules - their properties, structures and reactivity, chemists can shape and enrich the human experience unlike any other: energy security, climate stability, alleviating poverty, economic prosperity, and preserving life itself are just some of the endeavors where we may find chemists playing such a pivotal role.

I would like to express my utmost respect and gratitude towards Professor Wang and Professor Snieckus for their willingness to supervise the completion of my M.Sc. thesis. It is a privilege to explore the frontiers of organic synthesis under their guidance and patronage.

I would like to thank Professor Macartney and Professor Zechel being members of my graduate supervisory committee, and especially to Professor Macartney for his internal review

I would like to thank Professor Jerkiewicz, Professor Jessop and Professor Ross for being members of the examination committee.

Finally, to my family, friends and the many professors, mentors, and teachers who helped to make a difference in my time spent here at Queen's University, thank you!

Table of Contents

Abstract.....	ii
Acknowledgements.....	iii
List of Schemes.....	vi
List of Figures	viii
List of Tables	ix
List of Abbreviations	x
Chapter 1 Introduction	1
1.1 Indazoles	1
1.1.1 Introduction to Indazoles.....	1
1.1.2 Structure and Properties of Indazoles	2
1.1.3 Reactivity of Indazoles	4
1.1.4 Bioactivity and Material Science Applications of Indazoles.....	8
1.1.5 C-7 Substituted Indazoles	10
1.2 Organometallic Reactions	13
1.2.1 The Directed ortho Metalation (DoM) Reaction: An Overview	13
1.2.2 The DoM Reaction: Directed Metalation Groups (DMGs)	14
1.2.3 The DoM Reaction: Mechanism.....	16
1.2.4 The DoM Reaction: The Directed remote Metalation (DreM).....	20
1.2.5 Grignard Reactions: An Overview	23
1.3 N,C-Chelating Organoboron Compounds and Azaborines	24
1.3.1 Introduction to Azaborines	24
1.3.2 Key advancement of Azaborines.....	26
1.3.3 Four-Coordinate Chelated Organoboron Compounds	30
1.3.4 Recently Synthesized Azaborines.....	37
Chapter 2 Indazole Based Azaborines and the DoM Reaction of Indazoles	41
2.1 The DoM Approach towards Indazole-based Azaborines.....	41
2.1.1 Project Aims	41
2.1.2 N-1 Protection of 3-Iodo-1H-indazole.....	42
2.1.3 C-3 Functionalization of Indazoles via Suzuki-Miyaura Cross Coupling Reactions	42
2.1.4 Directed ortho Metalation of N-Benzyl 3-Aryl Indazoles.....	45
2.1.5 Debenzylation Attempts	47

2.1.6 DoM of N-H 3-Aryl Indazoles	49
2.1.7 DoM of N-1 Protected 3-Aryl Indazoles	51
2.2 C-7 Functionalization of Substituted Indazoles	54
2.2.1 Project Aims	54
2.2.2 C-3 Protection of 1H-Indazole.....	55
2.2.3 N-1 Functionalization of 3-chloro-1H-Indazole.....	56
2.2.4 Optimizing C-7 DoM Reaction Conditions	56
2.2.5 DoM of Substituted Indazoles.....	59
2.3 Hydroboration Approach Towards Indazole Based N,C-Chelating Organoboron Compounds	61
2.3.1 Project Aims	61
2.3.2 C-3 Functionalization of Indazoles via Sonogashira Cross Coupling Reactions	62
2.3.3 De-Silylation of 3-(TMS-Acetylene) Indazoles.....	63
2.3.4 Hydroboration Reactions	65
2.4 Conclusion and Future Work	68
2.5 Experimental Section	70
2.5.1 General Information	70
2.5.2 Representative Experimental Procedure for Suzuki-Miyaura Cross Coupling Reactions	71
2.5.3 Spectra Data for Products of Suzuki-Miyaura Cross Coupling Reactions	71
2.5.4 Representative Experimental Procedure for DoM reactions of N-benzyl 3-Aryl Indazoles	75
2.5.5 Spectra Data for Products of DoM reactions of N-benzyl 3-Aryl Indazoles.....	75
2.5.6 Representative Experimental Procedure for the N-1 Functionalization of Indazoles	76
2.5.7 Spectra Data for Products of N-1 Functionalization of Indazoles.....	77
2.5.8 Representative Experimental Procedure for C-3 Sonogashira Coupling Reactions.....	83
2.5.9 Spectra Data for Products of C-3 Sonogashira Coupling Reactions.....	83
2.5.10 Representative Experimental Procedure for De-silylation Reactions.....	85
2.5.11 Spectra Data for Products of De-silylation Reactions	86
2.5.12 Representative Experimental Procedure for Hydroboration Reactions	87
2.5.13 Spectra Data for Products of Hydroboration Reactions	87
2.5.14 Representative Experimental Procedure for C-7 DoM	88
2.5.15 Spectra Data for Products of C-7 DoM.....	89
Reference	98
Appendix	108

List of Schemes

Scheme 1-1 Fischer synthesis of 1H-indazole in 1885.	1
Scheme 1-2 Photochemical reactions of indazoles.	5
Scheme 1-3 Thermolysis of indazole at 600 – 950 °C.	6
Scheme 1-4 The synthesis of fused indazole ring systems.	7
Scheme 1-5 Regioselective protection of indazoles with the SEM protecting group.....	7
Scheme 1-6 Synthesis of 7-chloro-1H-indazole via S _N Ar type reactions.....	11
Scheme 1-7 Diazotization procedure towards substituted indazoles.	12
Scheme 1-8 [3+2] cycloaddition reactions towards substituted indazoles.	12
Scheme 1-9 Simplified representation of the DoM reaction.....	14
Scheme 1-10 Mechanisms of DoM according to the Complex Induced Proximity Effect (CIPE).....	17
Scheme 1-11 Evidence for CIPE in alpha-deprotonation.	17
Scheme 1-12 NMR and computation study on the ortho lithiation of anisole.....	19
Scheme 1-13 The DreM reaction in the synthesis of 7,8-dimethoxy phenanthridine.....	20
Scheme 1-14 The DreM reaction in the synthesis of 9-keto-9H-pyrolo-[1,2-a]indole.	21
Scheme 1-15 Progress towards 1,2-dihydro-1,2-azaborine.	28
Scheme 1-16 Synthesis of 1,2-dihydro-1,2-azaborine.	29
Scheme 1-17 Isomerisation pathways of photochromic N,C-chelating organoboron compounds.	33
Scheme 1-18 Inhibition of photoisomerization in N,C-chelating organoborons.	35
Scheme 1-19 Synthesis of N,C-chelating organoborons through trans-hydroboration of internal alkynes.	36
Scheme 1-20 Formation of azaborines through photoelimination of four-coordinate chelated organoboron compounds.	37
Scheme 1-21 Formation of azaborines through photoelimination reactions.	38
Scheme 1-22 Reversible 1,1-hydroboration reaction towards N,C-chelated four coordinate organoborons.....	40
Scheme 2-1 Proposed retro-synthetic pathway for targets 2.6 and 2.9.	41
Scheme 2-2 N-1 protection of 3-Iodo-1H-indazole.....	42

Scheme 2-3 Precedent for the Suzuki-Miyaura cross coupling reaction of 3-Chloro-1H-indazole.	43
Scheme 2-4 The Suzuki-Miyaura cross coupling reaction of 3-iodo-1H-indazole.	44
Scheme 2-5 Unsuccessful Suzuki-Miyaura cross coupling of N-1 protected 3-Iodo-1H-indazoles.	45
Scheme 2-6 Ziegler and Fowler's ortho lithiation of piperonal cyclohexylimine.....	45
Scheme 2-7 The DoM reaction of N-benzyl 3-aryl indazoles.....	46
Scheme 2-8 Unsuccessful generation of lithio-dianion.	47
Scheme 2-9 Enantioselective reduction of benzyl amines.	47
Scheme 2-10 N-1 protection of 3-aryl indazoles.	51
Scheme 2-11 C-7 Activation of substituted indazoles via DoM chemistry.	54
Scheme 2-12 Base-mediated ring opening of unprotected indazoles.....	55
Scheme 2-13 Synthesis of 3-chloro-1H-indazole.	55
Scheme 2-14 N-1 functionalization of 3-chloro-1H-indazole.....	56
Scheme 2-15 trans-hydroboration of internal alkynes.	61
Scheme 2-16 trans-hydroboration of internal alkynes incorporating indazole-based systems.	62
Scheme 2-17 Base-mediated de-silylation of substituted indazoles.	64
Scheme 2-18 Sonogashira cross coupling reactions of indazoles.	64
Scheme 2-19 cis-Hydrogenation of N-benzyl 3-phenylethynyl indazole.	67
Scheme 2-20 Grignard reagents based on indazoles.....	68
Scheme 2-21 Synthesis of indazole-based azaborines using Grignard reagents.....	69

List of Figures

Figure 1-1 Indazole based natural products.	2
Figure 1-2 Tautomers of indazole.	2
Figure 1-3 The crystal structure of 3-methyl-1H-indazole dimers.	3
Figure 1-4 Intramolecular hydrogen bonding of 7-nitro-1H-indazole.	3
Figure 1-5 Bioactive indazoles.	9
Figure 1-6 Crystal structure of an NH indazole anti-cancer derivative interacting with p110 γ kinase.	9
Figure 1-7 Bioactive C-7 substituted indazoles.	11
Figure 1-8 Examples of common DMGs.	15
Figure 1-9 Hierarchy of DMG power.	15
Figure 1-10 The Kinetically Enhanced Metalation (KEM) transition state.	20
Figure 1-11 Synthesis of natural products using the DreM strategy.	21
Figure 1-12 Sites of deprotonation in DoM compared with DreM.	22
Figure 1-13 Borazine formal charge and electronegativity.	24
Figure 1-14 The isoelectronic relationships of BN/CC isosterism.	25
Figure 1-15 Azaborine based hydrogen storage materials.	26
Figure 1-16 Azaborine products synthesized by Dewar.	27
Figure 1-17 Exemplary azaborine molecules.	30
Figure 1-18 Components of a four-coordinate organoboron compound.	31
Figure 1-19 Early work on N,O-chelating and N,N-chelating azaborines.	32
Figure 1-20 Visible fluorescence from N,C-chelating organoboron compounds.	34
Figure 1-21 Examples of azaborine compounds.	39
Figure 2-1 C-7 functionalization of substituted indazoles.	60
Figure 2-2 Theoretical azaborine molecule that incorporates indazole dimers.	69

List of Tables

Table 2-1 Optimization studies for N-1 debenylation reactions of substituted indazoles.....	48
Table 2-2 Unsuccessful ortho lithiation of N-H unprotected 3-aryl indazoles.	50
Table 2-3 Unsuccessful Directed ortho Metalation of N-trityl 3-ortho-tolyl indazole.....	52
Table 2-4 Directed ortho Metalation of N-diethylcarbamoyl 3-phenyl indazoles.....	53
Table 2-5 Condition optimization studies on C-7 metalation of substituted indazoles.	57
Table 2-6 Condition optimization studies on C-7 silylation of substituted indazoles.....	58
Table 2-7 Sonogashira cross coupling reactions of substituted indazoles.	63
Table 2-8 Unsuccessful hydroboration reactions towards N,C-chelating organoboron compounds.....	66

List of Abbreviations

Ac	acetyl
^t Am	<i>tert</i> -amyl
aq	aqueous
Ar	aryl
atm	atmosphere
ATR	attenuated total reflectance
9-BBN	9-borabicyclo(3.3.1)nonane
BINAP	2,2'-bis(diphenylphosphino)-1,1'-binaphthyl
Bn	benzyl
Boc	<i>tert</i> -butoxycarbonyl
bipy	2,2'-bipyridine
ⁿ Bu	<i>n</i> -butyl
^s Bu	<i>sec</i> -butyl
^t Bu	<i>tert</i> -butyl
Bz	benzoyl
°C	degrees Celsius
CIPE	complex-induced proximity effect
CNDO	complete neglect of differential overlap
Cp	cyclopentadienyl
Cy	cyclohexyl

dba	dibenzylideneacetone
DCE	dichloroethane
δ	chemical shift
DFT	density functional theory
DG	directing group
DME	1,2-dimethoxyethane
DMF	<i>N,N</i> -dimethylformamide
DMA	<i>N,N</i> -dimethylacetamide
DMG	directed metalation group
DMSO	dimethyl sulfoxide
DoM	Directed <i>ortho</i> Metalation
DreM	Directed <i>remote</i> Metalation
<i>E</i>	entgegen
E^+	electrophile
EDG	electron donating group
<i>ee</i>	enantiomeric excess
EI	electron impact
eqn	equation
equiv	equivalent
ESI	electrospray ionization
Et	ethyl
Et ₂ O	diethyl ether

EWG	electron withdrawing group
g	gram
GC	gas chromatography
GSK-3	glycogen synthase kinase 3
h	hours
HOMO	highest occupied molecular orbital
HPLC	high performance liquid chromatography
HRMS	high resolution mass spectrometry
Hz	hertz
INDO	intermediate neglect of differential overlap
IR	infrared
<i>J</i>	coupling constant
KIE	kinetic isotope effect
KEM	kinetically enhanced metalation
L_n	ligand set
LDA	lithium diisopropylamide
LIF	laser induced fluorescence
LiTMP	lithium 2,2,6,6-tetramethylpiperidine
LUMO	lowest unoccupied molecular orbital
M	molar
M^n	metal with an oxidation state n
Me	methyl

MetAP2	methionine aminopeptidase 2
MHz	megahertz
min	minutes
mL	milliliter
mm	millimeter
mmol	millimole
MNDO	modified neglect of diatomic overlap
mp	melting point
MOM	methoxymethyl
MS	mass spectrometry
NMR	nuclear magnetic resonance
Nu	nucleophile
OLED	organic light-emitting diode
PG	protecting group
Ph	phenyl
pin	pinacolato
PMMA	poly-methylmethacrylate
ppm	parts per million
ppy	phenyl pyridyl
<i>i</i> Pr	<i>iso</i> -propyl
PVK	poly-N-vinylcarbazole (PVK)
pz	pyrazole

(<i>R</i>)	rectus
rt	room temperature
(<i>S</i>)	sinister
SEM	2-(trimethylsilyl)ethoxymethyl
SEM-Cl	2-(Trimethylsilyl)ethoxymethyl chloride
SPhos	2-dicyclohexylphosphino-2',6'-dimethoxybiphenyl
S_EAr	electrophilic aromatic substitution
S_NAr	nucleophilic aromatic substitution
TBS	<i>tert</i> -butyldimethylsilyl
TEA	triethylamine
TFA	trifluoroacetic acid
THF	tetrahydrofuran
THP	tetrahydropyran
TLC	thin layer chromatography
TMEDA	tetramethylethylenediamine
TMP	2,2,6,6-tetramethylpiperidine
TMS	trimethylsilyl
<i>tol</i>	tolyl
Trityl	Triphenylmethyl
Ts	<i>p</i> -toluenesulfonyl
UV	ultraviolet
X-couple	cross-couple

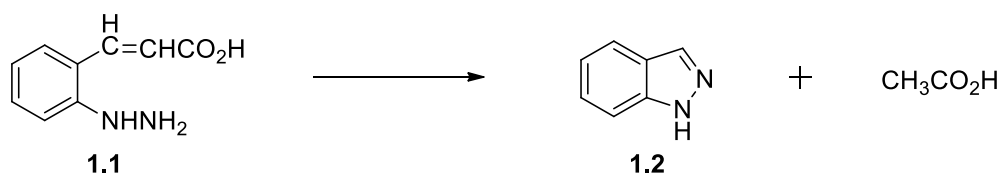
Chapter 1 Introduction

1.1 Indazoles

1.1.1 Introduction to Indazoles

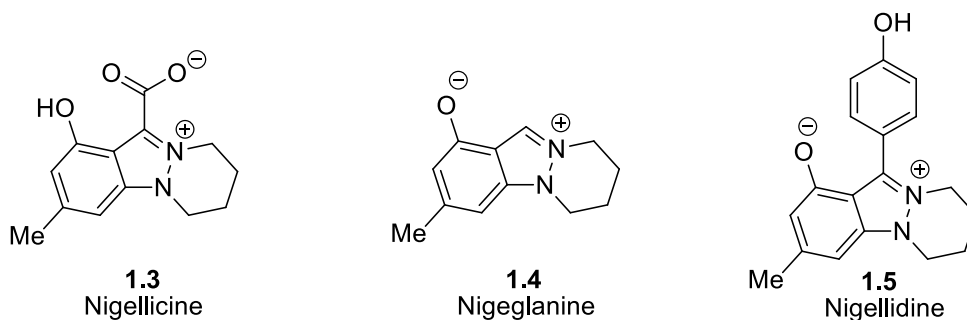
The history of the heterocycle indazole began with Emil Fisher, a Nobel laureate who fundamentally advanced the field of organic chemistry through his dedicated research on various natural products, dyes, narcotics, sugars, and proteins. In the early 1880s, he thermolyzed *o*-hydrozinoacetic acid **1.1** and from a number of products obtained, a new substance which by combustion analysis did not contain oxygen.¹ Fischer assigned structure **1.2** to the product and described this transformation as “remarkable in the highest degree”. He named it “indazole”, analogous to the already known indole.² Hence a new field of heterocyclic chemistry was born.

Scheme 1-1 Fischer synthesis of 1*H*-indazole in 1885.



As one of the fundamental heterocyclic building blocks, indazole and its derivatives have spurred significant research interest and patented applications since Fischer’s discovery. To fast-forward, the year 2009 alone witnessed more than 150 articles pertaining to the biological properties of indazole derivatives, and over 400 patents relating to the indazole core - mediated biological effects.³ On the other hand, indazole derivatives remain rare in nature,⁴ and only three naturally occurring indazoles are known (**Figure 1-1**).⁵

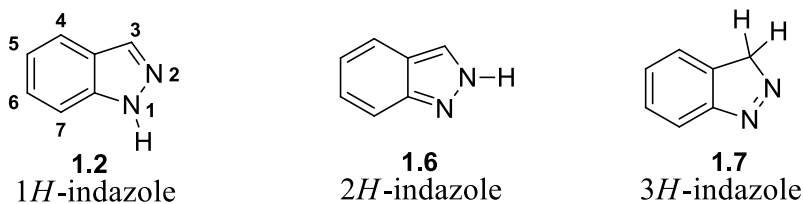
Figure 1-1 Indazole based natural products.



1.1.2 Structure and Properties of Indazoles

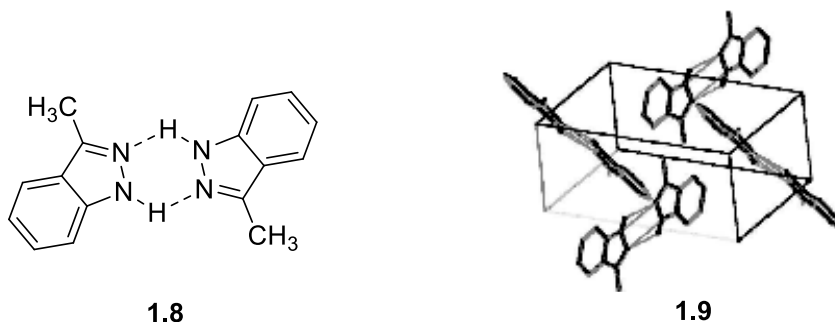
In the words of Emil Fischer, the molecular structure of indazole resembles that of “a pyrazole ring condensed with the benzene ring”. This system is a 10 π - electron heteroaromatic molecule for which there are three tautomeric forms (**Figure 1-2**).

Figure 1-2 Tautomers of indazole.



The 1H-tautomer **1.2** is determined to be approximately 2-4 kcal/mol more stable than the 2H-tautomer **1.6** in the majority of cases,^{5, 6, 7} and only few examples of the 3H-tautomers **1.7** are known. In comparison to pyrazole, indazole is a weaker base (indazole: $pK_{AH} = 1.31$, pyrazole: $pK_{AH} = 2.52$) but stronger NH acid (indazole NH: $pK_A = 13.86$, pyrazole NH: $pK_A = 14.21$).⁸ N-1 unsubstituted Indazole derivatives frequently crystallize in the form of dimers (**Figure 1-3**), trimers or catemers in which an intermolecular N-H \cdots N hydrogen bonding interaction is observed.⁹

Figure 1-3 The crystal structure of 3-methyl-1*H*-indazole dimers.



Structures bearing Intramolecular hydrogen bonding are also feasible as shown in the example of 7-nitro-1*H*-indazole, (**Figure 1-4**).¹⁰

Figure 1-4 Intramolecular hydrogen bonding of 7-nitro-1*H*-indazole.



Computational calculations in lieu of experimental data have revealed a great deal of insight for the fundamental properties of indazoles. Zimmermann and Geisenfelder¹¹ detailed the heats of combustion in the solid and gaseous phase of indazoles, which Dewar used to compute their heats of atomization.¹² An earlier work by Kamiya has used the Pariser-Parr-Pople method with configuration interaction to calculate the electronic spectra, ionization energy, π -electron distribution and total π -energy of indazole,¹³ and molecular diagrams stemming from these calculations for the lowest $^1(\pi, \pi^*)$ singlet and $^3(\pi, \pi^*)$ triplet states show that isomerization from the 1*H*-tautomer to the 2*H*-tautomer is easier in the excited state. Escande and coworkers have used X-ray structure geometries of indazoles as a basis for CNDO/2 and CNDO/S calculations with satisfactory agreement to experimental data, and proposed that indazole in a crystalline solid state to be of the 1*H* tautomeric form.¹⁴ INDO calculations

performed by Palmer and coworkers presented a previously unknown geometry for the indazole anion.¹⁵ Physical chemistry data on indazole and its derivatives are also available through NMR,¹⁶ MS,¹⁷ X-ray,¹⁸ IR,¹⁹ microwave,²⁰ Raman,²¹ UV,²² and laser-induced fluorescence (LIF) excitation spectroscopy.²³

Despite these advances, inherent limitations within such methods still can only provide a tentative guideline for real molecular properties. For instance, in contrary to experimental evidence proving the sites for electrophilic substitution to occur at positions C-3 and C-5 on indazoles, Kamiya's calculations predicted instead for the preference to follow C-7 > C-5 for 1*H*-indazole and C-3 > C-5 > C-7 > C-4 for 2*H*-indazole. Palmer's calculations on indazole dipole moments from *ab initio* LCGO methods (1.97)²⁴ are in disagreement with experimental values (1.60).²⁵

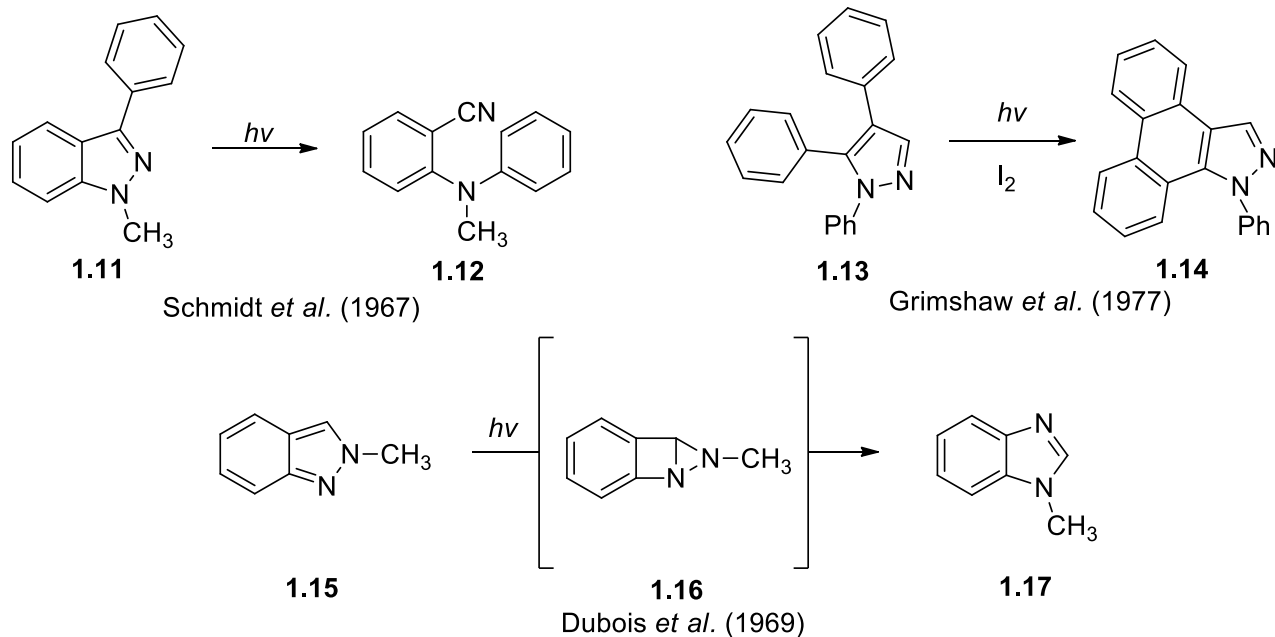
1.1.3 Reactivity of Indazoles

Indazoles exhibit similar reactivity as that of other aromatic moieties. However, there are notable differences. For instance, in comparison to pyrazole, the presence of the benzene ring decreases the overall 'aromaticity' in this system in a similar fashion as in the comparison of naphthalene to benzene, therefore, basic ring cleavage is reported to be easier in indazoles than in pyrazoles.²⁶

The photochemical reactivity of indazoles has been reported (**Scheme 1-2**). A classical study from 1967 by Schmid and colleagues observed the formation of a 1,2-disubstituted benzene derivative (**1.12**) which proceeded through a remarkable ring-opening reaction of 1-methyl-3-phenyl-1*H*-indazole (**1.11**) under UV irradiation.²⁷ Grimshaw and coworkers irradiated 1,4,5-triphenylpyrazole (**1.13**) under nitrogen atmosphere in the presence of iodine to afford 1-phenyl-1*H*-phenanthro[9,10-*c*]pyrazole (**1.14**), an indazole derivative extended in conjugation by 2 additional benzene rings to form the phenanthrene scaffold.²⁸ The phototransposition of 2*H*-indazoles into benzimidazoles (**1.15** → **1.17**), was studied in detail with regard to variations of quantum yield following conditional changes of wavelength, solvent,

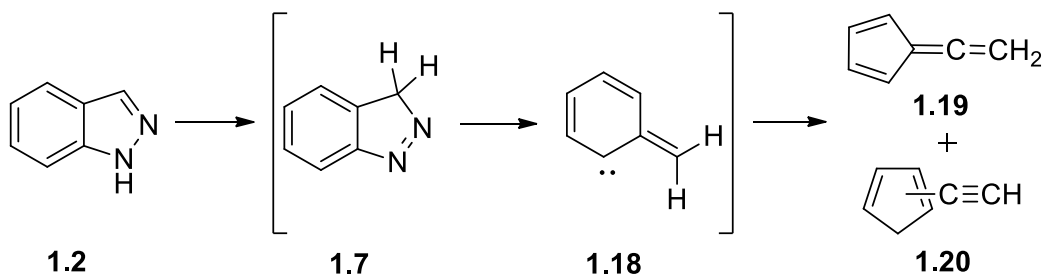
temperature and concentration.²⁹ The intermediate tricyclic compound (**1.16**) was hypothesized to form via a hypersurface crossing in quantitative yield at -60 °C.³⁰

Scheme 1-2 Photochemical reactions of indazoles.



Thermolysis studies by Crow and colleagues of commercial grade indazole over a temperature range of 600 – 950 °C led to the isolation of fulvenallene and ethynylcyclopentadiene in yields greater than 55% (**Scheme 1-3**). They proposed a mechanism involving the rare 3*H*-indazole tautomer **1.7**.

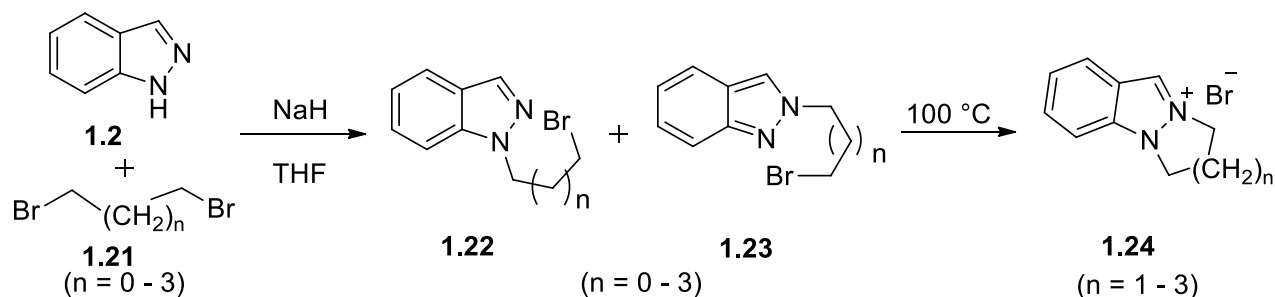
Scheme 1-3 Thermolysis of indazole at 600 – 950 °C.



An important feature of indazole reactivity is the regioselective N-1 and N-2 functionalization. INDO calculations and ^1H NMR spectroscopy aided Palmer and coworkers in their studies regarding the regioselective N-1 vs N-2 methylation of C-3 and C-7 substituted indazole N-anions, and established the electronic preference for N-1 over N-2 alkylation reactions.³¹ In addition, Palmer and Nunn experimentally determined that the ratio of methylation at N-1 vs N-2 positions is sensitive to steric effect of substituents at C-3 and C-7 positions, which favors N-1 and N-2 positions respectively.³²

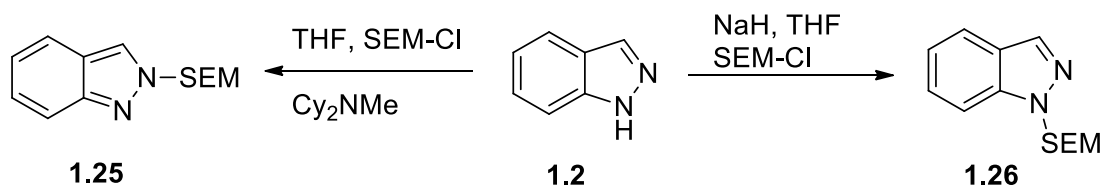
Yang and colleagues disclosed of a method for the synthesis of fused indazole ring systems **1.24** by starting with an alkylation reaction of **1.2** with **1.21** to give a mixture of N-1 and N-2 bromoalkylindazoles **1.22** and **1.23** (Scheme 1-4). Heating this mixture at 100 °C gave indazolinium **1.24** as products in > 95% yield.

Scheme 1-4 The synthesis of fused indazole ring systems.



Regioselective alkylation of indazoles may also be achieved through the careful selection of reaction conditions. Luo and colleagues introduced the 2-(trimethylsilyl)ethoxymethyl (SEM) protecting group with good regio control at either the N-1 or N-2 positions by variation of reaction conditions (**Scheme 1-5**).³³ A strong, non-nucleophilic base such as sodium hydride readily effects deprotonation of the acidic NH on indazoles, which then undergoes reaction as a nucleophile towards 2-(trimethylsilyl)ethoxymethyl chloride (SEM-Cl) to obtain the desired products (**1.26:1.25** ratio of 7.5:1) in 66 % combined yield. The authors proposed a mechanism in which deprotonation by sodium hydride results in the indazole anion where the negative charge primarily centers on the N-1 position but readily delocalizes between N-1 and N-2 without a significant energy barrier. On the other hand, when a weak base such as dicyclohexylmethylamine is introduced together with SEM-Cl, the reaction proceeds via N-2 quaternization followed by N-1 deprotonation since the electron pair at N-1 remains as part of the aromatic system, and only product **1.25** is formed.

Scheme 1-5 Regioselective protection of indazoles with the SEM protecting group.

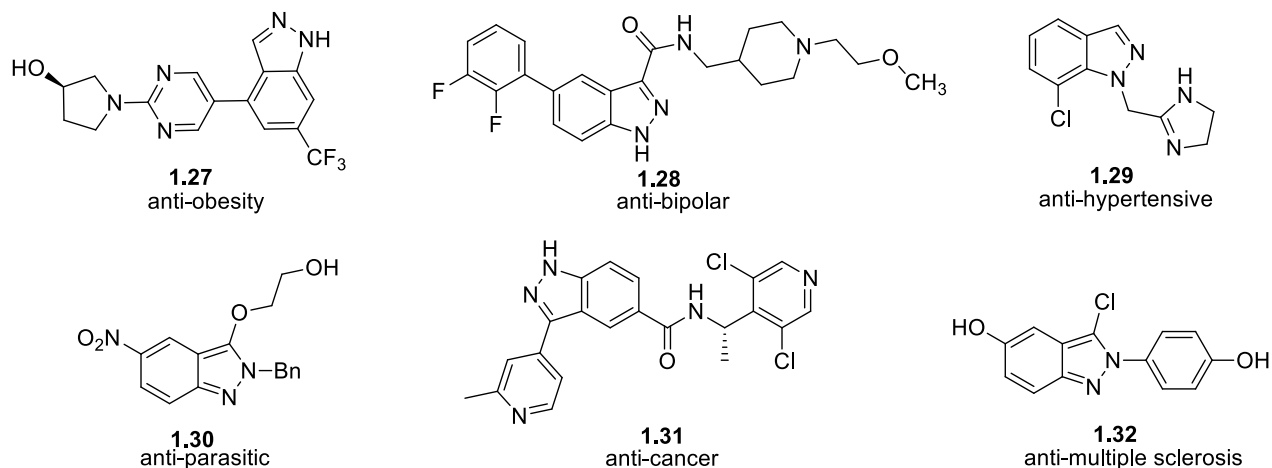


Indazole readily undergoes electrophilic aromatic substitution (S_EAr) with common reagents: results from nitration at C-3 and C-5,³⁴ sulfonation at C-7,³⁵ and bromination at C-5 and C-7 have been reported in classical studies.³⁶ The exact positions towards S_EAr reactivity varies depending on the overall electronic and steric factors of the system, but the general ranking of S_EAr tends to follow C-5 > C-3 > C-7 in the order of substitutions.²⁶

1.1.4 Bioactivity and Material Science Applications of Indazoles

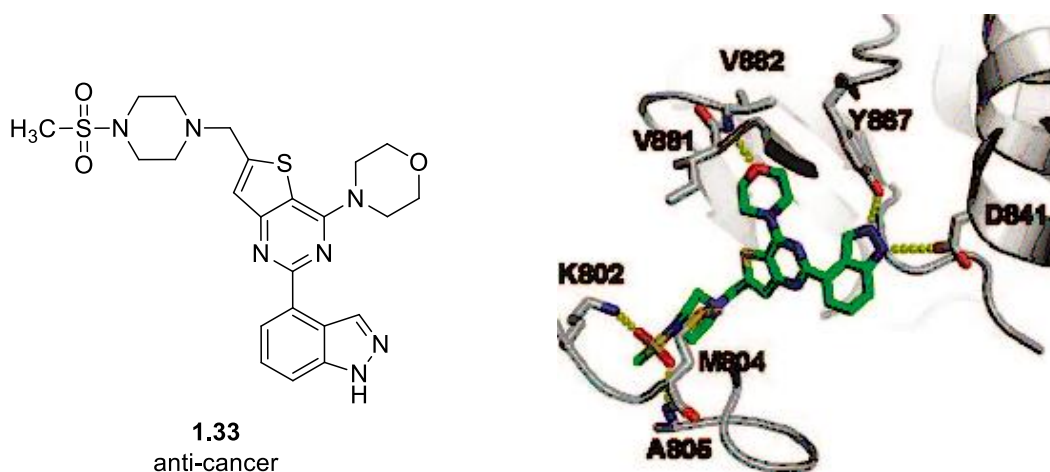
The known biological activities of indazole derivatives are far too copious for an exhaustive listing. Recent publications on the subject have highlighted the properties (**Figure 1-5**) of substituted indazole derivatives acting as a methionine aminopeptidase 2 (MetAP2) inhibitor for a possible treatment of obesity;³⁷ as a potent ERK1/2 enzyme inhibitor;³⁸ as a potential treatment of bipolar disorder through glycogen synthase kinase 3 beta (GSK-3 beta) inhibition;³⁹ as an anti-parasitic agents;⁴⁰ as a candidate for antihypertensive drugs,⁴¹ and as a potent therapeutic agent in the treatment of neural degenerative disorder multiple sclerosis.⁴² These are prime examples that attest to the potential of indazoles for the future betterment of human lives and health.

Figure 1-5 Bioactive indazoles.



Interestingly, the NH bond is often an essential component of ligand-protein interactions, as shown in the hydrogen bonding interaction between p110 γ kinase and compound **1.33**, an important anti-cancer 1*H*-indazole derivative (**Figure 1-6**).⁴³

Figure 1-6 Crystal structure of an NH indazole anti-cancer derivative interacting with p110 γ kinase.



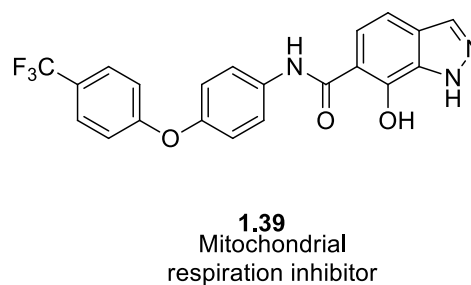
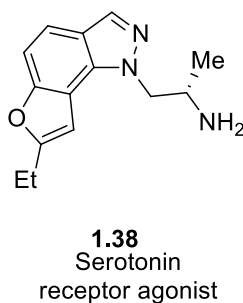
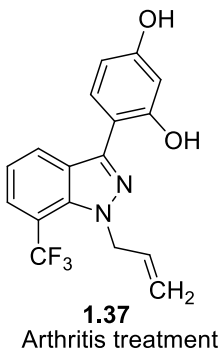
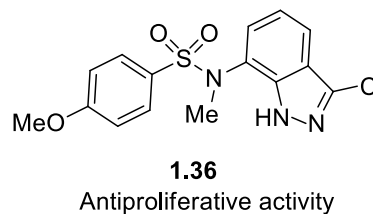
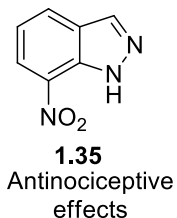
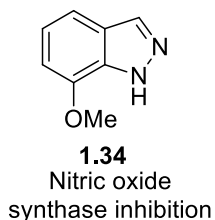
Indazole derivatives have also found utility in material sciences as copper corrosion inhibitors,⁴⁴ copolymerizing molecules for the fabrication of new materials,⁴⁵ effective film-forming additives over

high-voltage positive electrodes for battery applications,⁴⁶ and possible OLEDs through binding with lanthanide or transition metal complexes.⁴⁷

1.1.5 C-7 Substituted Indazoles

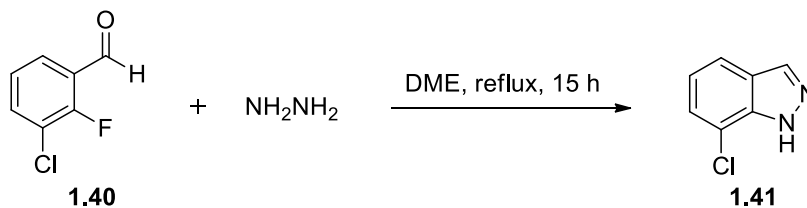
The progress in the study of the biological and physical properties of indazole derivatives would not have been possible without a similar spur of research in fundamental organic synthesis. Even though the drug discovery process is still being driven by decades old protocols, emerging technologies in microwave,⁴⁸ catalysis,⁴⁹ flow,⁵⁰ solvent-free,⁵¹ and green chemistry⁵² are all seeking to revolutionize the status quo. However, certain substituent patterns of indazole remain elusive and difficult to achieve by traditional means. Among these, C-7 substituted indazole derivatives are of prime interest due to their significant bioactivities as nitric oxide synthase inhibition,⁵³ antinociceptive effects,⁵⁴ anti-proliferation,⁵⁵ mitochondrial respiration inhibition,⁵⁶ anti-arthritic effects,⁵⁷ and serotonin receptor agonist (**Figure 1-7**).

Figure 1-7 Bioactive C-7 substituted indazoles.



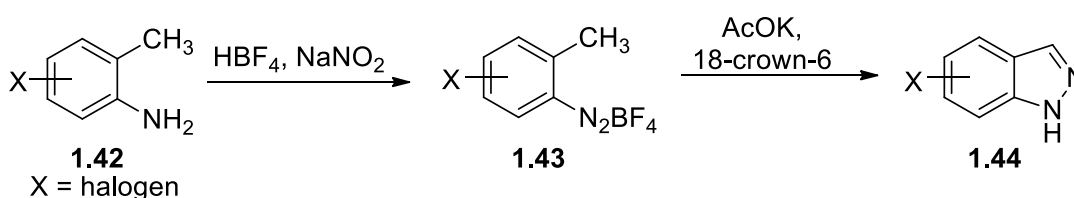
Traditional methods for the synthesis of C-7 substituted indazoles are cumbersome and indirect, and typically involve early stage prefunctionalization of the desired regio isomer of substituted benzene derivatives followed by various forms of cyclization reactions.^{58,59,60} The type and variety of C-7 substituted derivatives that may be obtained are often limited by harsh reaction conditions. A classical route towards indazoles involves the condensation reaction between substituted benzaldehydes with hydrazine.⁶⁰ In a more recent modification, 7-chloroindazole **1.41** was prepared by a condensation - S_NAr reaction of substituted *o*-fluorobenzaldehydes **1.40** with hydrazine (**Scheme 1-6**).

Scheme 1-6 Synthesis of 7-chloro-1H-indazole via S_NAr type reactions.



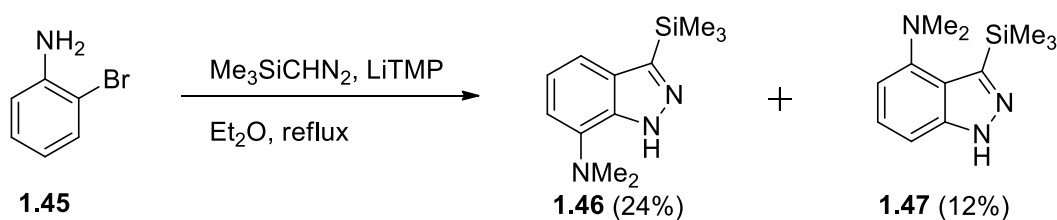
In another method,⁶¹ 2-bromo-6-methylaniline **1.42** is subjected to diazotization using aqueous sodium nitrite solution in fluoroboric acid to give the corresponding diazonium tetrafluoroborate salt **1.43**, which upon cyclization promoted by potassium acetate and 18-crown-6 gave 7-bromoindazole **1.44** in 90 % yield. Under these conditions, 4-, 5-, 6- and 7- halo substituted 1*H*-indazoles can be obtained dependent upon the substitution pattern of the initial methylaniline derivative (**Scheme 1-7**).

Scheme 1-7 Diazotization procedure towards substituted indazoles.



A rare example for the construction of C-7 substituted indazoles involves a [3 + 2]-cycloaddition reaction for the construction of C-7 substituted indazoles (**Scheme 1-8**). Thus, the generation of benzyne in the presence of in-situ generated lithium trimethylsilyldiazomethane (TMSC(Li)N₂), followed by cycloaddition leads to the formation of products **1.46** and **1.47**.⁵⁹ The starting reagent trimethylsilyldiazomethane is highly toxic that has caused fatalities upon fatal exposure.⁶² Safety hazards aside, this reaction suffers from poor regioselectivity and low yields under the used conditions of reaction.

Scheme 1-8 [3+2] cycloaddition reactions towards substituted indazoles.



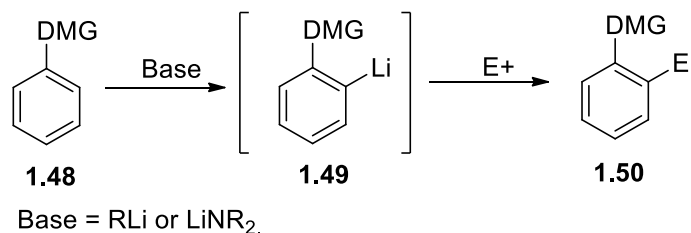
1.2 Organometallic Reactions

1.2.1 The Directed *ortho* Metalation (DoM) Reaction: An Overview

Given the importance and ubiquity of aromatic and heteroaromatic compounds, chemists have long sought to build and modify them through various means. Classically, the electrophilic aromatic substitution (S_EAr) reaction is the standard set of reactions with which chemists functionalize arenes. However, S_EAr reactions are not without their drawbacks in problems of regioselectivity, functional group tolerance, harsh conditions and low yields. Perhaps dissatisfied with the inherent limitations of S_EAr reactions, chemists have since developed methods using Directed *ortho* Metalation (DoM) and later C-H activation to better address the expectations of modern synthetic challenges.

Gilman and Wittig were the original discoverers of the power of alkyl lithiums to effect *ortho* deprotonation of anisole.⁶³ In which the OMe directed metalation group (DMG) regioselectively controls the site of deprotonation by a strong base, and the subsequent quench with an electrophile effectively traps the intermediate lithiated species to achieve *ortho* regioselective substitution of anisole (**Scheme 1-9**). Today, more than half a century since the inception of the DoM reaction, new DMGs are being developed, mechanisms are better understood, and the industry and academia alike rely heavily on the past achievements of Hauser⁶⁴, Gschwend,⁶⁵ Beak,⁶⁶ Meyers,⁶⁷ and Snieckus⁶⁸ among others for tackling modern synthetic challenges, and realizing, in part, the promise of DoM chemistry.

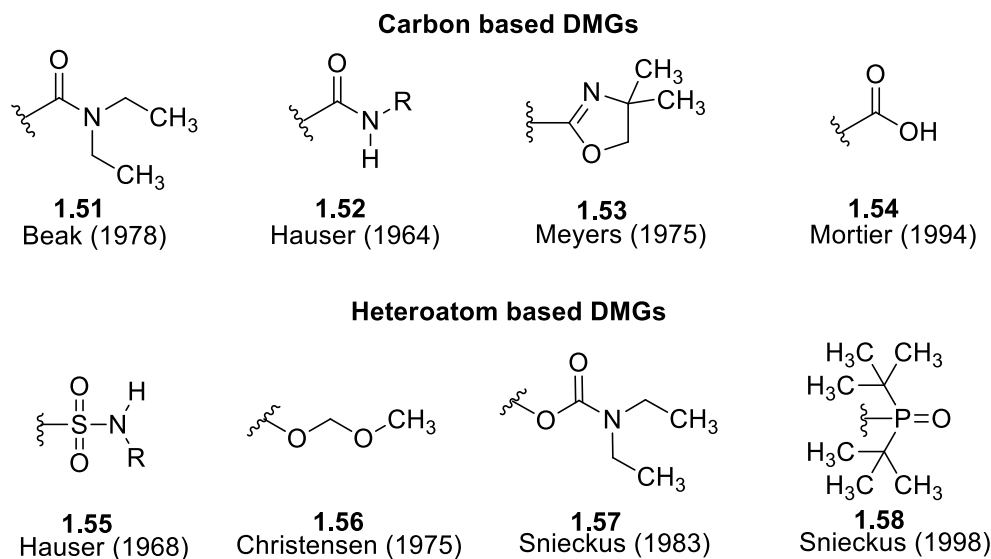
Scheme 1-9 Simplified representation of the DoM reaction.



1.2.2 The DoM Reaction: Directed Metalation Groups (DMGs)

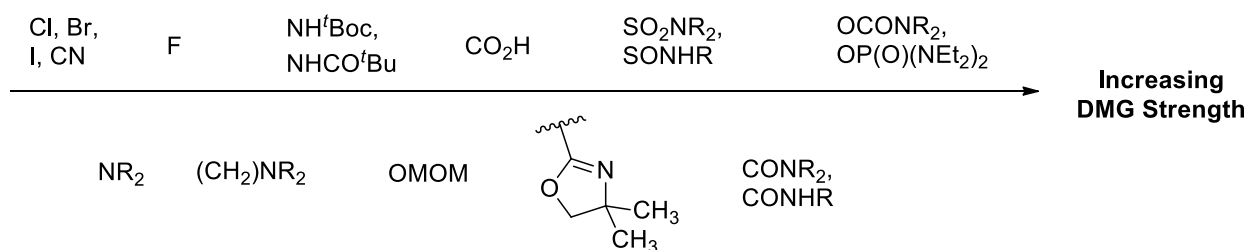
Directed metalation groups (DMGs) are generally classified into two camps: those based on carbons and those on heteroatoms. Each DMG is unique in its relative strength for *ortho* directing, sensitivity to reaction conditions such as temperature and solvent, and ease with which it may subsequently be removed or converted. A DMG should generally be a good coordinator for alkyllithium bases but not so electrophilic as to be attacked by these very same reagents, and strategies such as steric hindrance by introducing bulkier substituent and charge deactivation by anion formation on the DMG groups can sometimes be successful.⁶⁸ Generally, a heteroatom is included as a part of the DMG for coordination purposes, preferably through a 5-membered ring transition state during the deprotonation stage.⁶⁸ Selected examples of DMGs are shown in **Figure 1-8**.

Figure 1-8 Examples of common DMGs.



The relative *ortho* directing strengths of many DMGs has been established through competition experiments (**Figure 1-9**). Intramolecular competition studies using 1,4-disubstituted aromatics bearing different DMG groups were reported by Slocum,⁶⁹ Beak⁷⁰ and Macklin⁷¹ among others, and the preferred site of deprotonation is *ortho* to the stronger DMG and not the weaker DMG. Similarly, Meyers and Lutomski reported intermolecular competition studies using the oxazolino anchoring group.⁷²

Figure 1-9 Hierarchy of DMG power.



To rationalize the effectiveness of different DMGs, theories based on DMG dihedral angles⁷³ and triple ion model⁷⁴ have been proposed with varying degrees of success. The need for understanding

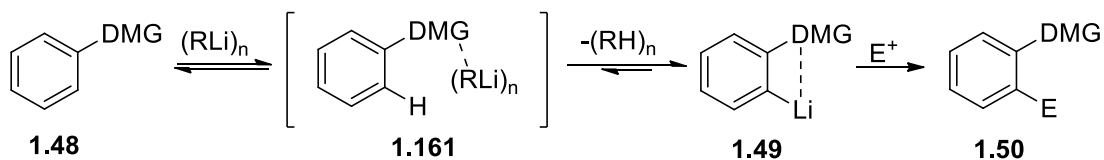
DMG activating strength requires fundamental kinetic and thermodynamic information. In an important study by Fraser and colleagues, pK_a data for monosubstituted benzenes in THF was determined, thereby providing a direct measure of the acidifying effect of a substituent on the *ortho* - proton.⁷⁵ Other than a few exceptions such as the *N,N*-diethyl *o*-carbamate directing group, the majority of substituents give rise to very similar pK_a values, thereby suggesting that kinetic effects are predominantly responsible for reactivity orders.

An important practical consideration when choosing any DMGs is the ease with which it may be modified or removed. For instance, Schwarz reagent generated *in situ* readily reduces DMGs such as the *N,N*-diethylcarboxamide to aldehydes that proceeds with very short reaction time, excellent functional group tolerance and the use of inexpensive reagents.⁷⁶ Tertiary amides are excellent DMGs, and their use in DoM chemistry prior to reduction can lead to unusually substituted aromatics. Cross coupling reactions of tertiary sulfonamides (SO_2NR_2)⁷⁷ or aryl *o*-carbamates⁷⁸ with Grignard reagents are also feasible under nickel (0) catalysis, thus making them latent DMGs. OMOM and NHBoc groups are relatively labile under hydrolysis to give unprotected phenols and anilines. The oxazoline DMG can also be hydrolyzed albeit by a complicated procedure to give the carboxylic acid.⁷⁹

1.2.3 The DoM Reaction: Mechanism

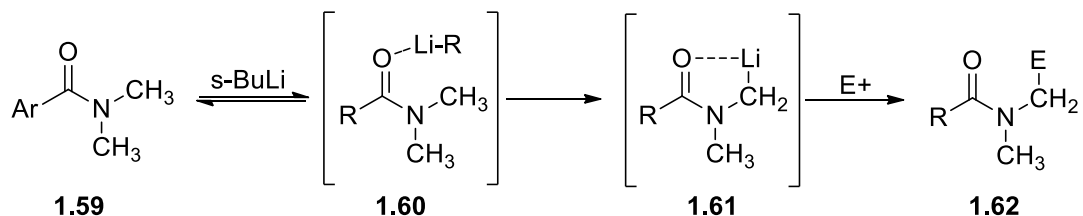
The mechanism of the DoM reaction may be simplified to a three stage process (**Scheme 1-10**). First, the base $(RLi)_n$ in the form of an aggregate undergoes coordination to the heteroatom-containing DMG. This forms a “preDoM” complex **1.161** which brings the base in close proximity to the *ortho* hydrogen. Deprotonation gives the coordinated *ortho*-lithiated species **1.49**, followed by the treatment with electrophiles to yield the product **1.50**. Beak and Myers termed this phenomenon the complex induced proximity effect (CIPE).⁸⁰

Scheme 1-10 Mechanisms of DoM according to the Complex Induced Proximity Effect (CIPE).



Beak and associates helped to establish evidence supporting the formation of a preDoM complex in an α -deprotonation reaction (**Scheme 1-11**).⁸¹ Using the stopped-flow IR technique, they observed the presence of the amide lithium complex **1.60** prior to α deprotonation, in which the organolithium base is brought by coordination to close proximity of α hydrogen. Energy calculations on species **1.61** suggest a stabilization of about 25 kcal/mol relative to an uncoordinated α -lithio amine species, with two thirds of this stabilization due to dipole-dipole interactions and one-third due to bonding by the lithium.⁸² Theoretically, the binding between the heteroatom of a DMG to the organolithium base contributes to a stabilization resulting from a favorable energetic interaction between the small positively charged lithium atom and the electron pair of that heteroatom.⁹⁶ Evidential support for lithium-electron pair complexation in the ground state is provided by X-ray crystallography.⁸³

Scheme 1-11 Evidence for CIPE in alpha-deprotonation.

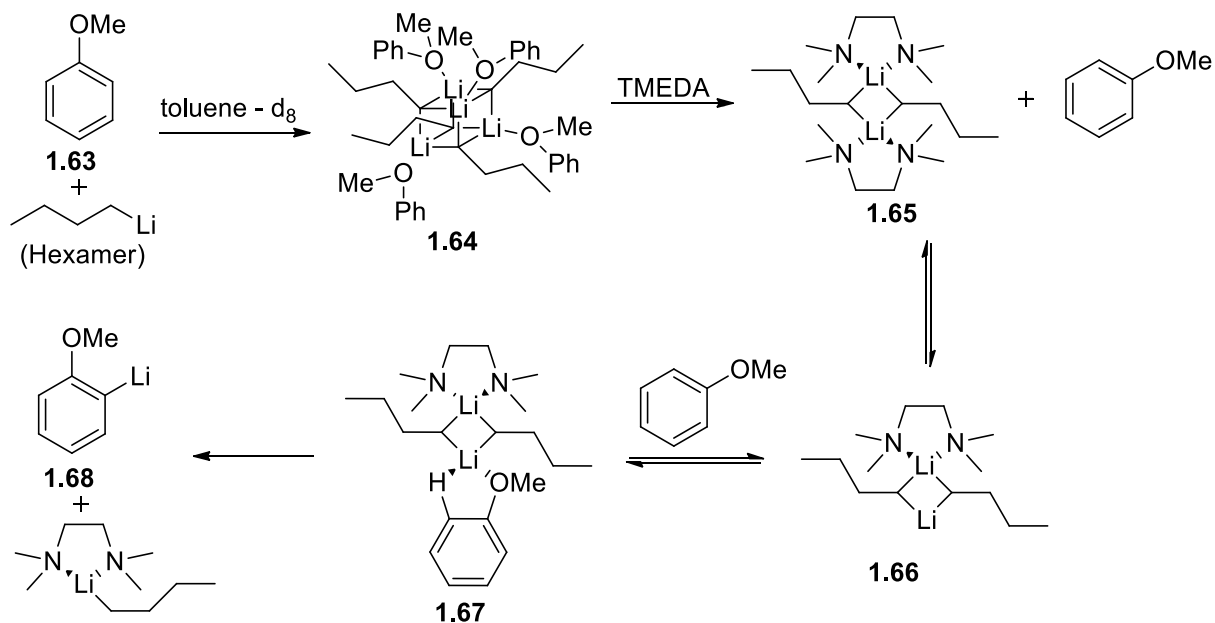


Evidence supporting the concept of DMG stabilization of the *ortho*-lithiated complex is also available. Thermodynamic data from Klumpp and Sinnige established that proton quench of (*p*-anisyl) lithium is 3.6 kcal/mol more exothermic than (*o*-anisyl) lithium, which is indicative for the greater thermodynamic stability of the *ortho*-lithiated anisole species.⁸⁴ Broaddus has demonstrated *ortho*-

deprotonation of anisole is 100 times faster than that of benzene.⁸⁵ Furthermore, the reaction of dimethylbenzylamine with *n*BuLi-TMEDA has been shown to produce an *ortho*-lithiated species, which was revealed by X-ray crystallographic analysis to be a tetrameric aggregate where each lithium atom is associated with three carbanionic carbon atoms and one nitrogen atom.⁸⁶ Significantly, the structure of the lithiated complex in Et₂O dynamically changes to produce a mixture of three different dimers, each exhibiting strong intramolecular chelation.⁸⁷ Through *Ab initio* calculations, the STO-3G stabilization energy versus phenyllithium were determined to be -7.1, -0.5, and 0.0 kcal/mol respectively, for *o*-, *m*-, and *p*-lithiophenol.⁸⁸ Similarly, *o*-, *m*-, and *p*-lithiofluorobenzene were reported to be more stable by 8.4, 1.2 and 0.7 kcal/mol relative to phenyllithium. The DMG stabilizing effect on the *ortho*-lithiated complex can be seen in these results.

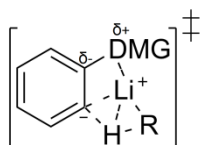
It is well known through ¹³C and ^{6,7}Li NMR spectroscopic studies that organolithiums exist as aggregates in organic solvents,⁸⁹ with *n*-BuLi existing in dimeric,⁹⁰ tetrameric⁹¹ and hexameric⁹² forms. In a detailed NMR and computational study (**Scheme 1-12**),⁹³ Bauer and Schleyer discovered that the hexameric *n*-BuLi aggregate can be disrupted upon addition of an equimolar concentration of anisole and replaced by a tetrameric 1:1 aggregate of anisole and *n*-BuLi **1.64** in toluene-*d*₈, which was observed through two-dimensional ⁷Li and ¹H-heteronuclear overhauser effect spectroscopy. The authors had initially anticipated the rapid metalation of anisole in the aggregate due to its close contacts with *n*-BuLi but this was not observed. Upon the addition of 1 equivalent of TMEDA, anisole undergoes decomplexation from the aggregate to give the *n*-BuLi dimer **1.65** which was observed spectroscopically. Under these conditions, anisole readily underwent metalation to give **1.68**, which was attributed to the formation of the reactive intermediate **1.67** with low stationary concentration undetectable by NMR. MNDO calculations supported these experimental results.

Scheme 1-12 NMR and computation study on the *ortho* lithiation of anisole.



A mechanistic proposal complementary to the CIPE was suggested by Hommes and Schleyer and termed the “kinetically enhanced metalation” (KEM). Based on the above NMR studies, this hypothesis argues that the pre-lithiation complex as an intermediate is not formed but replaced by a rate-determining proton transfer transition state.⁹⁴ In other words, the proton transfer occurs simultaneously with complexation as shown in **Figure 1-10**. This proposal is supported by the observation that halogens such as fluorine, chlorine and bromine which are poor coordination groups for alkyl-lithium bases are able to serve as moderate DMGs. The electron-withdrawing nature of these DMGs may play a role acidifying the *ortho* C-H bond. The KEM hypothesis is supported by *ab initio* calculations.⁹⁴ However, for DMGs with strongly coordinating groups such as amide, oxazoline, the onset of CIPE-type mechanism is still not ruled out.⁹⁵

Figure 1-10 The Kinetically Enhanced Metalation (KEM) transition state.



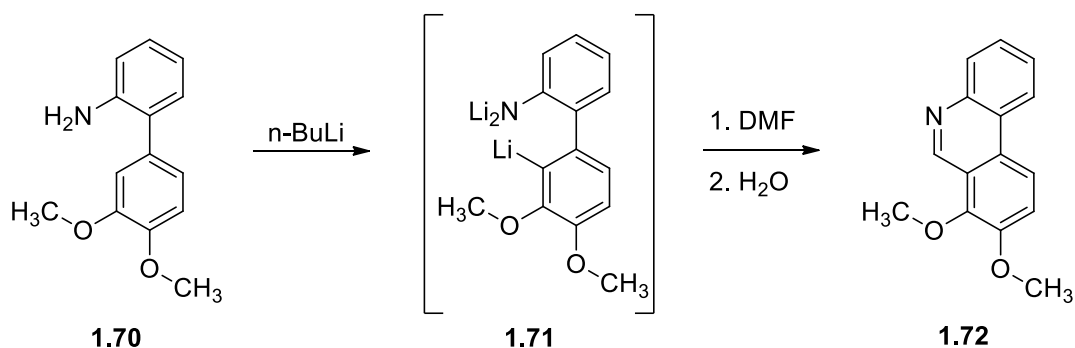
1.69

Over the years, extensive research efforts were invested towards understanding the mechanism of DoM reactions, and an excellent review from 2004 comprehensively summarized the most important findings.⁹⁶

1.2.4 The DoM Reaction: The Directed *remote* Metalation (*DreM*)

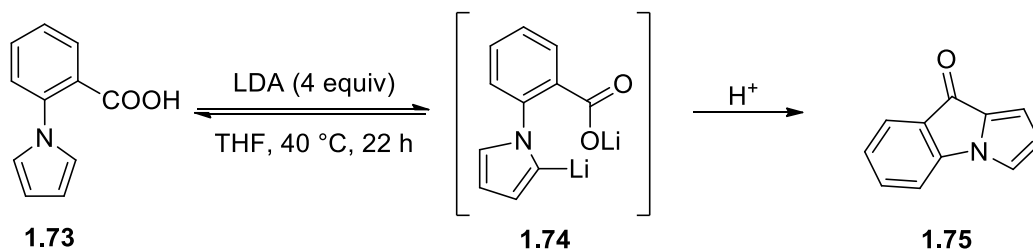
The application of DoM chemistry in the metalation of a remote arene in a biaryl/hetaryl system has led to the development of the directed remote metalation reaction (*DreM*). In one of the earlier examples, Narasimhan and colleagues established a synthetic route towards the difficult to access 7,8-dimethoxy phenanthridine **1.72** using *DreM* chemistry (**Scheme 1-13**).⁹⁷

Scheme 1-13 The *DreM* reaction in the synthesis of 7,8-dimethoxy phenanthridine.



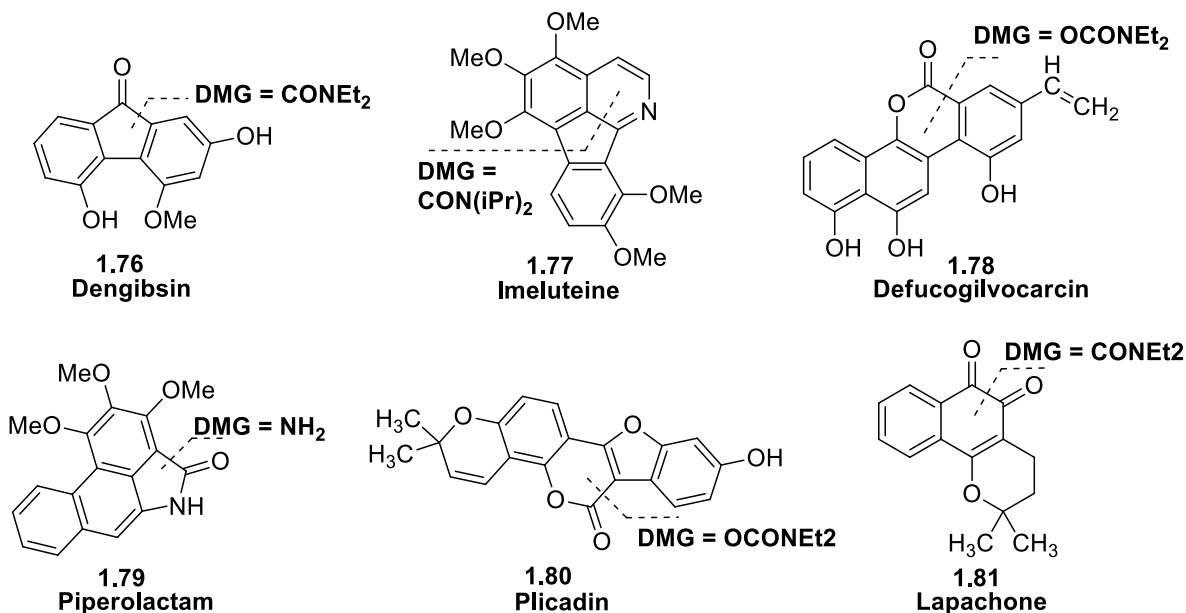
In another example, Cartoon and coworkers reported on the *DreM* reaction of 1-(2'-carboxyphenyl)pyrrole **1.73** with lithium diisopropylamide (LDA) to form 9-keto-9*H*-pyrrolo-[1,2-*a*]indole **1.75** (**Scheme 1-14**).⁹⁸ The reaction proceeds through an intramolecular cyclization of the remotely 2-lithiated pyrrole onto the carboxylic acid DMG in forming a ketone after acidic quench.

Scheme 1-14 The DreM reaction in the synthesis of 9-keto-9*H*-pyrolo-[1,2-*a*]indole.



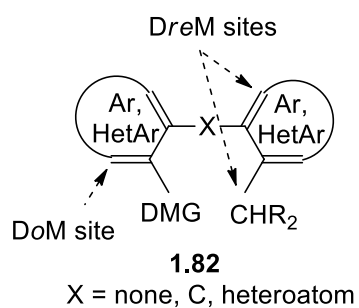
This important discovery of a self-quenching DMG upon metalation was further elaborated with CONEt₂ and OCONEt₂ as DMGs and developed into a robust methodology by the Snieckus group towards the total synthesis of a long list of important natural products (**Figure 1-11**), including dengibsin,⁹⁹ Imeluteine,¹⁰⁰ defucogilvocarin,¹⁰¹ piperolactam,¹⁰² lapachone,¹⁰³ plicadin,¹⁰⁴ eupolauramine,¹⁰⁵ and gymnopusin.¹⁰⁶

Figure 1-11 Synthesis of natural products using the DreM strategy.



The key aspect of *DreM* chemistry lies in its ability to selectively affect lithiation at positions remote from the arene which bears the DMG (**Figure 1-12**). It is often viewed as an extension of directed *ortho* metalation even though its development has lagged behind that of DoM.¹⁰⁷ Mechanistically, CIPE and KEM are both relevant and sometimes invoked together to rationalize the concept of *DreM* reaction.^{107, 108}

Figure 1-12 Sites of deprotonation in DoM compared with *DreM*.



1.2.5 Grignard Reactions: An Overview

With the exception of DoM reactions, few reactions can rival the synthetic utility and versatility of the Grignard reaction in classical C-C bond formation. First discovered in 1912 for which Victor Grignard received the Nobel Prize in Chemistry, it has since been the subject of intensive studies totaling over 40,000 papers published by 1975.¹⁰⁹ Today, it is an extremely valuable and widely-used transformation in organic synthesis.

A variety of methods for the preparation of Grignard reagents have since then developed, and these include: carbenoid-homologation possibly proceeding through an halide-Ate complex,¹¹⁰ reaction with activated magnesium through reduction of its salt with an alkali metal,¹¹¹ reaction with magnesium anthracene complex through its decomposition,¹¹² metal-catalyzed Grignard formation with iron,¹¹³ as well as numerous exchange reactions involving magnesium with halogens.¹¹⁴ The developments of chiral Grignard reagents were also outlined both theoretically and experimentally.¹¹⁵

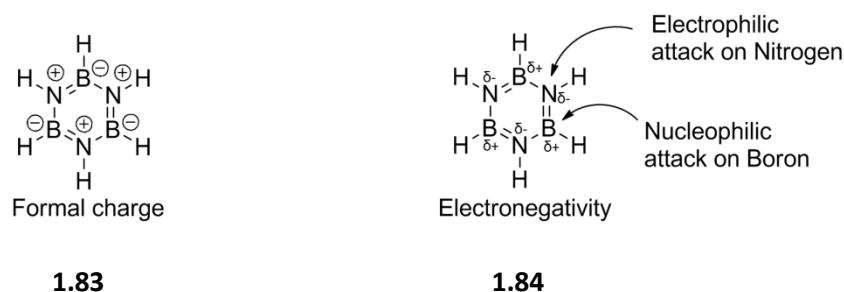
The cross-coupling reaction of a Grignard reagent received a great deal of attention from both the Corriu and Kumada research groups in the late 1960s, which culminated in the discovery of the Kumada-Corriu coupling reaction in 1972,¹¹⁶ an important synthetic milestone predating many of the mainstream cross-coupling reactions such as the Sonogashira (1975), Negishi (1976), Stille (1977), Suzuki (1979), and Hiyama (1988) reactions.

1.3 N,C-Chelating Organoboron Compounds and Azaborines

1.3.1 Introduction to Azaborines

The history of azaborines can be traced to 1926 with the synthesis of borazine by German chemist Alfred Stock.¹¹⁷ By heating diborane with ammonia at 300 degrees, Stock obtained the desired borazine **1.83** (Figure 1-13) in 50% conversion. As an isoelectronic and isostructural analogue of benzene, it is frequently termed as the “inorganic benzene”, which appears as a colorless liquid (bp = 53 °C) with an aromatic odour and similar physical properties.^{117, 118} The B-N bonding distances in the planar structure are equal (144 pm), with delocalization of electron density from the lone pairs on nitrogen into the empty p orbitals of boron. The relative electronegativity of boron ($\chi^p = 2.0$) and nitrogen ($\chi^p = 3.0$) places the site of nucleophilic and electrophilic attack on these two atoms respectively, opposite to what is expected based on the distributions of its formal charge (Figure 1-13).^{117,118}

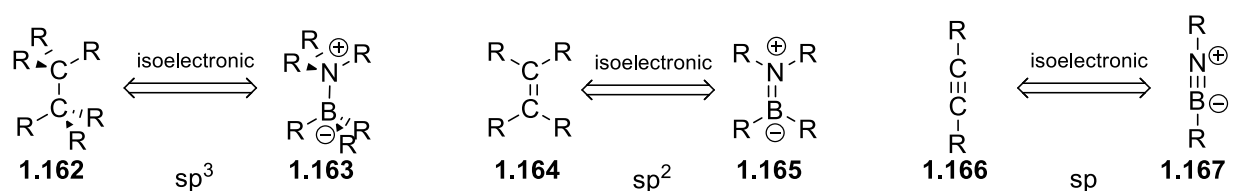
Figure 1-13 Borazine formal charge and electronegativity.



The conceptual framework with which one may attempt to understand the azaborine motif should be based on the idea of BN/CC isosterism, which is the replacement of bonding carbons with an isoelectronic and isosteric B-N unit.^{119, 120} There are three different relationships by which BN/CC isosterism can occur, and these are based on the hybridization of the atomic orbitals belonging to the bonding B-N pair in question (Figure 1-14). Despite the same total valence electron count, fundamentally different molecular properties and chemistry may be expected when such replacements are made.^{119, 120} Comparisons can be made in the simplest case when the R groups are hydrogen atoms.

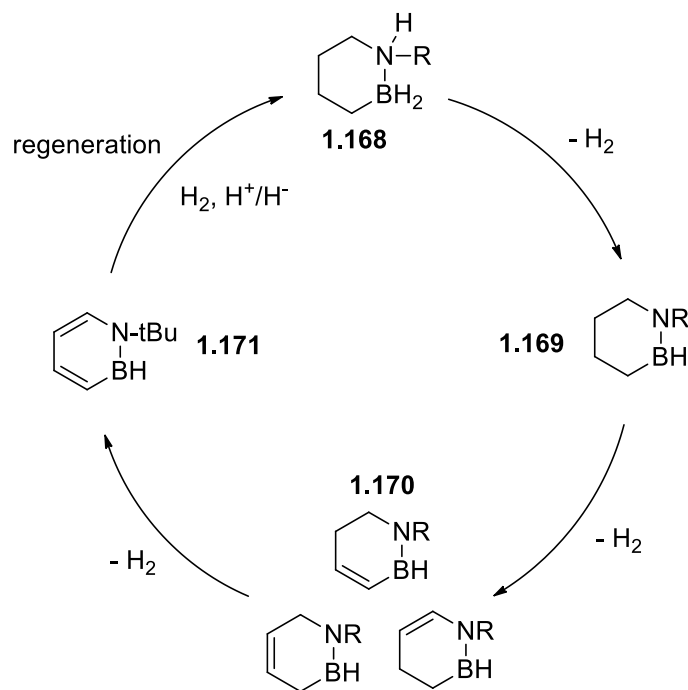
For instance, the sp^3 hybridized ethane molecule is a volatile gas under standard conditions (bp: $-89\text{ }^\circ\text{C}$), with zero net dipole moment from symmetry and a C-C bond dissociation energy of 90.1 kcal/mol .¹²¹ In contrast, the BN analogue of ethane, ammonia-borane, is a solid under standard conditions (mp: $104\text{ }^\circ\text{C}$), and due to its electronegativity differences, ammonia-borane has a dipole moment of 5.2 D and a bond dissociation energy of 27.2 kcal/mol .¹²²

Figure 1-14 The isoelectronic relationships of BN/CC isosterism.



While azaborine derivatives have recently shown some signs of promise as biologically relevant molecules,¹²³ the true extent of their prominence belongs to the field of material sciences. Their use as hydrogen storage materials (**Figure 1-15**),¹²⁴ OLEDs,¹²⁵ fluoride sensors,¹²⁶ cyanide sensors¹²⁷ and optoelectronic devices¹²⁸ are just some of the functionalities that attest to the importance of azaborine derivatives.

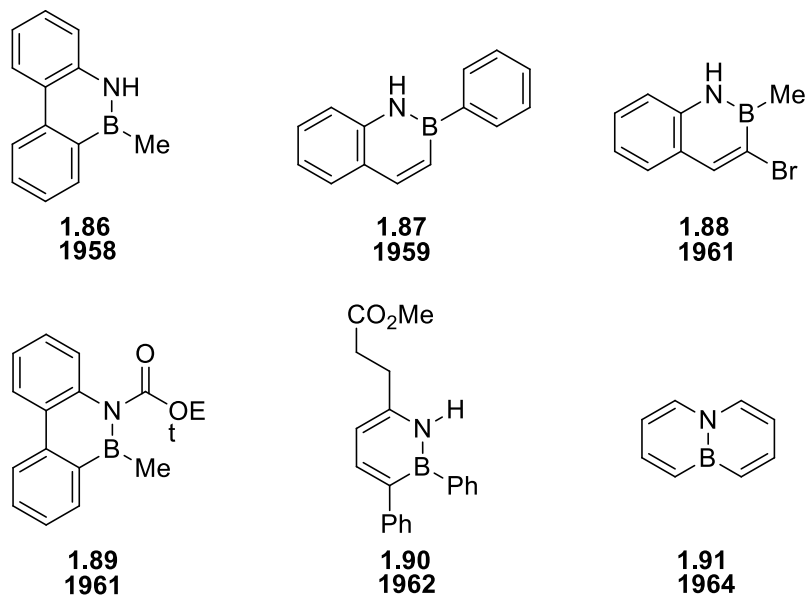
Figure 1-15 Azaborine based hydrogen storage materials.



1.3.2 Key advancement of Azaborines

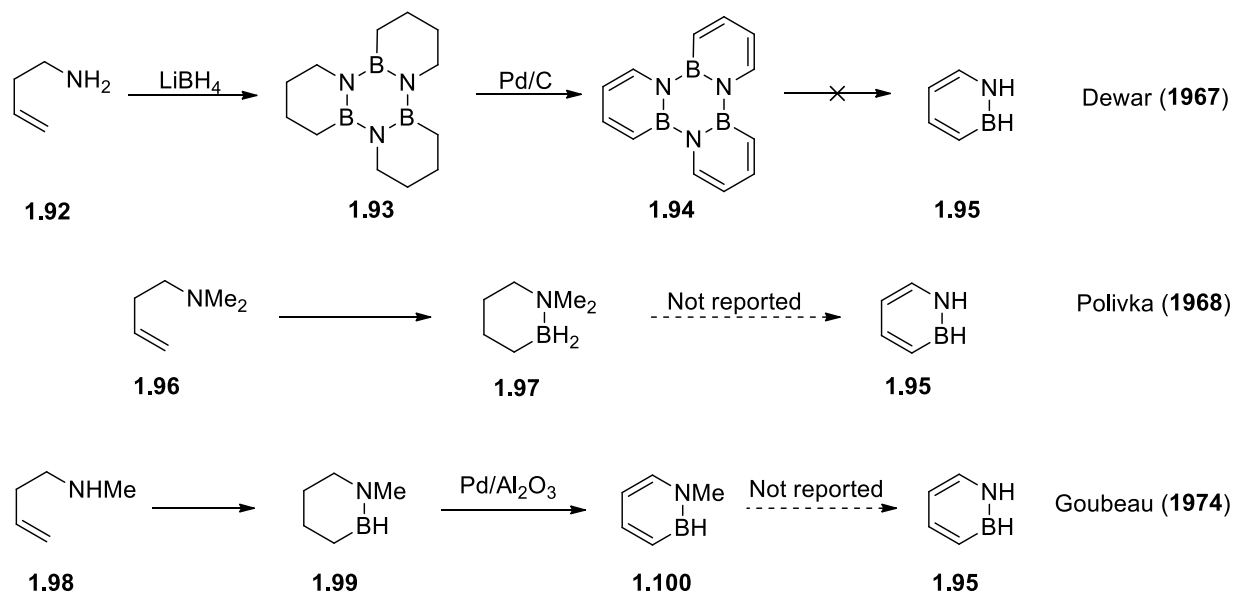
Since Alfred Stock, numerous other research groups have made headway into the field of azaborines. An important pioneer in the early development of azaborines was Dewar (**Figure 1-16**), a theoretical chemist who developed synthetic pathways to BN analogues of phenanthrene **1.86**¹²⁹ and naphthalene **1.87**,¹³⁰ and who was the first to achieve the synthesis of a monocyclic 1,2-azaborine derivative **1.90**,¹³¹ which was reported to be stable to Raney Nickel reduction as well as acidic and basic conditions in ethanol.

Figure 1-16 Azaborine products synthesized by Dewar.



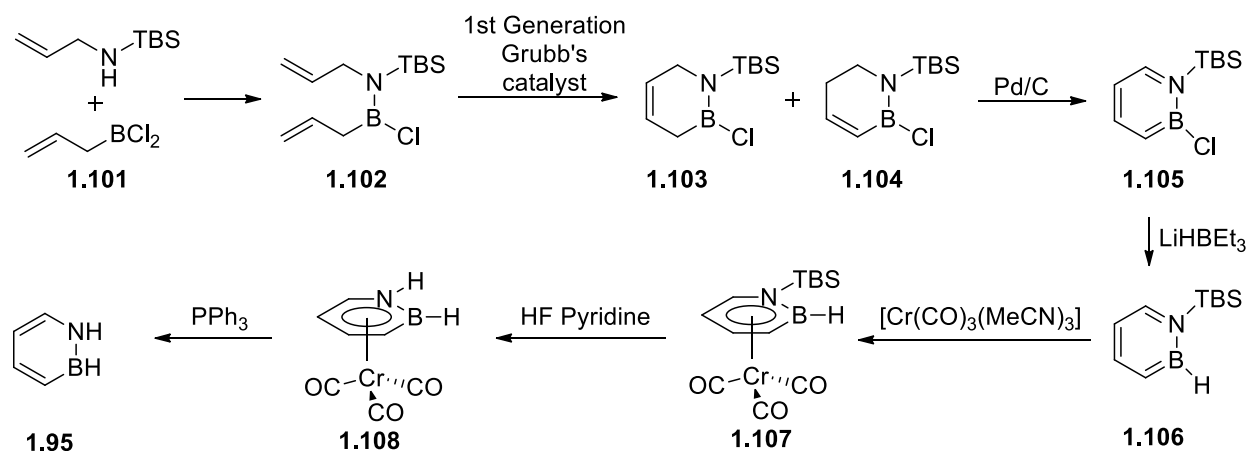
The parent 1,2-dihydro-1,2-azaborine **1.95** proved to be a much more elusive target than its substituted derivatives (**Scheme 1-15**). The Dewar group attempted its synthesis via a hydroboration-oxidation pathway which proved unsuccessful.¹³² The Polivka group managed to synthesize a hydrogenated version of the desired compound with full saturation and doubly substituted methyl groups on nitrogen **1.97**.¹³³ The Goubeau group got even closer to the target compound by synthesizing the B-H substituted 1,2-azaborine, but still N-methylated **1.100**.¹³⁴

Scheme 1-15 Progress towards 1,2-dihydro-1,2-azaborine.



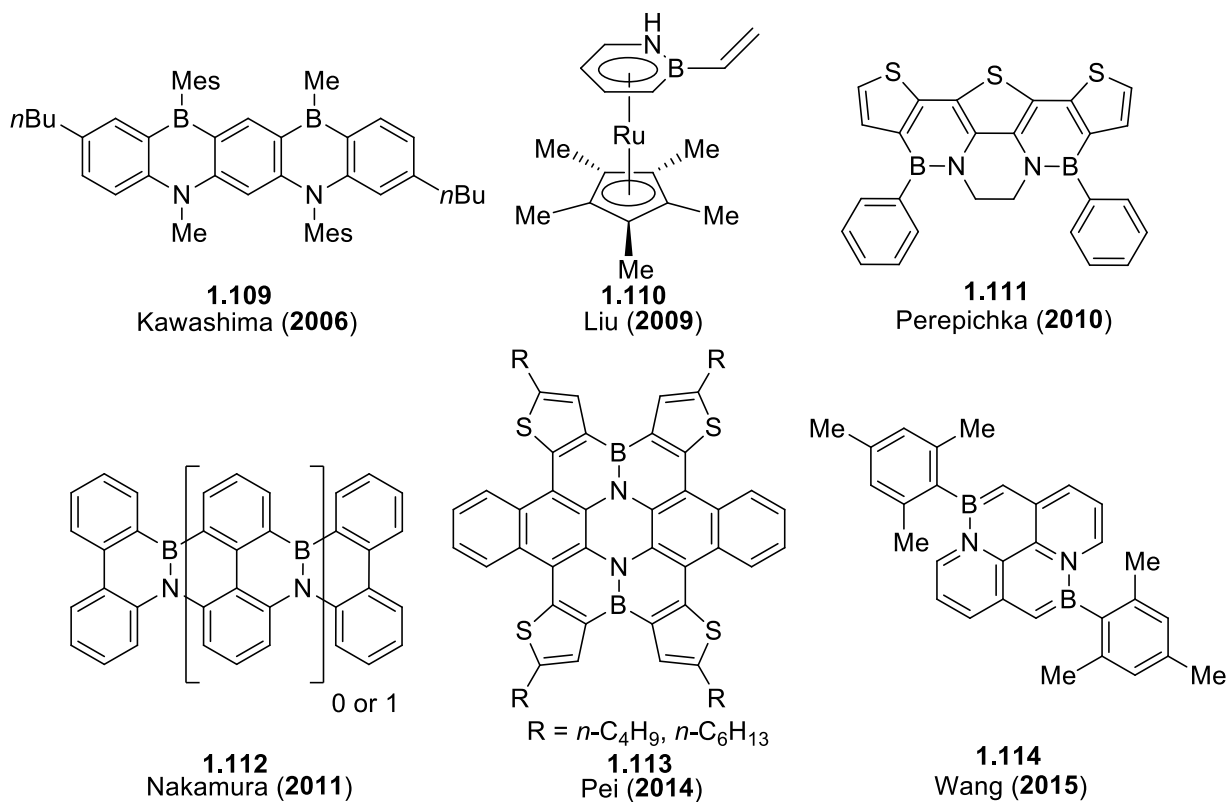
Almost half a decade following Dewar's synthesis of the monocyclic 1,2-azaborine derivative **1.90**, the breakthrough was finally achieved by the Liu group in 2009 when they reported on the first successful synthesis of this elusive target **1.95** (Scheme 1-16).¹³⁵ Worthy of note is the relative importance of the ring-closing metathesis reaction, a modern synthetic methodology characterized by mild reaction conditions which made further advancement into azaborine chemistry possible, and has been adopted by a number of research groups towards the synthesis of this class of molecules.¹³⁶ In Liu's synthesis, the use of chromium tricarbonyl as an activating agent that formed a piano-stool complex with the azaborine cycle **1.107** was necessary for the subsequent removal of the TBS protecting group.¹³⁵

Scheme 1-16 Synthesis of 1,2-dihydro-1,2-azaborine.



The idea of BN/CC isosterism became a theoretical justification for tackling new synthetic challenges. Motivated to expand the frontiers of aromatic chemistry and developing new synthetic methodologies, scientists such as Dewar, Polivka and Goubeau took on the challenge to replace the CC unit in the arene motif with the equivalent BN units in a variety of substrates. Many of Dewar's original azaborine targets did not reveal any significant applications in the years following their conceptions.^{129,130} However, interest did not subside and azaborine chemistry has undergone a renaissance in the recent decade as research groups lead by Ashe,¹³⁷ Wang,¹³⁸ Perepichka,¹³⁹ Yamaguchi,¹⁴⁰ Liu,¹³⁵ Kawashima¹⁴¹, Pei¹⁴², Piers,¹⁴³ and Nakamura¹⁴⁴ joined the fray in an effort to unveil the future potential of these molecules (**Figure 1-17**).

Figure 1-17 Exemplary azaborine molecules.



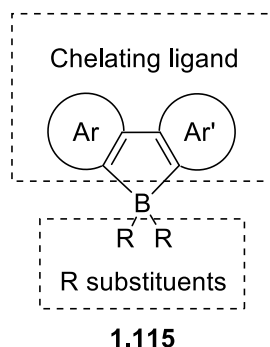
1.3.3 Four-Coordinate Chelated Organoboron Compounds

Recently, the Wang research group has made significant progress in azaborine chemistry both by expanding the synthetic methodologies for accessing these molecules as well as elaborating on the azaborine scaffold for fine tuning their photo luminescent properties (Figure 1-21).¹³⁸ These achievements were predated by, and perhaps impossible without a systematic investigation into the unique photo luminescence and electronic configurations of four-coordinate chelated organoboron compounds (Figure 1-18).

The Wang research group has been studying organoboron molecules for almost two decades.¹⁴⁵ In particular, they have focused on four-coordinate organoboron compounds bearing a π -conjugated chelate backbone **1.115**, where the electronic properties of the chelating scaffold as well as the charge

transfer transitions from the aromatic substituent attached to the coordinated boron center and their associated steric congestions impart broader molecular properties with practical applications as organic light-emitting diodes (OLEDs), organic field transistors, photo responsive materials, and sensory and imaging materials.¹⁴⁵ In this class of compounds, the lowest unoccupied molecular (LUMO) is usually localized on the π -conjugated chelate ligand stabilized by boron coordination. The highest occupied molecular orbital (HOMO) may be localized on either the chelate ligand or the R group attached as substituent on the coordinated boron atom. The photochemical properties of such compounds are usually the result of $\pi \rightarrow \pi^*$ electronic transitions of the chelate or charge-transfer transition for the R group to the chelating ligand (**Figure 1-18**).¹⁴⁷

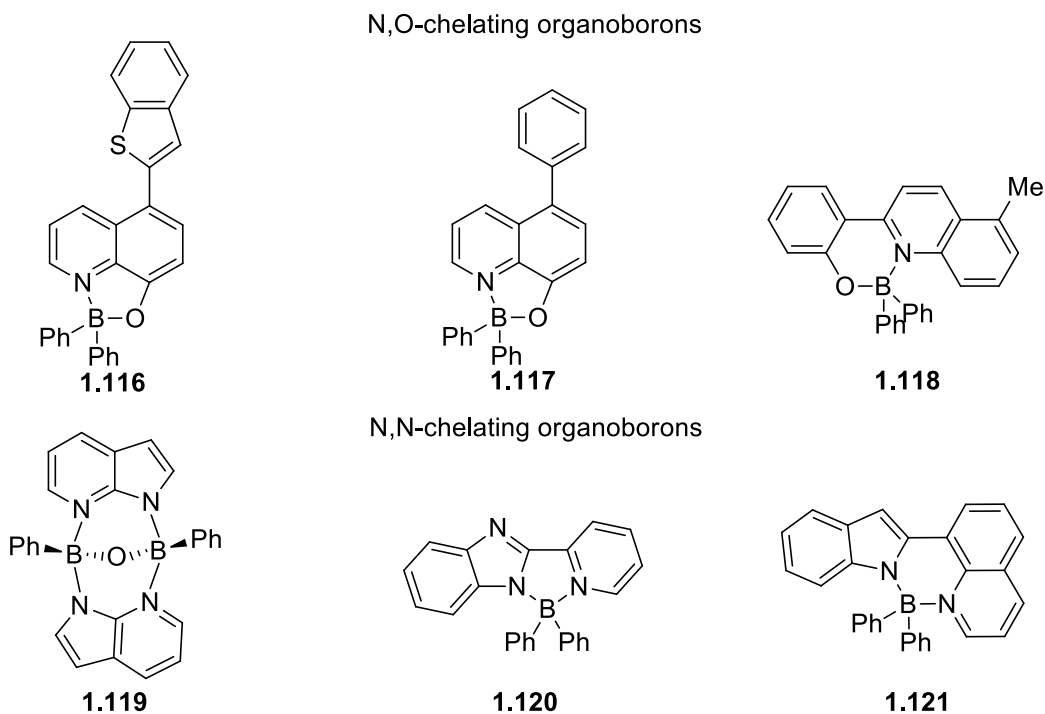
Figure 1-18 Components of a four-coordinate organoboron compound.



In their earlier works (**Figure 1-19**), Wang studied N,O-chelating azaborines 8-hydroxyquinolate **1.116** and **1.117** in hopes of discovering blue emitters for OLED applications with limited success.¹⁴⁶ N,N-chelating compounds based on the 7-azaindoly chromophore **1.119** were later developed that addressed some of the short comings in the N,O-chelating series with greater stability with regards to thermal degradation and irreversible oxidation in OLED devices.¹⁴⁷ The deprotonated 7-azaindole anion emitting a bright-blue color can be stabilized by metals and tetrahedral boron centers,¹⁴⁸ including the diboron compound **1.119**. This motif of N,N-chelating scaffold was later extended to indolyl **1.121**, pyridyl, thiazolyl, quinolyl, and benzoimidazolyl systems **1.120**, some of which

emits in the bright blue region.¹⁴⁹ Color tuning from blue to red and vice versa for this class of compounds was achieved via introduction of various electron donating/withdrawing substituents such as chloro, fluoro and methoxy groups.¹⁵⁰

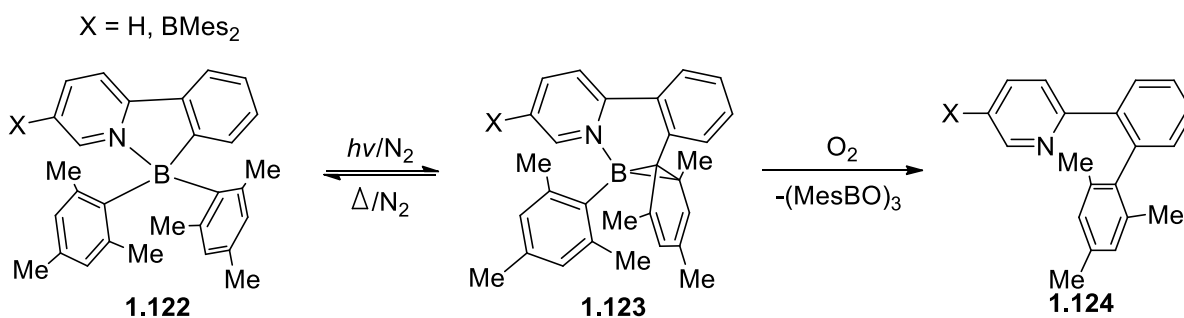
Figure 1-19 Early work on N,O-chelating and N,N-chelating azaborines.



In 2008, the Wang group discovered a reversible intramolecular C-C bond formation/breaking process involving a tetrahedral boron center that is accompanied by distinct color switching (**Scheme 1-17**).¹⁵¹ When irradiated by UV light (365 nm) under N₂, **1.123** was formed from **1.122** accompanied by a rapid loss of fluorescence and a shift from colorless to olive green or navy blue, depending on the exact isomer. Noticeable changes in UV-Vis and NMR spectra correlated with the reaction progress. Supported by DFT calculations, **1.123** was initially proposed to contain the borabicyclo[4.1.0]hepta-2,4-diene structure, where a C-C bond is formed between the phenyl and one of the mesityl groups. This hypothesis was subsequently confirmed through an X-ray crystal structure of an analogue based on the

pyridyl-indolyl chelating ligand.¹⁵² Remarkably, **1.123** exhibits photochromic behavior as it readily reverts back to the parent compounds **1.122** in quantitative conversion after heating in C₆D₆. The thermal reversibility of **1.123** was unprecedented and believed to be facilitated by the chelating scaffold holding the boron center and aryl groups in fixed positions.

Scheme 1-17 Isomerisation pathways of photochromic N,C-chelating organoboron compounds.

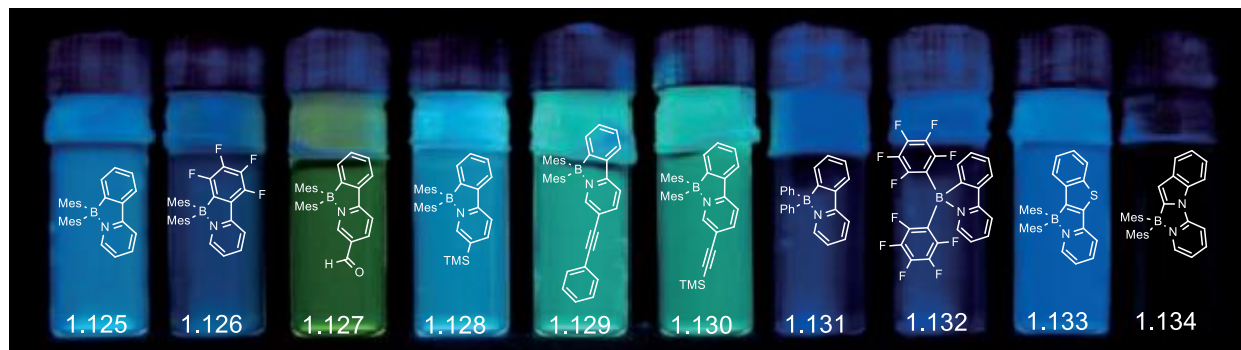


It was necessary to understand the various factors that influence the photochemical stability and photochromic switching behaviour for this class of N,C-chelate boryl systems both from a fundamental perspective as well as for their potential future application as OLEDs. Over the next decade, by pursuing new synthetic directions and probing fundamental assumptions, the Wang group have broadened the photoisomerization of the parent compound **1.122** that can be controlled, modified, stabilized or inhibited by introducing a variety of structural motifs that operate through a myriad of kinetic, electronic and steric factors.

In a comprehensive report, a variety of N,C-chelate boryl systems based on the 2-phenylpyridyl **1.125 – 1.132** (ppy), benzo[*b*]thiophenylpyridine **1.133** and indolylpyridine **1.134** chelating ligands and mesityl or phenyl substituent on the boron center were synthesized and systematically investigated by the Wang group (**Figure 1-20**).¹⁵³ It was discovered that the mesityl substituent plays a significant role in affecting low energy charge-transfer transition from the mesityl groups to the chelating ligands

stemming from its steric congestion and electron donating properties. In sharp contrast, boryl centers bearing phenyl substituent **1.131** do not exhibit photochromic behavior. The electron-donating and electron with-drawing groups were found to have a distinct impact on the photoisomerization rate and the photochemical stability of the molecules, with the former increasing and the latter reducing the overall rate of photo-conversion.¹⁵³ In a subsequent study, the mechanism for the photoisomerization process was elucidated to proceed via photoactive triplet states, which implicate the potential for modulating photoreactivity by introducing triplet sensitizers or acceptors onto the chelate backbone.¹⁵⁴ Furthermore, unprecedented multistructural transformations extending beyond the simple formation of isomer **1.123** was observed in the case of 2-phenylbenzothiazolyl, 2-phenyl 4-methylthiazolyl, 2-phenylbenzoxazolyl, 2-phenylbenzimidazolyl as chelating ligands. In these systems, the formation of isomer **1.123** upon photoexcitation was followed by thermal intramolecular H-atom transfer, azole ring reductions and further ring expansions to generate novel azaborine derivatives.¹⁵⁵

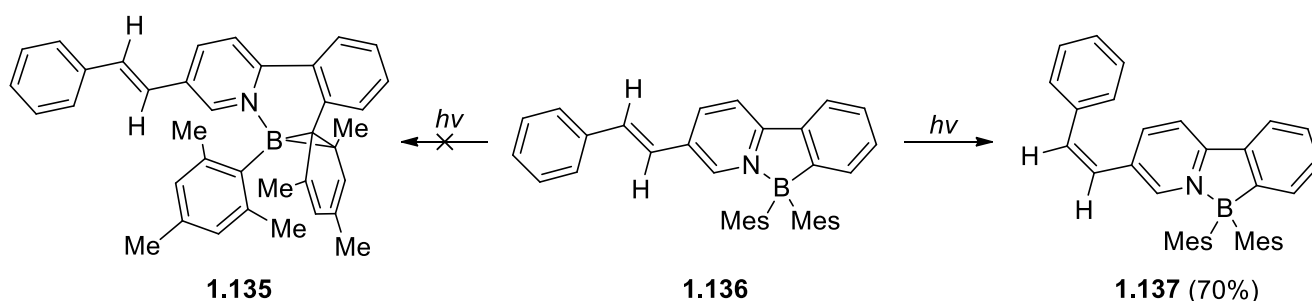
Figure 1-20 Visible fluorescence from N,C-chelating organoboron compounds.



Extension of π -conjugation in the chelating ligand using vinyl or acetylene linkers was found to introduce photostability to the parent isomer **1.136** under UV radiation, which instead of forming isomer **1.135**, undergoes *cis-trans* isomerization **1.137** and completely inhibits the photo-switching process (**Scheme 1-18**).¹⁵⁶ Time-dependent density functional theory (TD-DFT) computations probing the mechanism of this photo-excitation established that the presence of an olefinic bond provides an

alternate energy dissipation pathway for this series of substrates, hence stabilizing them towards photochromic switching. An alternative method using a dithienyl unit conjugated with the chelate backbone was also effective at disrupting photo-switching in this class of N,C-chelate boryl compounds. Other transition metals (Au(I), Pt(II), Re(I)) attached to the chelating ligand through an acetylene linker were shown to similarly inhibit or reduce photoisomerization in the parent chromophore **1.123**.

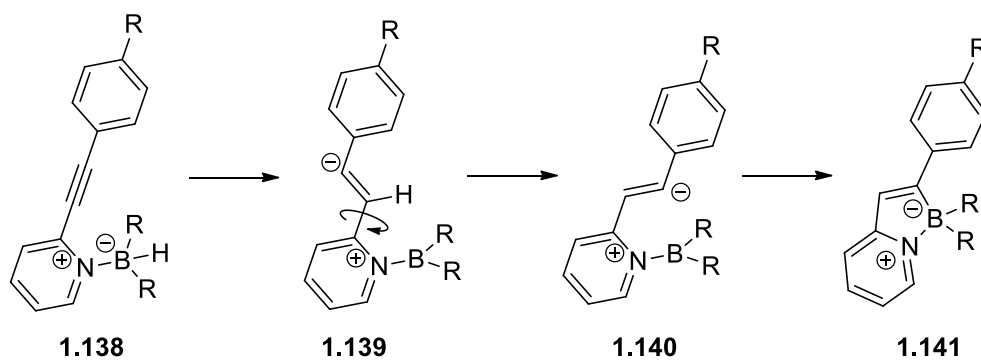
Scheme 1-18 Inhibition of photoisomerization in N,C-chelating organoborons.



To study the impact of incorporating multiple photochromic boron centers, Wang synthesized a series of π -conjugated N,C-chelate boryl systems based on the parent chromophore **1.123** in the forms of dimers, trimers and hexamers, and subjected them to the same photo-excitation under UV light. The Wang group discovered that the isomerization of one chromophore prevents the isomerization of others, which leads to amplified and reversible fluorescence quenching of the entire molecule. It was postulated that upon photo-excitation, photo-switching at a single boryl will be significantly faster than the simultaneous switching at multiple boryl centers due to substantial structural rearrangements, hence making it kinetically favored. Once a monoisomerized product is formed, the energy of its excited state can be dissipated by fast intramolecular energy transfer in accordance with Kasha's rule, effectively preventing any further isomerization.¹⁵⁷ This property may prove beneficial in organic charge-transport materials or transistors where the integrity of the conjugated system is important.¹⁵⁸ Non-conjugated silyl-bridged linkers were shown to achieve the same effect.¹⁵⁹

In a 2016 paper, Wang disclosed the synthesis for a new class of N,C-chelating organoborons through *trans*-hydroboration of internal alkynes at room temperature with 9-BBN, producing five-membered BN-heterocycles **1.141** (**Scheme 1-19**).¹⁶⁰ The mechanistic rationale supported by DFT calculations proposes the formation of a Lewis adduct **1.138** upon mixing of the substrate with borane, which then proceeds with a hydride migration from the borane to the *sp*-hybridized carbon of the acetylene unit to give **1.139**. Finally, rotation about the vinylpyridine C-C single bond and ring closure affords the *trans* product **1.141**.

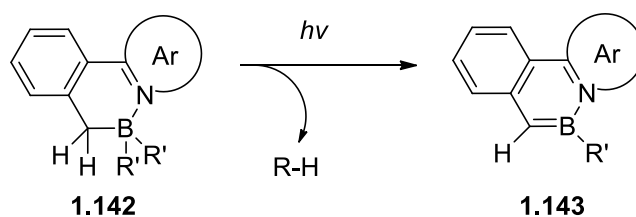
Scheme 1-19 Synthesis of N,C-chelating organoborons through *trans*-hydroboration of internal alkynes.



1.3.4 Recently Synthesized Azaborines

A breakthrough in 2013 marked the beginning of Wang's synthesis of azaborines **1.143** through highly unusual photoelimination pathway that involves the breakage of a C-H bond and of a B-C bond from a four-coordinate chelated organoboron compound **1.142** (Scheme 1-20).¹⁶¹ This process appears to be a generic reaction that works for this type of B, N-heterocyclic compounds. The R' groups may be alkyl or aryl and the N heterocycle can be either a pyridyl or a benzothiazolyl. Under UV irradiation at 300 nm in dry toluene or benzene under nitrogen atmosphere, it was observed that the solutions readily changed from colorless to bright yellow. The photoelimination reaction also occurs readily in the solid state with polymer films such poly-methylmethacrylate (PMMA) or poly-N-vinylcarbazole (PVK).

Scheme 1-20 Formation of azaborines through photoelimination of four-coordinate chelated organoboron compounds.



The course of the reaction shown in **Scheme 1-20** was monitored spectroscopically, and a new absorption band appeared in the 360-520 nm region of the UV/Vis spectra that increased in intensity with longer irradiation time, correlating with the color change. The reactions were monitored by ¹H and ¹¹B NMR spectroscopy, and changes were observed in the chemical shift and integration of the methylene protons, and the ¹¹B chemical shifts further downfield as the tetrahedral sp³ hybridized boron centers in the starting materials **1.142** adopt sp² hybridization in the final products **1.143**. The final azaborine product **1.148** as shown in **Scheme 1-21** constitute previously unknown isomers of B,N phenanthrene.¹⁶² They were stable as solids but slowly degrade upon exposure to air. Unlike their non-

emissive precursors **1.145** - **1.147**, the azaborine products are fluorophores with bright green or yellow-green fluorescence emission, and reported as the brightest emitters among all known B,N phenanthrene compounds.

Scheme 1-21 Formation of azaborines through photoelimination reactions.

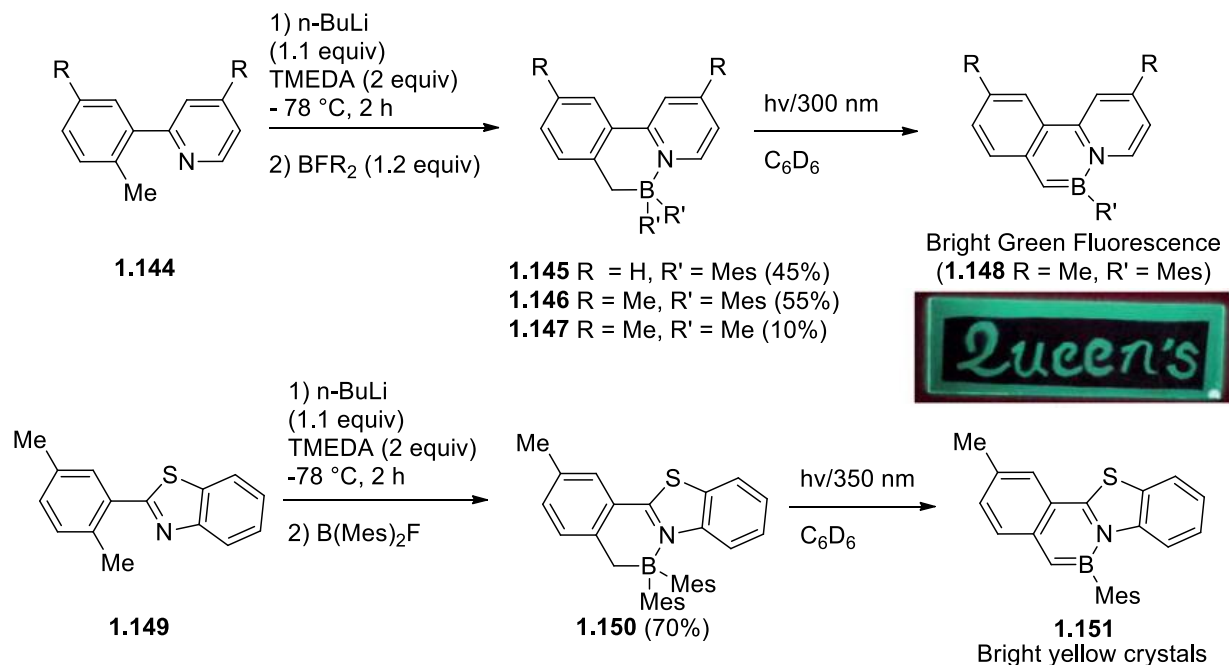
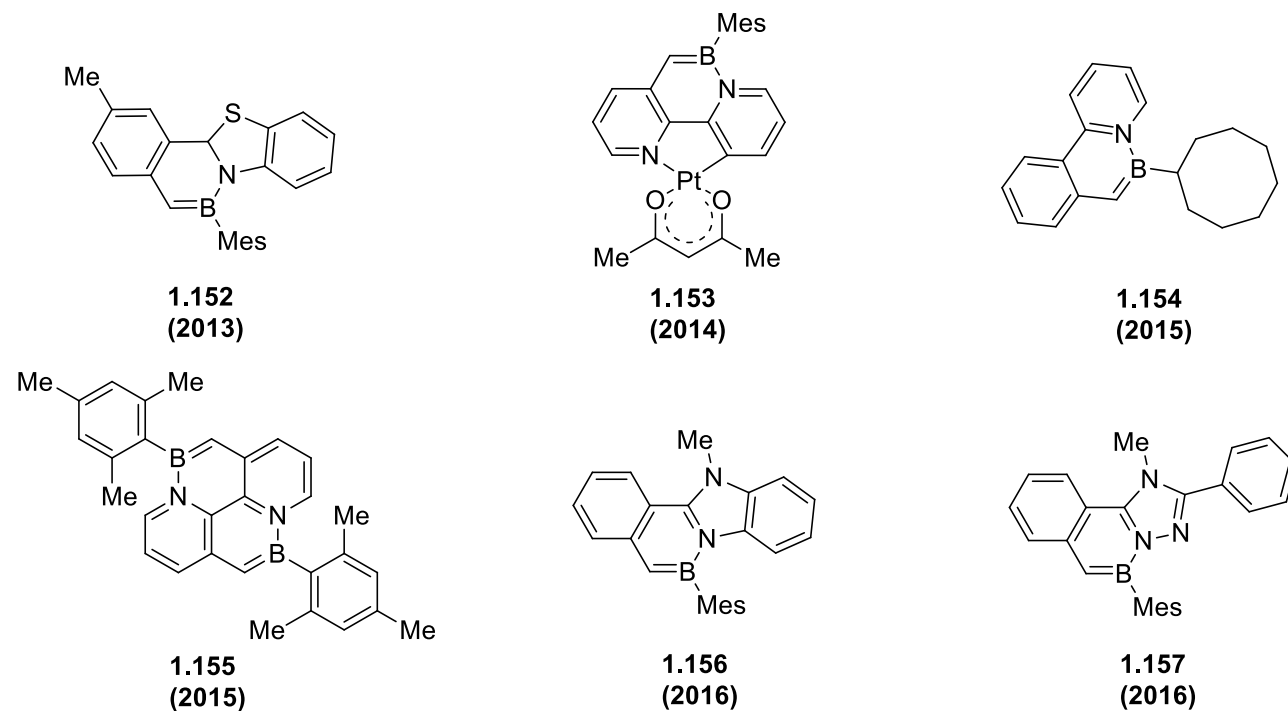
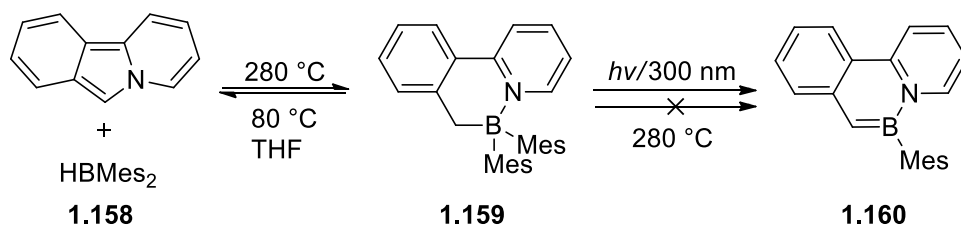


Figure 1-21 Examples of azaborine compounds.



Subsequent work in this area have focused on fine tuning the electronic and photo-luminescent properties of azaborines as well as developing new synthetic pathways for accessing these molecules. It was discovered that metal chelation with Pt(II) enhances the photoelimination quantum efficiency by two orders of magnitude and enables phosphorescence in the analogous B,N-benzoquinolines **1.153**.¹⁶³ Double photoelimination was observed to form fluorescent BN-pyrenes containing two B-N units (**1.155**).¹⁶⁴ In 2015, Wang expanded upon the original discovery by showing that pyrido[1,2-a]isoindole **1.158** readily undergoes a reversible 1,1-hydroboration reaction thermally with certain boranes to give the four-coordinate chelated organoboron compounds **1.159**, which subsequently proceeds through a photoelimination pathway to yield the final azaborine product **1.160** (Scheme 1-22).¹⁶⁵

Scheme 1-22 Reversible 1,1-hydroboration reaction towards N,C-chelated four coordinate organoborons.

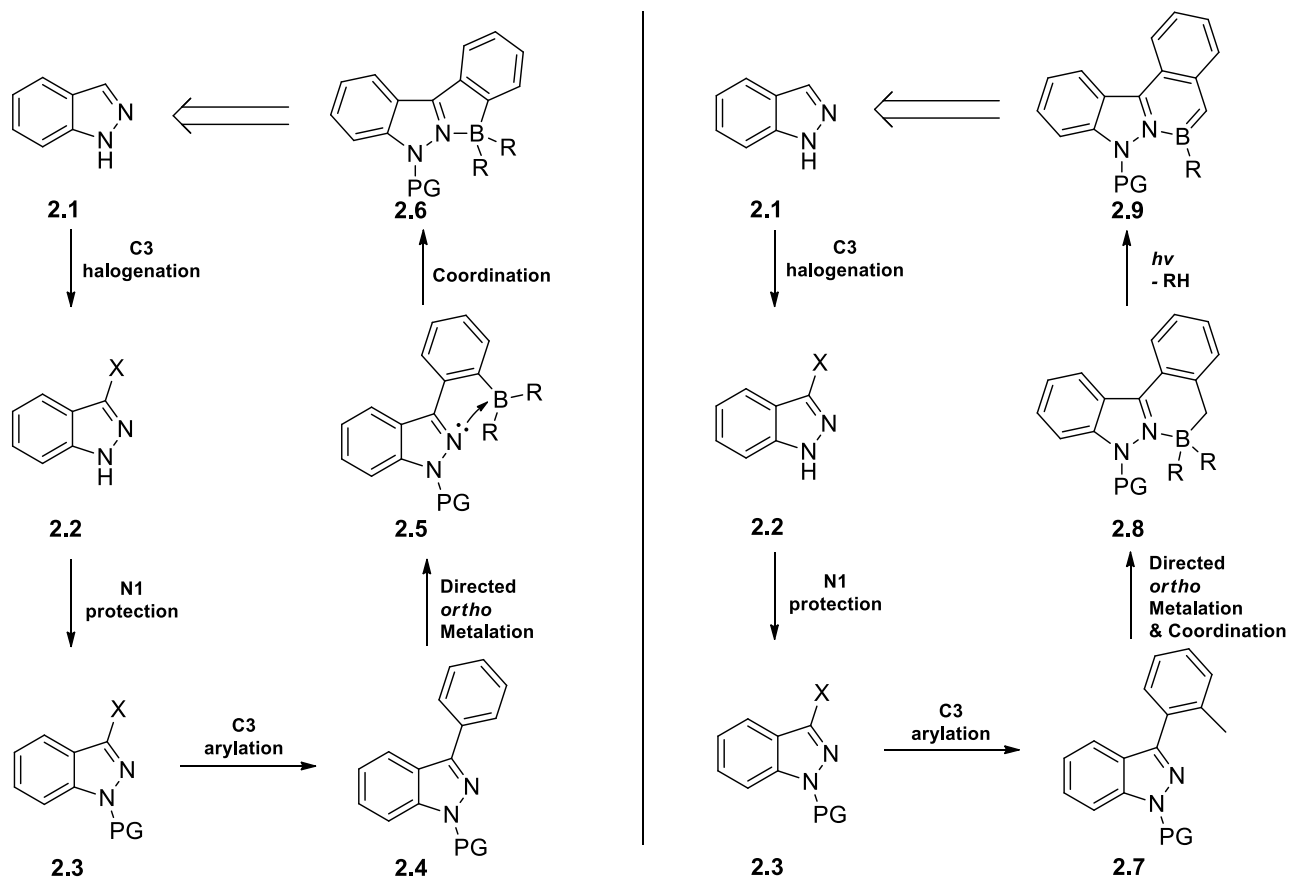


Chapter 2 Indazole Based Azaborines and the DoM Reaction of Indazoles

2.1 The DoM Approach towards Indazole-based Azaborines

2.1.1 Project Aims

Scheme 2-1 Proposed retro-synthetic pathway for targets 2.6 and 2.9.



Scheme 2-1 outlines the proposed retrosynthetic strategy towards target molecules **2.6** and **2.9**.

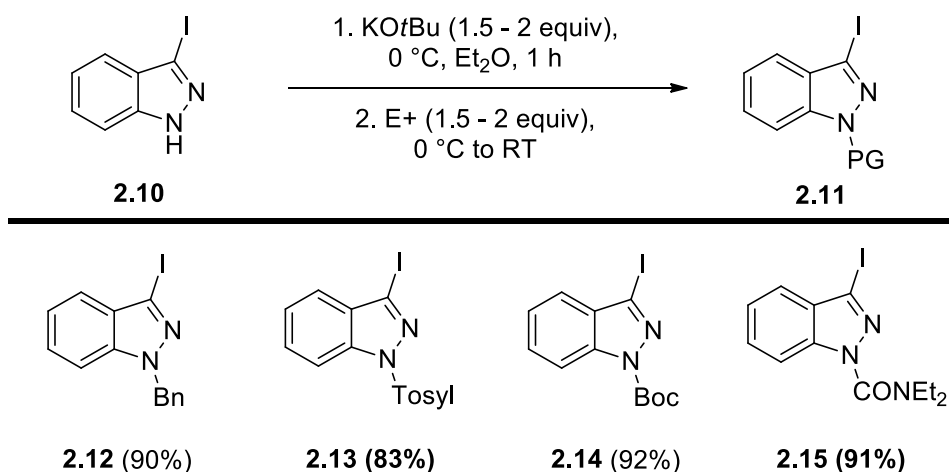
Both targets follow a similar pathway that involves C-3 iodination, N-1 protection, C-3 arylation, and the late stage DoM reactions. Target **2.6** serves as a proof of concept for N,C-chelating organoboron compounds based on the indazole heterocycle, which undergoes reaction through a direct coordination of N-2 to boron center. For target **2.9**, we envisage a photoelimination reaction pathway on compound **2.8** to afford the azaborine products. The efforts expended toward the synthesis of the final target

molecules constitute a methodological study into modern ways of functionalizing indazoles. In addition, the targets were chosen with the aims of expanding the library of known N,C-chelating organoboron and azaborine compounds, many of which possess unusual and highly desirable properties as outlined in the introductory section.

2.1.2 N-1 Protection of 3-Iodo-1H-indazole

Work started with commercially available 1H-indazole. By following a literature procedure for iodination,¹⁶⁶ 3-iodoindazole (**2.10**) was obtained in good yield. Next, N-1 protection was explored using potassium *tert*-butoxide as a base in a variety of solvents, and the best results in Et₂O are reported in **Scheme 2-2**. Potassium *tert*-butoxide (pK_aH ~ 17) was chosen as a readily available strong base that is capable of deprotonating the aforementioned position. Even though a variety of other bases such as carbonates, sodium hydride, and amides could also function in a similar capacity, it was advantageous to find a base whose conjugate acid is only slightly higher in pK_a value than that of the target. With the optimized conditions in hand, we were able to successfully incorporate benzyl (**2.12**, 90%), tosyl (**2.13**, 83%), Boc (**2.14**, 92%), and diethyl carbamoyl (**2.15**, 91%) as N-1 protecting groups (**Scheme 2-2**).

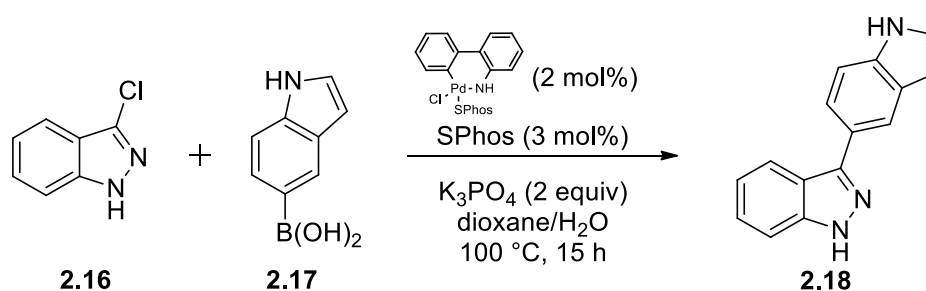
Scheme 2-2 N-1 protection of 3-Iodo-1H-indazole.



2.1.3 C-3 Functionalization of Indazoles via Suzuki-Miyaura Cross Coupling Reactions

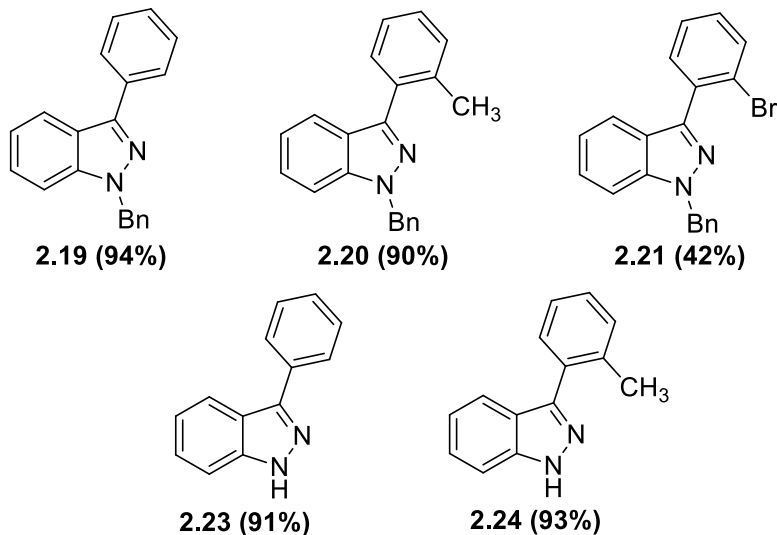
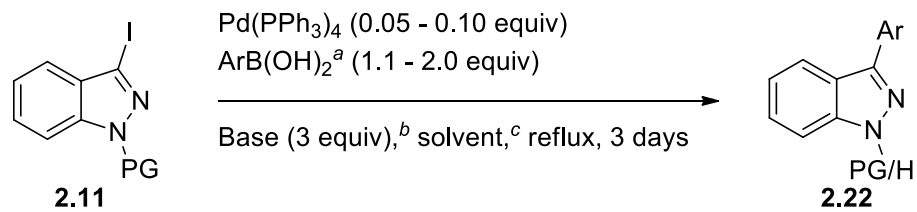
From retrosynthetic analysis, N-1 protection was recognized as a crucial step as the acidic N-H proton ($pK_a \sim 13.8$) will interfere with subsequent coupling reactions at the C-3 position under standard conditions.¹⁶⁷ A recent report had in fact disclosed of unprotected N-H indazoles undergoing Suzuki-Miyaura cross coupling reactions at the C-3 position.¹⁶⁸ However; this required an expensive and uncommon catalyst and ligand system (**Scheme 2-3**).

Scheme 2-3 Precedent for the Suzuki-Miyaura cross coupling reaction of 3-Chloro-1H-indazole.



With the desired protecting groups in place, work was begun to effect C-3 cross coupling reactions. In a 1999 paper, Rault *et al.* disclosed that the Suzuki-Miyaura reaction was successful in the reaction of compound **2.12** with a variety of aryl and hetero-aryl boronic acids.¹⁶⁷ The Rault procedure was followed with modifications extending the duration of the reaction time and using different base/solvent systems as appropriate. The isolated yield of product **2.19** (94%) obtained under the modified conditions was greater than that reported (72%).¹⁶⁷ Extension of this methodology to other aryl boronic acids successfully introduced *o*-tolyl (**2.20**) and 2-bromophenyl (**2.21**) at the C-3 position of N-benzyl indazoles (**Scheme 2-4**).

Scheme 2-4 The Suzuki-Miyaura cross coupling reaction of 3-iodo-1*H*-indazole.



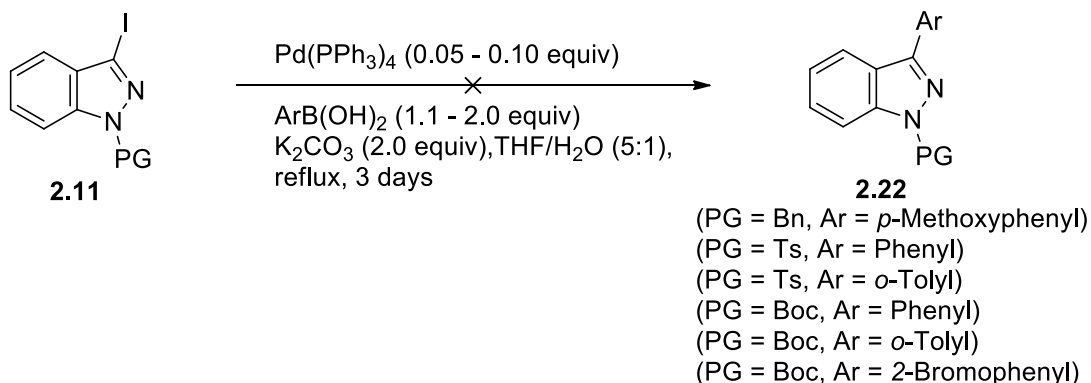
^aAr = phenyl in **2.19**, **2.23**; *o*-tolyl in **2.20**, **2.24**; 2-bromophenyl in **2.21**

^bNaHCO₃ in **2.19**, **2.20**; K₂CO₃ in **2.21**; Na₂CO₃ in **2.23**, **2.24**

^cToluene/EtOH/H₂O (20/1/4) in **2.19**; DME/H₂O (2/1) in **2.20**; THF/H₂O (1.2/1) in **2.21**;
 1,4-Dioxane/H₂O (4/1) in **2.23**, **2.24**

Extension of this methodology to N-Boc protected indazoles (**2.14**) was initially unsuccessful with either phenylboronic acid or *o*-tolylboronic acid using K₂CO₃ as a base and THF/H₂O (5:1) solvent mixtures, as were attempts to functionalize the C-3 position of N-tosyl protected indazoles (**2.13**) under reported conditions (**Scheme 2-5**). However, changing the base and solvent systems to Na₂CO₃ and 1,4-dioxane/H₂O (4/1) respectively resulted in the *in-situ* loss of the Boc group to furnish N-H C-3 aryl functionalized indazoles (**2.23**, **2.24**) in very good yields (**Scheme 2-4**).

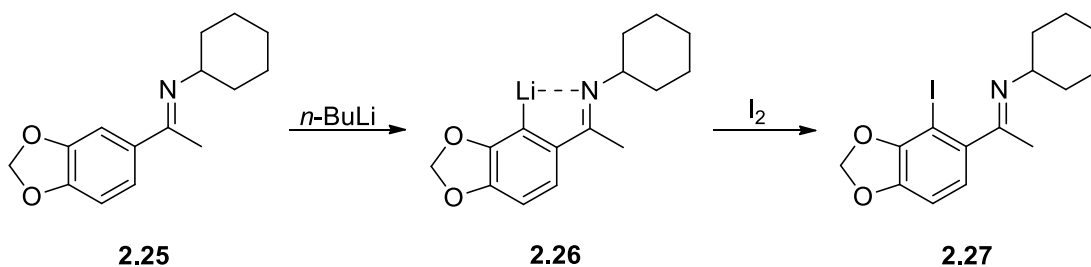
Scheme 2-5 Unsuccessful Suzuki-Miyaura cross coupling of N-1 protected 3-Iodo-1H-indazoles.



2.1.4 Directed *ortho* Metalation of N-Benzyl 3-Aryl Indazoles

With the desired starting molecules **2.19** and **2.20** now available, DoM reactions were attempted on these substrates in the hope of accessing the remote *ortho* positions on the C-3 aryl groups. While many different types of functional groups were previously identified as potential DMGs for DoM reactions as outlined in the introduction **1.2.2 The DoM Reaction: Directed Metalation Groups (DMGs)**, we did not find any literature precedent for using indazoles or pyrazoles as a directing group. The closest analogy upon which to base the precedent would be that of Ziegler and Fowler's work in achieving *ortho* lithiation of piperonal cyclohexylimine¹⁶⁹ (**Scheme 2-6**).

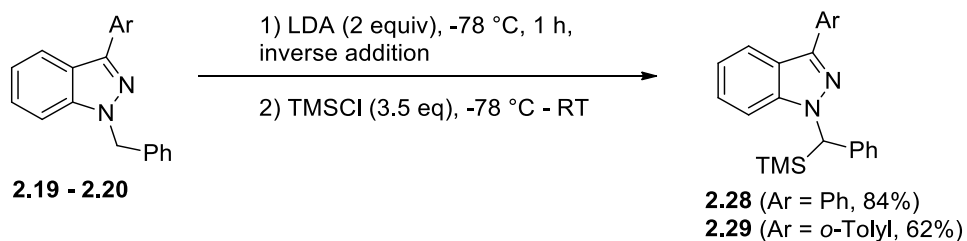
Scheme 2-6 Ziegler and Fowler's *ortho* lithiation of piperonal cyclohexylimine.



An extensive review on DoM reactions by Snieckus¹⁷⁰ identified *s*-BuLi in combination with TMEDA as a potent and effective lithiation reagent. Our initial attempts following these conditions

resulted only in the recovery of starting materials, and the unsuccessful reaction was attributed to trace amounts of moisture in the reaction vessel. The experiment was repeated with care for stringent anhydrous conditions and a new result was obtained as shown in **Scheme 2-7**:

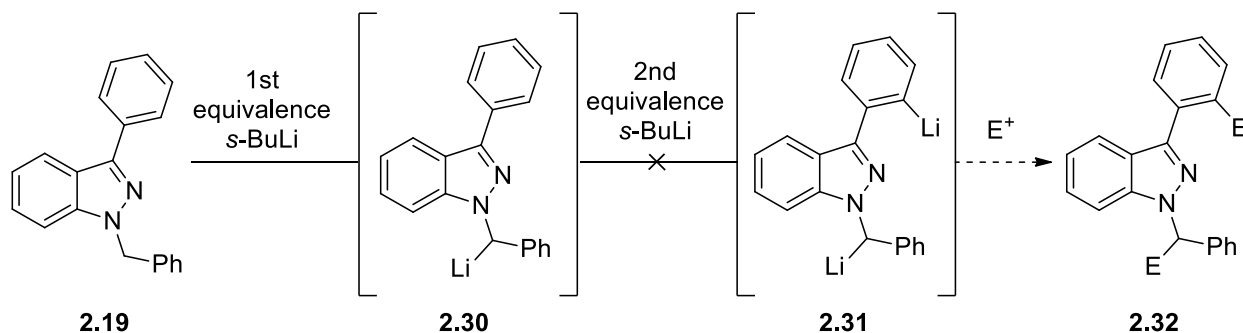
Scheme 2-7 The DoM reaction of N-benzyl 3-aryl indazoles.



The same products (**2.28**, **2.29**) were obtained with *s*-BuLi/TMEDA as the base/ligand combination and yields of the respective products were within 10% of that obtained under LDA conditions. ¹H NMR spectra shows the incorporation of the TMS group in the products with a characteristic up-field singlet integrating for nine protons. In the aromatic region, signals found between the 7.0 and 8.0 ppm window integrate for fourteen protons as expected. The most revealing change is that of the singlet peak located near 5 ppm belonging to the benzyl protecting group as its integration had reduced from two protons in the starting material to one in the product. In the case of **2.29**, the *o*-tolyl methyl group remains at 2.48 ppm and integrates for three protons as it had in the starting material **2.20**. This suggests that the site of deprotonation and subsequent electrophile quench with TMSCl had occurred on the N-1 benzyl protecting group instead of the remote *ortho* positions on the 3-aryl groups. This result falls within our expectations as the N-1 substituted benzyl position can be deemed to be the most acidic position, hence the most thermodynamically favored site for lithiation. Subsequent attempts reducing the duration of DoM reactions from 1 hour to 15 minutes resulted only in similar yields for products **2.28** (80%) and **2.29** (66%). Additional equivalents of base (3 equiv) were added in subsequent experiments with the hopes of facilitating the generation of lithio-dianions (**2.31**)

on both the benzyl position and the remote *ortho* positions (**Scheme 2-8**), but the reaction did not proceed as hypothesized.

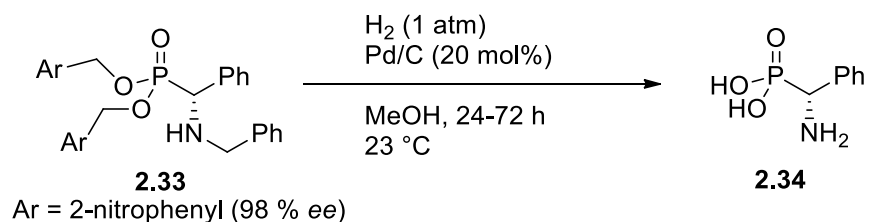
Scheme 2-8 Unsuccessful generation of lithio-dianion.



2.1.5 Debenzylation Attempts

Although useful in their purpose as a protecting group during the Suzuki-Miyaura cross coupling stage, the N-1 benzyl protecting group of **2.19** and **2.20** now becomes a hindrance for the subsequent DoM reactions step, therefore justifying for their removal. The cleavage of benzyl protecting groups may be accomplished via hydrogenolysis over a transition metal catalyst, such as palladium. One such example demonstrates the viability of this methodology for the enantioselective reduction of benzyl amines (**Scheme 2-9**).¹⁷¹

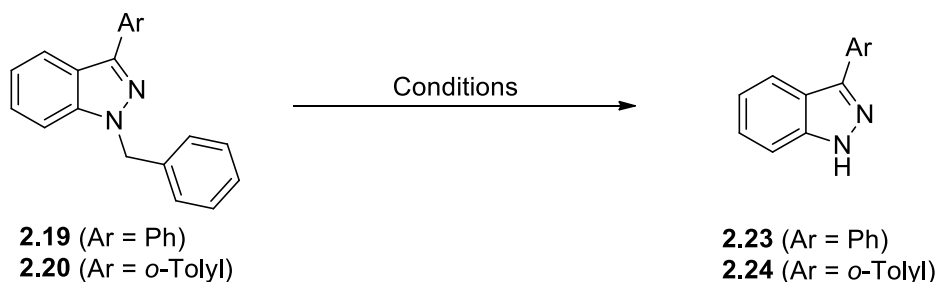
Scheme 2-9 Enantioselective reduction of benzyl amines.



Given the precedent reported in **Scheme 2-9**, this general reductive technique was attempted under a variety of conditions for molecules **2.19** & **2.20** albeit with little success (**Table 2-1**). In a majority

of cases, no conversion was observed and only starting materials were recovered. Acidic conditions appear to facilitate the process notwithstanding the low yield (entry 6). Eventual success was achieved by following literature precedent using potassium *tert*-butoxide in DMSO under oxygen¹⁷², which afforded the products **2.23** and **2.24** in very good yields (entries 8 & 12).

Table 2-1 Optimization studies for N-1 debenzyltion reactions of substituted indazoles.

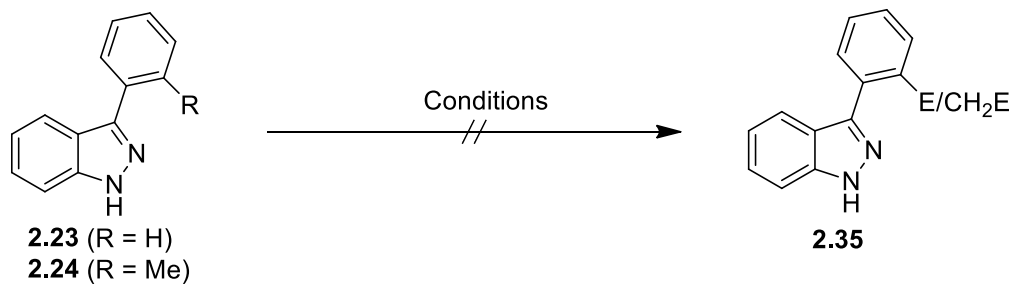


Entry	Starting Materials	Conditions	Yield
1	2.19	H ₂ (1 atm), Pt/C (10 mol %), EtOH, 24 h	No conversion
2	"	H ₂ (1 atm), Pt/C (10 mol %), 60°C, EtOH, 24 h	"
3	"	H ₂ (1 atm), Pd/C (10 mol %), EtOH, 24 h	"
4	"	H ₂ (1 atm), Pd/C (10 mol %), CH ₃ COOH (0.1 equiv), EtOH	"
5	"	NH ₄ HCO ₂ (10 equiv), Pd/C (10 mol %), EtOH	"
6	"	H ₂ (1 atm), Pd/C (10 mol %), Formic acid (0.1 equiv), MeOH	2.23 (3 %)
7	"	KOtBu (3 equiv), O ₂ , DMSO, 6 h	2.23 (21 %)
8	2.19	KOtBu (6 equiv), O₂, DMSO, 24 h	2.23 (90 %)
9	2.20	H ₂ (1 atm), Pt/C (10 mol %), EtOH, 24 h	No conversion
10	"	H ₂ (1 atm), Pt/C (10 mol %), 60°C, EtOH, 24 h	"
11	"	KOtBu (3 equiv), O ₂ , DMSO, 8 h	2.24 (86 %)
12	2.20	KOtBu (6 equiv), O₂, DMSO, 24 h	2.24 (91 %)

2.1.6 DoM of N-H 3-Aryl Indazoles

Successful removal of the benzyl protecting groups furnishes N-H substituted indazoles for subsequent experiments. The DoM reactions were attempted on both C-3 phenyl (**2.23**) and C-3 *o*-tolyl (**2.24**) N-H indazoles under 3 equivalents of *s*-BuLi and TMEDA combination for 1 h at -78 °C, and immediately subjected to electrophilic quench under an excess of TMSCl (4 equiv). We initially anticipate for the quantitative deprotonation of the N-H acidic proton upon base addition, and it was hoped that the excess of alkyl-lithiums will subsequently afford C-3 phenyl as well as C-3 *o*-tolyl deprotonations, and the site will be directed *ortho* to the indazole N-2 nitrogen. This hypothesis necessitates the formation of a lithio-dianion intermediate that will subsequently afford the desired products upon quench by the appropriate electrophiles. The initial attempts were unsuccessful with only starting materials recovered from the reaction mixture. Other bases such as *t*-BuLi and LiTMP were also utilized in an effort to affect *ortho*-lithiation but to no avail.

Table 2-2 Unsuccessful *ortho* lithiation of N-H unprotected 3-aryl indazoles.

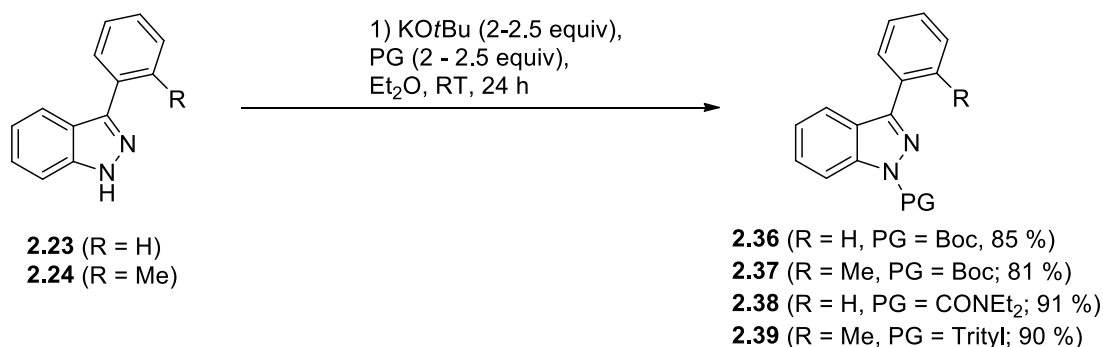


Entry	Starting Materials	Conditions
1	2.23 & 2.24	1) <i>s</i> -BuLi (3 equiv), TMEDA (3 equiv), - 78 °C, 1 h (inverse) 2) TMSCl (4 equiv), - 78 °C – RT
2	“	1) <i>s</i> -BuLi (5 equiv), TMEDA (5 equiv), - 78 °C, 1 h (inverse) 2) TMSCl (10 equiv), - 78 °C – RT
3	“	1) LiTMP (5 equiv), TMSCl (5 equiv), - 78 °C, 1 h (Martin)
4	“	1) <i>t</i> -BuLi (5 equiv), TMEDA (5 equiv), - 78 °C, 1 h 2) TMSCl (6 equiv), 1 h
5	“	1) <i>t</i> -BuLi (5 equiv), TMEDA (5 equiv), - 78 °C, 1 h 2) CO ₂ (excess), - 78 °C – RT
6	“	1) <i>t</i> -BuLi (5 equiv), TMEDA (5 equiv), - 40 °C, 1 h 2) <i>d</i> ₄ -MeOH (6 equiv), - 40 °C - RT

2.1.7 DoM of N-1 Protected 3-Aryl Indazoles

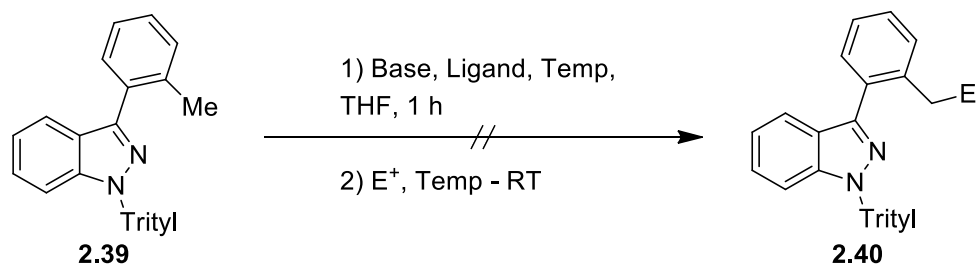
Due to unsuccessful results functionalizing N-H unprotected indazoles under DoM conditions, our attention turns to functionalizing the N-1 position of 3-aryl indazoles. The strategy aims to introduce alkyl-lithium inert protecting groups that would also permit for their facile removal under mild conditions. To that end, we functionalized molecule **2.23** with *tert*-butoyloxycarbonyl (Boc), and N,N-diethylcarbamoyl groups and molecule **2.24** with Boc and triphenylmethyl (trityl) protecting groups (Scheme 2-10).

Scheme 2-10 N-1 protection of 3-aryl indazoles.



DoM reactions with this subset of molecules were attempted. Upon treatment with *t*-BuLi (1.5 equiv) under cryogenic conditions (-78 °C, THF, 1 h) followed by quench with 2 equivalents of TMSCl, the Boc derivative **2.36** gave 25 % of **2.23** resulting from Boc cleavage, and the rest remained as starting material **2.36**. Switching to the sterically encumbered base lithium 2,2,6,6-tetramethylpiperidine (LiTMP) eliminated this side reaction completely but metalation was not achieved as evidenced by recovery of starting material **2.36** (88 %). Similar results were observed with **2.37** (82 %) under identical reaction conditions. Detailed investigation of DoM reactions of the trityl derivative **2.39** was then undertaken and the results are reported **Table 2-3**.

Table 2-3 Unsuccessful Directed *ortho* Metalation of N-trityl 3-*ortho*-tolyl indazole.



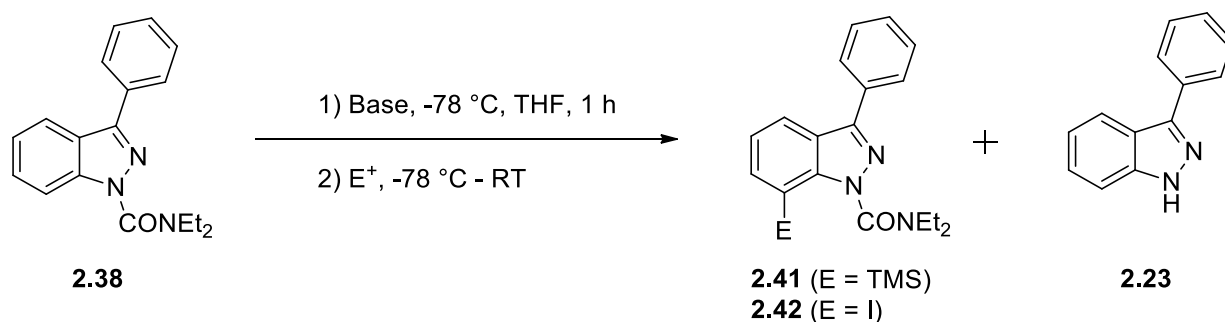
Entry	Base & Ligand	Temp (°C)	E ⁺	recovery of 2.39 ^a
1	<i>n</i> -BuLi (3 equiv), TMEDA (3 equiv)	-78	TMSCl (3 equiv)	89 %
2	<i>n</i> -BuLi (4 equiv), TMEDA (4 equiv)	0	TMSCl (4 equiv)	86 %
3	"	"	<i>d</i> 4-MeOH (4 equiv)	"
4	<i>s</i> -BuLi (3 equiv), TMEDA (3 equiv)	-78	TMSCl (3 equiv)	83 %
5	<i>s</i> -BuLi (4 equiv), TMEDA (4 equiv)	0	TMSCl (4 equiv)	89 %
6	"	"	<i>d</i> 4-MeOH (4 equiv)	91 %
7	<i>t</i> -BuLi (3 equiv), TMEDA (3 equiv)	-78	TMSCl (3 equiv)	82 %
8	<i>t</i> -BuLi (4 equiv), TMEDA (4 equiv)	0	TMSCl (4 equiv)	79 %
9	"	"	<i>d</i> 4-MeOH (4 equiv)	82 %
10	LDA (3 equiv)	-78	TMSCl (3 equiv)	91 %
11	LDA (4 equiv)	0	TMSCl (4 equiv)	90 %
12	"	"	<i>d</i> 4-MeOH (4 equiv)	92 %

^aYields of isolated products after column chromatography

Positive results were obtained upon treatment of molecule **2.38** under DoM conditions (Table 2-4). Using LiTMP as a base, we were able to regioselectively functionalize the C-7 position of indazoles with trimethylsilyl (TMS) using the corresponding trimethylsilyl chloride (TMSCl) as the electrophile. Entries 3 to 5 details the gradual improvement in isolated yield of product **2.41** as LiTMP was increased

from 3.0 to 4.0 equivalence. As detailed in 1.2.2 The DoM Reaction: Directed Metalation Groups (DMGs), N,N-diethylcarbamoyl group is an effective and potent DMG commonly utilized to direct *ortho*-lithiation on a variety of substrates. Although compound **2.38** (Table 2-4) has two potential DoM sites, the C-2' and C-7 for favorable 5-membered ring chelated intermediate formation, previous work on azaindoles¹⁷³ and benzimidazoles¹⁷⁴ provided precedent for C-7 metalation. The preliminary results require work in optimization and generalization to provide a valuable methodology for the difficult to obtain 7-substituted indazoles.

Table 2-4 Directed *ortho* Metalation of N-diethylcarbamoyl 3-phenyl indazoles.



Entry	Base	E^+	Yields ^a
1	<i>t</i> -BuLi (1.5 equiv)	TMSCl (2.5 equiv)	2.23 (15%), 2.38 (61%)
2	<i>t</i> -BuLi (3.0 equiv)	TMSCl (5 equiv)	2.23 (29%), 2.38 (30%), 2.41 (10%)
3	LiTMP (3.0 equiv, inverse)	"	2.38 (32%), 2.41 (57%)
4	LiTMP (3.5 equiv, inverse)	"	2.38 (33 %), 2.41 (58 %)
5	LiTMP (4.0 equiv)	"	2.38 (24 %), 2.41 (70 %)
6	LiTMP (3.0 equiv, inverse)	I ₂ (3.5 equiv)	2.38 (52 %), 2.42 (44 %)
7	LiTMP (3.0 equiv, inverse)	CO ₂ (excess)	No conversion, 2.38 (79 %)

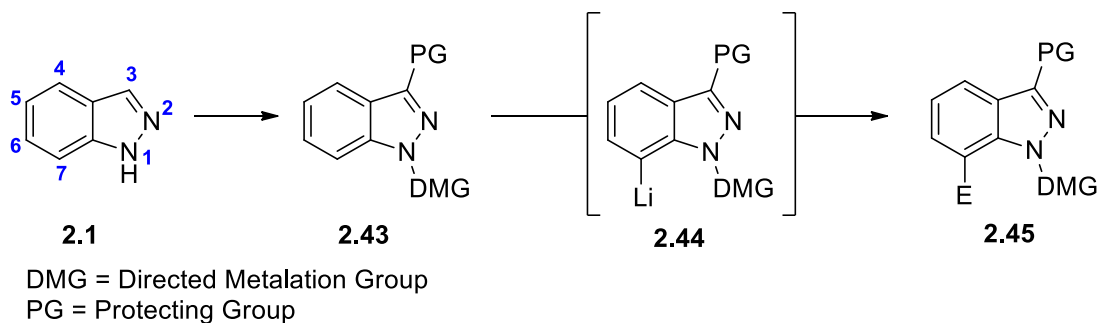
^aYields of isolated products after column chromatography

2.2 C-7 Functionalization of Substituted Indazoles

2.2.1 Project Aims

We were pleased by the relative efficiency and high regio-selectivity of C-7 activation of indazoles using DoM chemistry (Table 2-4). Given the difficulties in accessing this position through traditional methodologies, we aim to expand upon our preliminary results and further develop the DoM approach towards C-7 substituted indazoles which are of great interests to medicinal chemists. Our approach involves attempts to effect the directed *ortho* metalation (DoM) reactions on C-3 protected indazoles bearing N-directed metalation groups (DMG) to obtain the C-7 deprotonated species, which by quench reactions with various electrophiles would lead to 7-substituted 1*H*-indazoles, and thereby facilitate the development of a new general route to these derivatives.

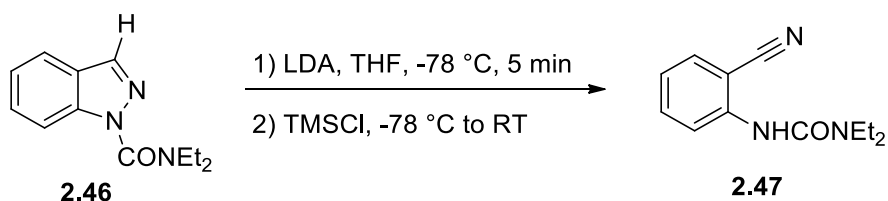
Scheme 2-11 C-7 Activation of substituted indazoles via DoM chemistry.



2.2.2 C-3 Protection of 1*H*-Indazole

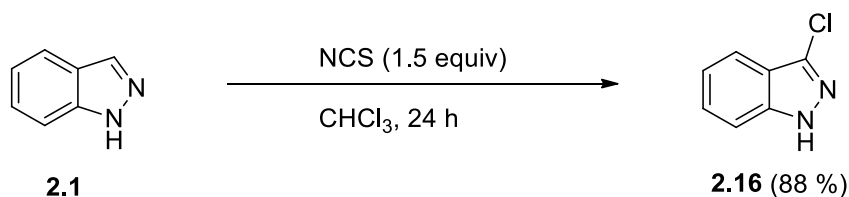
Previous results from the Snieckus lab reported that without C-3 protection, 1*H*-indazole undergoes deprotonation and subsequent ring opening to form di-substituted aryl derivatives **2.47**, as shown in **Scheme 2-12**.

Scheme 2-12 Base-mediated ring opening of unprotected indazoles.



Mechanistic studies probing the nature of metal-halogen exchange reactions have identified chloride as a suitable protecting group towards alkyl-lithium bases.¹⁷⁵ Upon treatment with *N*-chlorosuccinimide (NCS), we obtained 3-chloro-1*H*-indazole in good yield (**Scheme 2-13**).

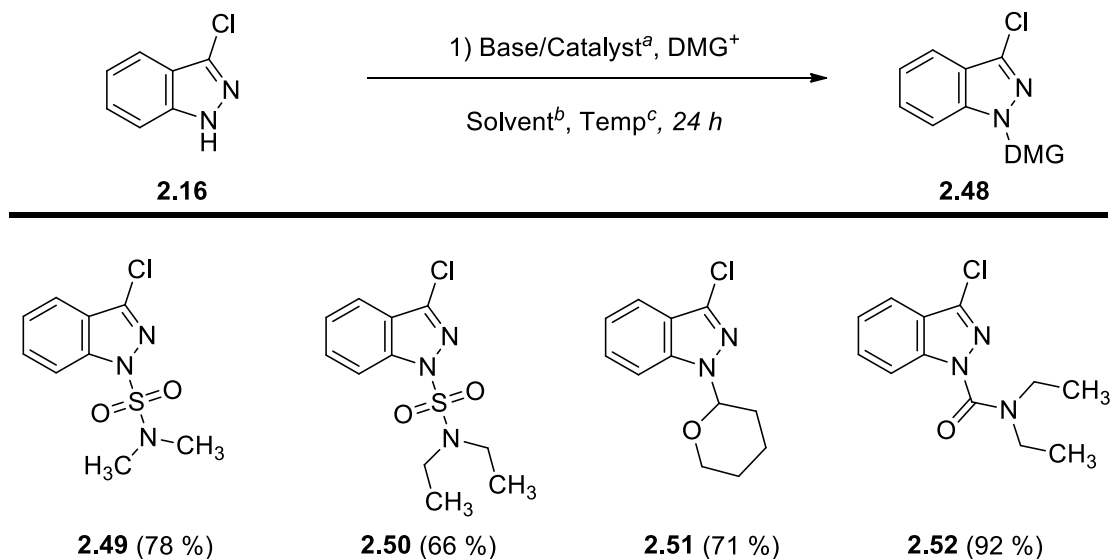
Scheme 2-13 Synthesis of 3-chloro-1*H*-indazole.



2.2.3 N-1 Functionalization of 3-chloro-1H-Indazole

Base mediated deprotonation and nucleophilic addition of 3-chloro-1H-indazole to the electrophilic form of several directing groups affords N-1 substituted 3-chloro-1H-indazoles in good yields.

Scheme 2-14 N-1 functionalization of 3-chloro-1H-indazole.



^aDABCO (1.1 equiv) in **2.49**, **2.50**; PPTS (0.01 equiv) as catalyst in **2.51**; K₂CO₃ (2 equiv) in **2.52**

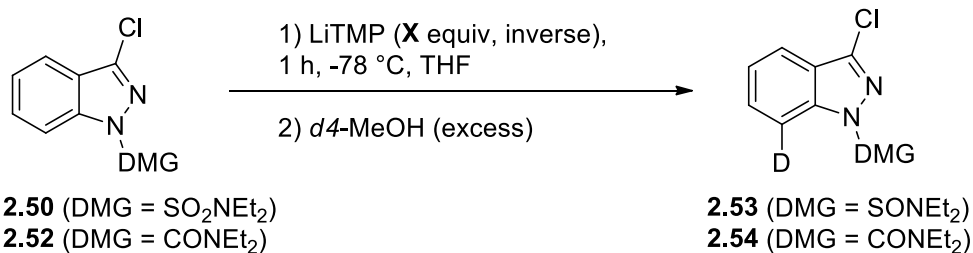
^bAcetonitrile in **2.49**, **2.50**, **2.52**; CH₂Cl₂ in **2.51**

^cRT in **2.49**, **2.50**; Reflux in **2.51**; 50 °C in **2.52**

2.2.4 Optimizing C-7 DoM Reaction Conditions

Preliminary attempts to direct C-7 lithiation of **2.49** and **2.51** using *n*-BuLi and TMEDA combination was unsuccessful, presumably attributed to relative weak directing abilities of the *N,N*-dimethylsulfonamide and tetrahydropyran (THP) groups. Encouragingly, **2.50** and **2.52** bearing *N,N*-diethylsulfonamide and *N,N*-diethylcarboxamide directing groups enabled the selective activation of the C-7 position on indazole derivatives using DoM reactions. Condition optimizations were conducted using LiTMP as the base and upon generation of the C-7 lithiated species for 1 hour at -78 °C in THF, it is quenched using *d*₄-MeOH as the electrophile, and effectively replacing the proton with deuterium for the purpose of determining reaction conversions (**Table 2-5**).

Table 2-5 Condition optimization studies on C-7 metalation of substituted indazoles.



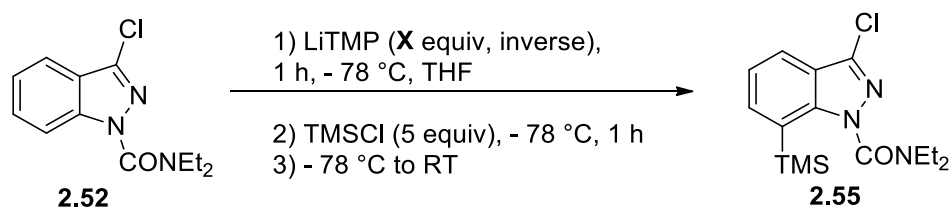
Entry ^a	Starting Material	X	Deuteration (%) ^b
1	2.50	2.0	66
2	"	2.0	73
3	"	2.0	63
4	"	3.0	65
5	"	3.0	79
6	"	5.0	80
7	"	5.0	78
8	"	8.0	79
9	2.52	1.5	22
10	"	1.5	9
11	"	2.0	76
12	"	3.0	76
13	"	3.0	87
14	"	5.0	84
15	"	5.0	90
16	"	8.0	97

^aAll reactions were performed at 0.1M concentration of starting material excess (greater than 10 equivalence) of electrophiles

^bDeuteration was determined by 400 Mhz ¹H NMR on the purified reaction mixture

While keeping the concentration of the starting materials **2.50** and **2.52** constant at 0.1 M, the trend from **Table 2-5** suggests that the level of deuterium incorporation for compounds **2.53** and **2.54** increases steadily as the equivalents of base increase. The observed increase of deuterium incorporation may be attributed to the increasing molarity of base in solution. Hence it may be possible to maintain the same percentage of deuteration with lower equivalents of base by reducing the overall volume of solution. We conducted additional reaction optimization experiments by substituting *d4*-MeOH with TMSCl as the electrophile instead, and the best result is highlighted in entry 6 (**Table 2-6**).

Table 2-6 Condition optimization studies on C-7 silylation of substituted indazoles.



Entry ^a	X	Yield (%) ^b
1	1.5	2.52 (21 %); 2.55 (56 %)
2	1.5	2.52 (49 %); 2.55 (45 %)
3	2.0	2.52 (8 %); 2.55 (82 %)
4	2.0	2.55 (90 %)
5	2.0	2.55 (89 %)
6	2.0	2.55 (92 %)
7	2.5	2.55 (92 %)

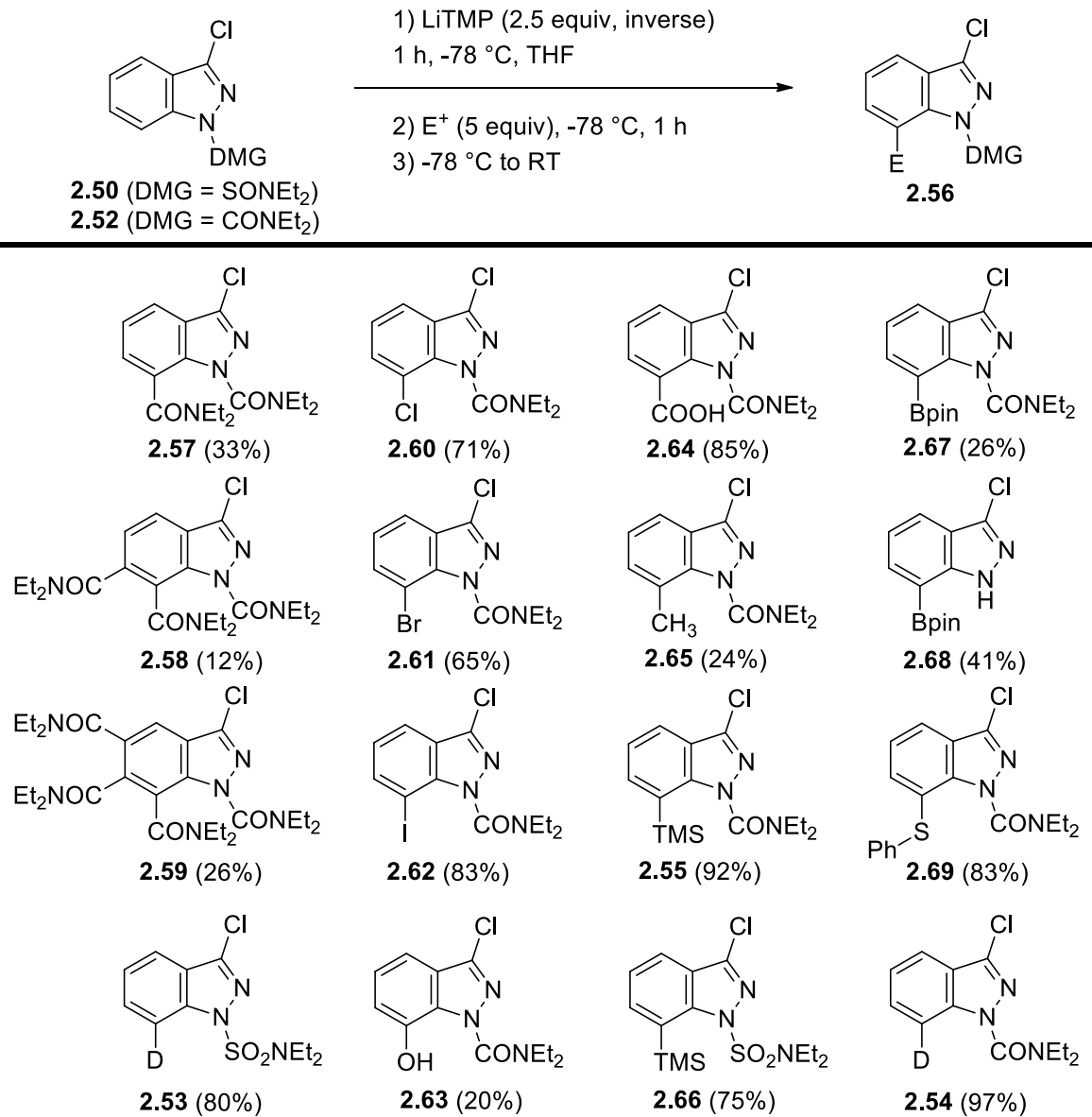
^aAll reactions were performed at 0.1M concentration of starting material excess (greater than 10 equivalents) of electrophiles

^bIsolated yields of pure compounds

2.2.5 DoM of Substituted Indazoles

We were satisfied with the optimized condition outlined in entry 6 of **Table 2-6**, and applied this to subsequent reactions with a variety of carbon and heteroatom based electrophiles to demonstrate the scope and applicability of this methodology. The halogen series in the form of chloro, bromo and iodo substituents were introduced at the C-7 position via hexachloroethane (C_2Cl_6), bromine (Br_2) and iodine (I_2) respectively. Carbon based electrophiles such as CO_2 and MeI were also easily incorporated as their acid (COOH) and methyl derivatives. Phenyl disulfide (PhS)₂ provide for an example of C-7 incorporation of sulfur based electrophiles in good yield (**2.69**, 83%). When we introduced bis(pinacolato)diboron (B_2pin_2) to the reaction mixture, the expected organoboron compound was isolated upon workup in modest yields (**2.67**, 26 %), in addition, we also isolated the N-1 decarbamoylated 3-chloro 7-Bpin indazole as the major product (**2.68**, 41%), presumably the consequence of hydroxide mediated carboxamide cleavage during basic work-up. Upon C-7 metalation, the ensuing electrophilic quench using trimethylborate and hydrogen peroxide successfully incorporates hydroxyl group at the C-7 position (**2.63**). An interesting result was obtained by introducing the electrophilic diethylcarbamoyl chloride to the reaction mixture, which as a strong directing group for *ortho* lithiation, presumably enabled in the presence of excess base and electrophiles a series of successive quench-metalating cycles that gradually introduced the diethylcarbamoyl group around the indazole ring. The mono- (**2.57**), bis- (**2.58**), and tri- (**2.59**) substituted derivatives appear as a light yellow liquid and various attempts for their recrystallization were unsuccessful.

Figure 2-1 C-7 functionalization of substituted indazoles.

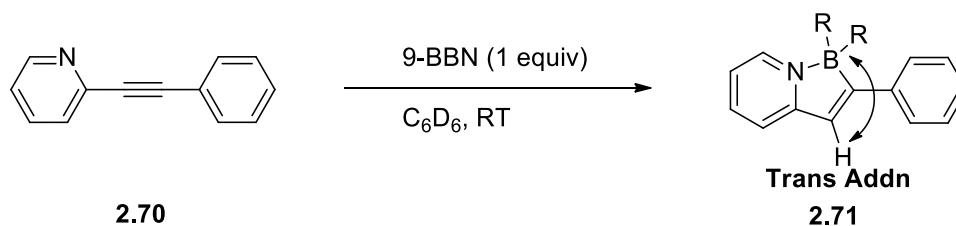


2.3 Hydroboration Approach Towards Indazole Based N,C-Chelating Organoboron Compounds

2.3.1 Project Aims

The Wang research group have disclosed a novel approach towards the synthesis of N,C-chelating organoboron compounds via *trans*-hydroboration reaction of 9-BBN and internal alkynes (Scheme 2-15).¹⁷⁶

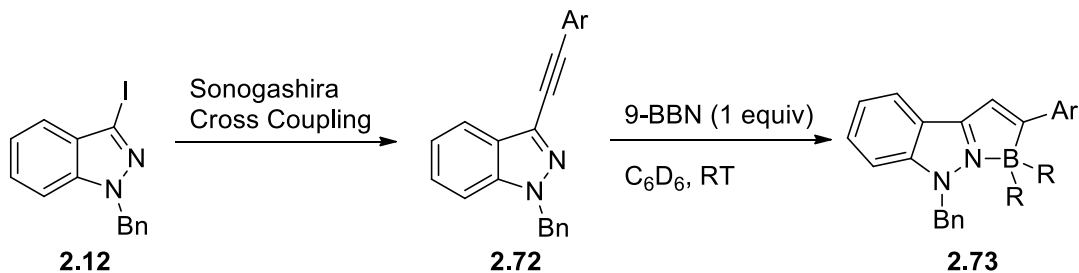
Scheme 2-15 *trans*-hydroboration of internal alkynes.



Hydroboration is one of the simplest methods for generating organoboron compounds.¹⁷⁷ The mechanism for such reactions is generally accepted to occur via four-membered transition states between the borane and the alkyne. The geometry of the transition state during which B-H bond breakage and C-H/C-B bond formation occur simultaneously will lead to *cis*-addition products. The remarkable results in *trans*-stereoselectivity as shown by the Wang research group also proceeds within minutes to yield the final products at room temperature (Scheme 1-19). Such stereo-selectivity is not usually observed in the standard hydroboration reactions without the addition of a transition metal catalyst, for instance, Miyaura *et al.* reported the use of Ir or Rh catalysts for the *trans*-hydroboration of terminal alkynes.¹⁷⁸ Furstner *et al.* reported a series of Ru catalysts for the *trans*-hydroboration of internal alkynes.¹⁷⁹ Other groups had also discovered the utility of Ru and Co complexes as effective *trans*-hydroboration catalysts with good selectivity and high yields.¹⁸⁰

We envisaged a similar structural motif based on the indazole heterocycle (**2.73**) instead of pyridine in the configuration of an internal alkyne, and to affect *trans*-hydroboration on this system in the manner as shown by **Scheme 2-16**. The goal of this project is to evaluate the robustness and utility of the *trans*-hydroboration reaction discovered by the Wang research group when it is extended to aromatic systems incorporating the indazole backbone, as well as expanding the library of related organoboron compounds.

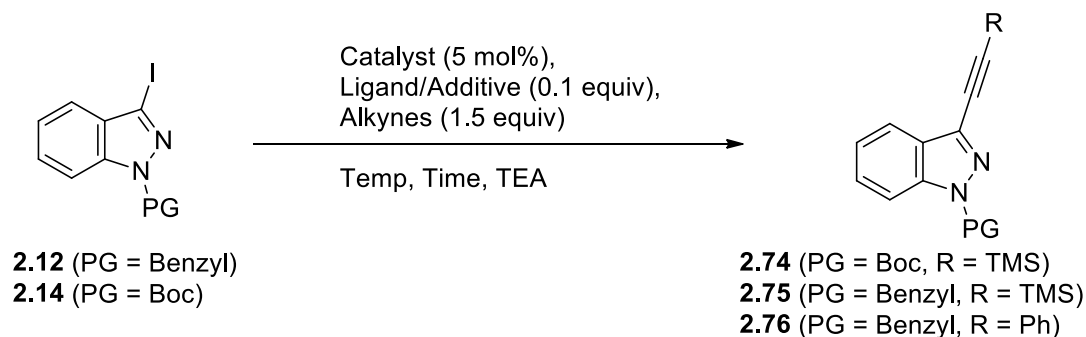
Scheme 2-16 *trans*-hydroboration of internal alkynes incorporating indazole-based systems.



2.3.2 C-3 Functionalization of Indazoles via Sonogashira Cross Coupling Reactions

We attempted the Sonogashira cross coupling reactions of N-1 protected 3-iodo-1*H*-indazoles by following a modified literature procedure.¹⁸¹ For compound **2.14**, the best conditions were reported using tetrakis(triphenylphosphine)palladium(0) with copper(I) iodide as the catalyst/ligand system. Stirring for twelve hours at room temperature in triethylamine (TEA) affords 3-TMS acetylene coupled indazole in good yield (entry 3). However, we did not observe any conversion when phenyl-acetylene was substituted as the alkyne coupling partner (entry 4). The optimized condition was extended to compound **2.12** which affords 3-TMS acetylene (entry 7) and 3-phenyl acetylene coupled indazoles (entry 9).

Table 2-7 Sonogashira cross coupling reactions of substituted indazoles.



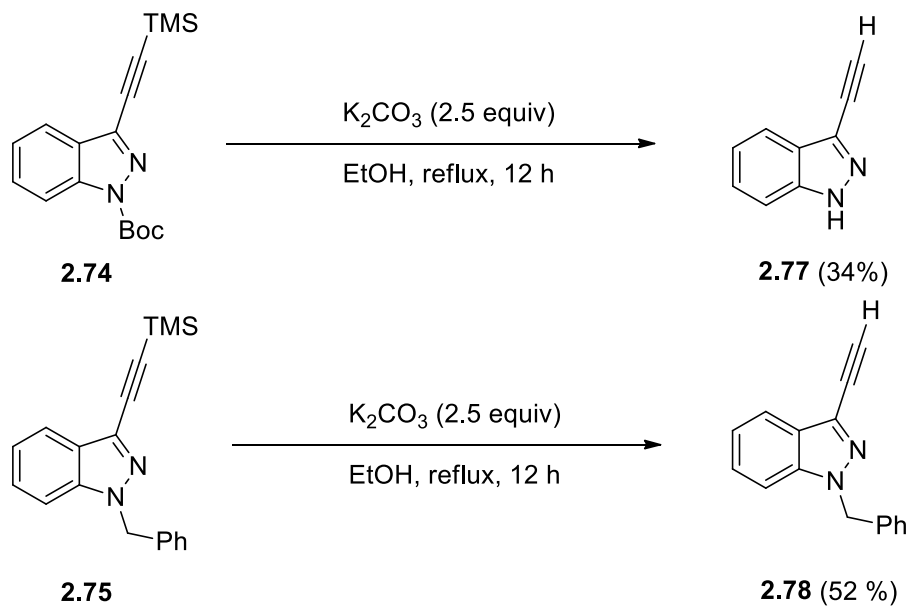
Entry	Starting material	Catalyst	Ligand/Additive	Alkynes	Temp	Time	Compounds ^a
1	2.14	PdCl ₂ (PPh ₃) ₂		TMS-acetylene	50 °C	5 h	2.74 (25 %)
2	"	Pd(OAc) ₂	PPh ₃ , CuI	"	80 °C	"	2.74 (50 %)
3	2.14	Pd(PPh₃)₄	CuI	TMS-acetylene	RT	12 h	2.74 (71 %)
4	"	"	"	Ph-acetylene	"	"	2.14 recovery (76 %)
5	2.12	"	"	TMS-acetylene	"	1 h	2.12 recovery (72 %)
6	"	"	"	"	"	3 h	2.12 recovery (73 %)
7	2.12	Pd(PPh₃)₄	CuI	TMS-acetylene	95 °C	12 h	2.75 (22 %)
8	"	"	"	Ph-acetylene	RT	3 h	2.76 (89 %)
9	"	"	"	Ph-acetylene	"	12 h	2.76 (90 %)

^aYields of isolated products after column chromatography

2.3.3 De-Silylation of 3-(TMS-Acetylene) Indazoles

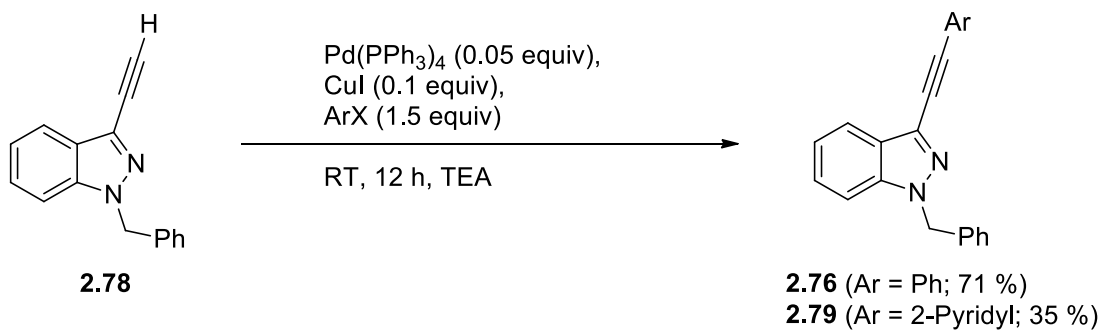
Successful de-silylation of compounds **2.74** and **2.75** was achieved with the treatment of potassium carbonate (K₂CO₃) in refluxing EtOH (**Scheme 2-17**). Under these conditions, compound **2.74** also undergoes base-mediated decarboxylation, thus re-exposing the N-H acidic proton at the N-1 position.

Scheme 2-17 Base-mediated de-silylation of substituted indazoles.



As an extension, compound **2.78** was subjected to the optimized Sonogashira reaction condition with aryl halide coupling partners, which offers a powerful synthetic handle for further elaborations on the substituted indazole nucleus.

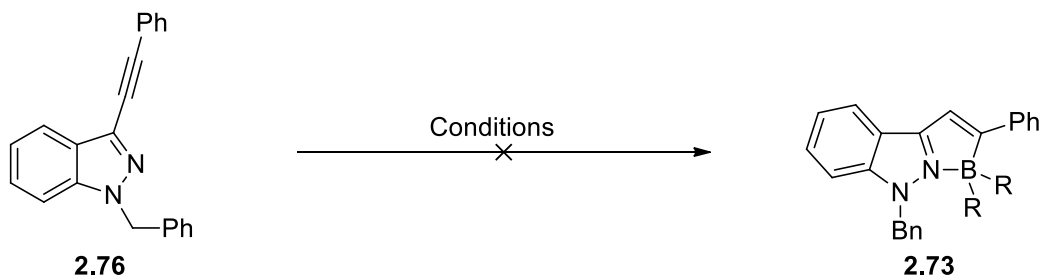
Scheme 2-18 Sonogashira cross coupling reactions of indazoles.



2.3.4 Hydroboration Reactions

With starting material **2.76** readily available, we attempted the hydroboration reactions under conditions optimized by the Wang research group (**Table 2-8**).¹⁷⁶ The air and moisture sensitive properties of 9-borabicyclo[3.3.1]nonane (9-BBN) led to careful preparations prior to experimental work. Entry 1 details the first attempt at the hydroboration reaction by following procedural precedent.¹⁷⁶ ¹H and ¹¹B NMR experiments within 1 hour of reaction initiation show only the presence of starting materials, and subsequent examinations at later times using NMR spectroscopy did not suggest any conversion towards the desired product. Concerns regarding the relative permeability of standard NMR tubes to gases and moisture led to the adoption of standard round bottom flasks under an inert atmosphere of argon for ensuing experiments. Disappointingly, only starting materials were recovered with THF as the solvent under reflux (Entry 2). Similarly, we did not observe significant changes in ¹H and ¹¹B NMR spectroscopy except for the decomposition of 9-BBN reagent when the reaction mixture was heated at 50 °C for 3 days in benzene (Entry 3). Switching from 9-BBN to B(Mes)₂H did not facilitate the process. (Entries 3 & 4)

Table 2-8 Unsuccessful hydroboration reactions towards N,C-chelating organoboron compounds.

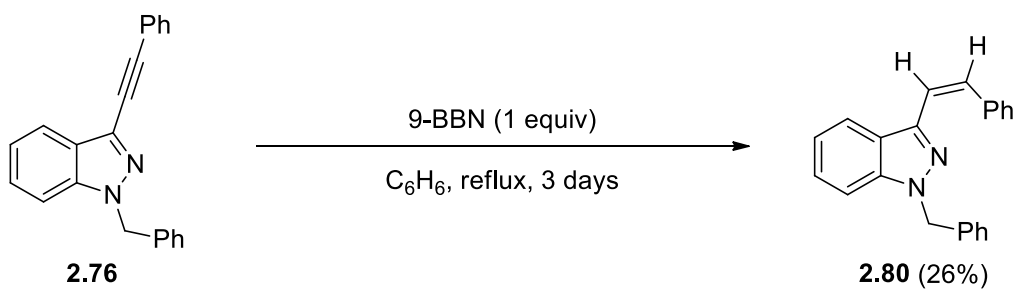


Entry	Conditions ^a
1	9-BBN (1 equiv), C ₆ D ₆ , RT, 1 week
2	9-BBN (1 equiv), THF, reflux, 3 days
3	9-BBN (1 equiv), C ₆ D ₆ , 50 °C, 3 days
4	B(Mes) ₂ H (1 equiv), C ₆ D ₆ , RT, 3 days
5	B(Mes) ₂ H (1 equiv), C ₆ D ₆ , 80°C, 3 days

^aEntry 1: reaction within standard NMR tube; Entry 2: reaction within round bottom flask; Entries 3, 4, 5: reactions within J-young NMR tube;

However, a new product (**2.80**) was obtained from heating the reaction mixture to reflux in benzene (**Scheme 2-19**). The *cis*-hydrogenated regio-isomer was established through the observed 12.5 Hz coupling constant doublet in the ¹H NMR spectra. The mass (311.15u, (M+H)⁺) and atomic composition (C₂₂H₁₉N₂, (M+H)⁺) of the product by HRMS analysis provides further evidence in support. The product appears as light yellow oil and attempts to crystallize this compound in a variety of solvents were unsuccessful. 9-BBN was confirmed to be the reductant as control experiment under identical conditions except for its addition gave only the recovery of starting materials.

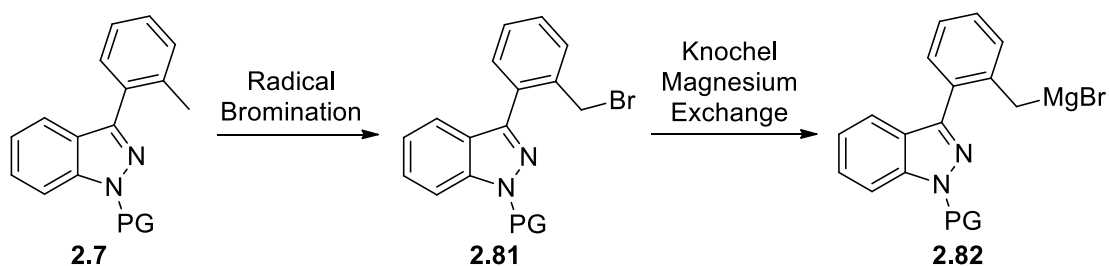
Scheme 2-19 *cis*-Hydrogenation of N-benzyl 3-phenylethynyl indazole.



2.4 Conclusion and Future Work

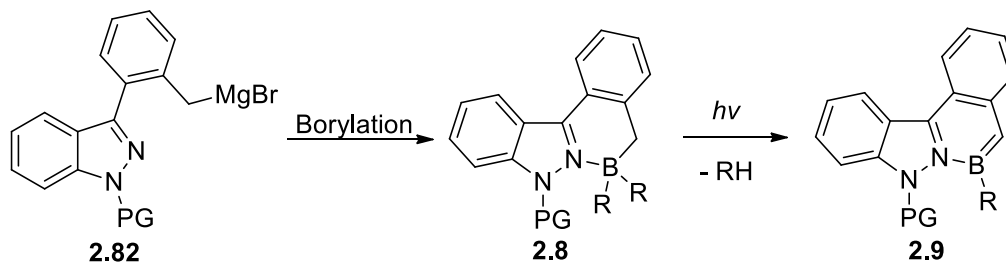
Progress towards the synthesis of novel azaborine compounds have shown that DoM reactions may be of limited utility in the late stage borylation steps (**Table 2-3**). Given the difficulties experienced thus far in our efforts, alternative strategies are proposed to mitigate these problems. We may attempt radical bromination on compound **2.7**,¹⁸² and if successful, magnesium-halogen exchange may be feasible under Knochel conditions to afford Grignard reagents **2.82** (**Scheme 2-20**).¹⁸³ Alternatively, C-H activation may be explored as a potential pathway albeit few literature precedents exist to support indazole as a directing group for that purpose.¹⁸⁴

Scheme 2-20 Grignard reagents based on indazoles.



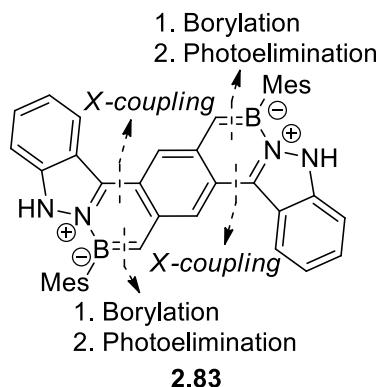
If these efforts prove successful in accessing the *ortho* position of C-3 coupled aryl groups, we hope to achieve quantitative anion formation, a standard that may be characterized as having >95% deuterium incorporation. Upon treatment with electrophilic boron reagents such as B(Mes)₂F, BCl₃, BF₃ or B(Ph)₂F, nucleophilic attack by the Grignard reagent **2.82** may afford the desired product **2.8**, which may then proceed through the photoelimination pathway to generate indazole-based azaborines **2.9** (**Scheme 2-21**).

Scheme 2-21 Synthesis of indazole-based azaborines using Grignard reagents.



New indazole-based azaborines may involve the installation of electron withdrawing/donating groups and further extension of the pi-conjugated framework, an example of which can be seen in **Figure 2-2**.

Figure 2-2 Theoretical azaborine molecule that incorporates indazole dimers.



Directed *ortho* Metalation is indeed a powerful method for the regioselective functionalization of substituted aromatics and provides direct access to unusually substituted indazoles. 3-chloro-1*H*-indazoles bearing *N,N*-diethylsulfamoyl or *N,N*-diethylcarbamoyl DMGs enabled C-7 functionalization using DoM chemistry, and successfully introduced deuterium >95% at this position. Optimized conditions settled on the use of LiTMP as the amine base during DoM reactions which enabled the synthesis for a variety of substrates incorporating carbon and heteroatom based electrophiles at the C-7 position.

2.5 Experimental Section

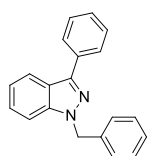
2.5.1 General Information

All reactions were carried out under argon atmosphere using flame-dried glassware. Anhydrous solvent was obtained from an SPS Solvent Purification System. All compounds were purified by flash chromatography using silica gel 60 (40-63 μm , *Silicycle*) and gave spectroscopic data consistent with being $\geq 95\%$ by ^1H NMR. Analytical thin layer chromatography (TLC) was performed on pre-coated 0.2 mm thick silica gel 60-F254 plates (*Merck*); visualized using UV light and by treatment with a KMnO_4 dip, followed by heating. Melting points were obtained from a Büchi M560 melting point instrument. IR spectra were recorded on a *Agilent Technologies Cary 630 FT-IR* (ATR) spectrometer; wavenumbers (ν) are given in cm^{-1} ; Mass spectra were obtained through the Chemistry Department Mass Spectrometry Service, Queen's University. ^1H NMR and ^{13}C NMR spectra were recorded on a *Bruker Avance-400* spectrometer operating at 400 MHz (^1H NMR frequency, corresponding ^{13}C frequencies are 100 MHz) in CDCl_3 at ambient temperature; chemical shifts (δ) are given in ppm and calibrated using the signal of residual undeuterated solvent as internal reference. ^1H NMR data are reported as follows: chemical shift (multiplicity, coupling constant, integration). Coupling constants (J) are reported in Hz and apparent splitting patterns are designated using the following abbreviations: s (singlet), d (doublet), t (triplet), q (quartet), m (multiplet), br (broad), app. (apparent) and the appropriate combinations. Unless otherwise indicated, reagents were obtained from commercial sources and were used without further purification. Solutions of *n*BuLi and *t*BuLi bases were purchased from Sigma-Aldrich and were titrated using *N*-benzylbenzamide as indicator. Indazole, $\text{Pd}(\text{PPh}_3)_4$, Pd_2dba_3 , and $\text{Pd}(\text{OAc})_2$ were purchased from Sigma-Aldrich.

2.5.2 Representative Experimental Procedure for Suzuki-Miyaura Cross Coupling Reactions

1-Benzyl-3-iodo-1H-indazole **2.12** (100 mg, 0.30 mmol, 1.0 equiv) was added to a mixture Pd(PPh₃)₄ (17 mg, 5 mol%), phenylboronic acid (37 mg, 0.31 mmol, 1.1 equiv) and NaHCO₃ (70 mg, 0.83 mmol, 3 equiv) in a flame-dried round bottom flask attached to a reflux condenser under an inert atmosphere. Degassed solvent mixture toluene/EtOH/H₂O (20/1/4 mL) was added and the reaction mixture was stirred at reflux for *ca.* 72 hours. The reaction mixture was concentrated *in vacuo* and purified by flash column chromatography (silica gel, eluting with Et₂O / hexane) to afford 1-benzyl-3-phenyl-1H-indazole **2.19** (80 mg, 0.28 mmol, 94%) as a colourless solid.

2.5.3 Spectra Data for Products of Suzuki-Miyaura Cross Coupling Reactions



1-benzyl-3-phenyl-1H-indazole (**2.19**)

Color and State: colourless solid (mp = 66 – 67 °C)

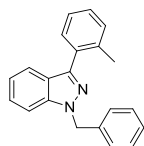
Recrystallization solvent - Et₂O : Hexanes (1 : 2)

¹H NMR (400 MHz, Acetone-*d*₆) δ 7.98 – 7.87 (m, 3H), 7.49 – 7.42 (m, 1H), 7.35 (dd, *J* = 8.4, 7.0 Hz, 2H), 7.26 – 7.19 (m, 2H), 7.18 – 7.10 (m, 4H), 7.09 – 7.02 (m, 2H), 5.54 (s, 2H).

¹³C NMR (100 MHz, Acetone-*d*₆) δ 144.25, 142.18, 138.50, 134.92, 129.67, 129.47, 128.64, 128.47, 128.28, 128.06, 127.19, 122.71, 122.15, 122.03, 110.92, 53.33.

IR (ATR) ν 3051, 2939, 1604, 1492, 1297, 1150, 1111cm⁻¹

HRMS (EI [M]⁺) calcd for C₂₀H₁₆N₂ 284.1313, found 284.1317



1-benzyl-3-(o-tolyl)-1H-indazole (2.20)

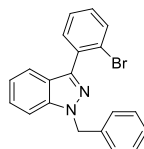
Color and State: colourless liquid

¹H NMR (400 MHz, Acetone-*d*₆) δ 7.48 (m, 2H), 7.41 (m, 1H), 7.27 – 7.04 (m, 9H), 6.99 (m, 1H), 5.55 (s, 2H), 2.26 (s, 3H).

¹³C NMR (100 MHz, Acetone-*d*₆) δ 145.21, 141.38, 138.66, 137.90, 133.54, 131.72, 131.15, 129.44, 128.85, 128.43, 128.29, 127.11, 126.60, 124.21, 121.84, 121.73, 110.68, 53.27, 21.03.

IR (ATR) ν 3059, 2922, 2854, 1613, 1454, 1311, 1152, 1100, 697 cm⁻¹

HRMS (EI [M]⁺) calcd for C₂₁H₁₈N₂ 298.1470, found 298.1477



1-benzyl-3-(2-bromophenyl)-1H-indazole (2.21)

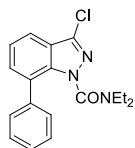
Color and State: colourless liquid

¹H NMR (400 MHz, CDCl₃) δ 7.67 (dd, *J* = 8.0, 1.3 Hz, 1H), 7.60 (d, *J* = 8.2 Hz, 1H), 7.50 (dd, *J* = 7.6, 1.8 Hz, 1H), 7.35 (t, *J* = 7.5, 1H), 7.31 – 7.16 (m, 8H), 7.09 (m, 1H), 5.61 (s, 2H).

¹³C NMR (101 MHz, CDCl₃) δ 144.26, 140.27, 136.85, 134.28, 133.36, 132.44, 129.80, 128.73, 127.74, 127.29, 127.19, 126.46, 123.54, 123.05, 121.90, 120.83, 109.56, 53.19

IR (ATR) ν 3058, 1614, 1492, 1312, 1153, 723, 703 cm⁻¹

HRMS (EI [M]⁺) calcd for C₂₀H₁₅N₂Br 362.0419, found 362.0422



3-chloro-N,N-diethyl-7-phenyl-1H-indazole-1-carboxamide (2.84)

Color and State: grey solid (104 – 105 °C)

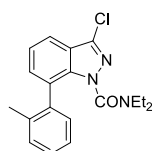
Recrystallization solvent – EtOAc : Hexane (1 : 3)

¹H NMR (400 MHz, Acetone-*d*₆) δ 7.59 (dd, *J* = 7.7, 1.4 Hz, 1H), 7.41 – 7.27 (m, 6H), 7.23 (m, 1H), 3.45 (q, *J* = 7.1 Hz, 2H), 3.06 (q, *J* = 7.1 Hz, 2H), 1.17 (t, *J* = 7.1 Hz, 3H), 0.81 (t, *J* = 7.1 Hz, 3H).

¹³C NMR (101 MHz, Acetone-*d*₆) δ 151.51, 140.97, 139.48, 137.88, 131.05, 129.46, 128.80, 128.58, 128.37, 124.83, 124.33, 119.19, 43.94, 41.90, 14.14, 12.35

IR (ATR) ν 2981, 1696, 1460, 1432, 1159, 761, 700 cm⁻¹

HRMS (EI [M]⁺) calcd for C₁₈H₁₈ClN₃O 327.1138, found 327.1141



3-chloro-N,N-diethyl-7-(o-tolyl)-1H-indazole-1-carboxamide (2.85)

Color and State: colourless solid (136 – 137 °C)

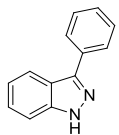
Recrystallization solvent – EtOAc: Hexane (1 : 3)

¹H NMR (400 MHz, Acetone-*d*₆) δ 7.61 (dd, *J* = 8.0, 1.2 Hz, 1H), 7.33 (dd, *J* = 8.1, 7.1 Hz, 1H), 7.25 (dd, *J* = 7.1, 1.2 Hz, 1H), 7.18 – 7.10 (m, 2H), 7.07 (m, 1H), 7.00 (dd, *J* = 7.4, 1.5 Hz, 1H), 3.24 (q, *J* = 7.1 Hz, 2H), 2.96 (dq, *J* = 6.8 Hz, 2H), 2.00 (s, 3H), 1.09 (t, *J* = 7.0 Hz, 4H), 0.64 (t, *J* = 7.1 Hz, 4H).

¹³C NMR (100 MHz, Acetone-*d*₆) δ 151.32, 141.34, 138.35, 137.32, 137.06, 131.44, 131.03, 130.00, 128.71, 128.49, 126.33, 124.33, 123.79, 119.14, 43.99, 41.86, 20.33, 14.10, 12.17.

IR (ATR) ν 2994, 2984, 1702, 1432, 1260, 1217, 1068, 760 cm⁻¹

HRMS (EI [M]⁺) calcd for C₁₉H₂₀N₃OCl 341.1295, found 341.1299



3-phenyl-1H-indazole (2.23)

Color and State: colourless solid (108 – 109 °C)

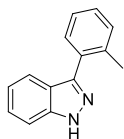
Recrystallization solvent – DCM slow evaporation

¹H NMR (400 MHz, Acetone-*d*₆) δ 12.25 (s, 1H), 7.98 (d, *J* = 8.3 Hz, 1H), 7.93 (d, *J* = 7.0 Hz, 2H), 7.50 (d, *J* = 8.4 Hz, 1H), 7.39 (t, *J* = 7.7 Hz, 2H), 7.35 – 7.21 (m, 2H), 7.15 – 7.05 (m, 1H).

¹³C NMR (101 MHz, CDCl₃) δ 145.83, 141.69, 133.57, 128.92, 128.18, 127.67, 126.83, 121.40, 121.17, 121.02, 110.12

IR (ATR) ν 3148, 2985, 1343, 1101, 775, 738, 694 cm⁻¹

HRMS (EI [M]⁺) calcd for C₁₃H₁₀N₂ 194.0844, found 194.0842



3-(*o*-tolyl)-1H-indazole (2.24)

Color and State: colourless solid (120 - 122 °C)

Recrystallization solvent – DCM slow evaporation

¹H NMR (400 MHz, CDCl₃) δ 10.16 (s, 1H), 7.60 (d, *J* = 8.1 Hz, 1H), 7.54 – 7.39 (m, 2H), 7.36 (dd, *J* = 6.9, 1.2 Hz, 1H), 7.29 (dd, *J* = 4.1, 1.9 Hz, 3H), 7.12 (ddd, *J* = 7.9, 6.8, 0.9 Hz, 1H), 2.34 (s, 3H).

¹³C NMR (101 MHz, CDCl₃) δ 140.92, 137.48, 132.35, 130.81, 130.64, 129.05, 128.38, 128.24, 126.72, 125.81, 122.36, 121.14, 109.97, 20.51

IR (ATR) ν 3146, 2925, 1338, 1093, 905, 724 cm⁻¹

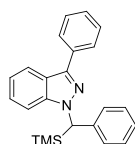
HRMS (EI [M]⁺) calcd for C₁₄H₁₂N₂ 208.1000, found 208.1004

2.5.4 Representative Experimental Procedure for DoM reactions of N-benzyl 3-Aryl

Indazoles

1-Benzyl-3-phenyl-1H-indazole **2.19** (100 mg, 0.35 mmol, 1 equiv) was dissolved in anhydrous tetrahydrofuran (1.5 mL) in a flame-dried round bottom flask under an inert atmosphere. The solution was cooled down to $-78\text{ }^{\circ}\text{C}$ before LDA (0.35 mL, 2.0 M, 2 equiv) was added to it drop wise *via* syringe pump (1.0 mL / min). The reaction mixture was stirred at $-78\text{ }^{\circ}\text{C}$ for *ca.* 1 hour, and then TMSCl (0.16 mL, 1.24 mmol, 3.5 equiv) was added *via* drop wise addition into the flask at $-78\text{ }^{\circ}\text{C}$, ensuring $T < -72\text{ }^{\circ}\text{C}$. The reaction mixture was then allowed to warm up to room temperature, and subsequently quenched with water. The reaction mixture was extracted into EtOAc ($3 \times 10\text{ mL}$), washed with water ($2 \times 10\text{ mL}$) and brine ($1 \times 10\text{ mL}$). The combined organic layers were dried with MgSO_4 , filtered and concentrated *in vacuo*. The crude product was purified by flash column chromatography (silica gel, eluting with Et_2O / hexane) to afford 3-phenyl-1-(phenyl(trimethylsilyl)methyl)-1H-indazole **2.28** (105 mg, 0.29 mmol, 84%) as a colourless solid.

2.5.5 Spectra Data for Products of DoM reactions of N-benzyl 3-Aryl Indazoles



3-phenyl-1-(phenyl(trimethylsilyl)methyl)-1H-indazole (**2.28**)

Color and State: colourless solid (mp = $153 - 154\text{ }^{\circ}\text{C}$)

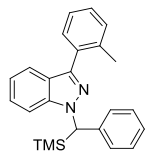
Recrystallization solvent – DCM slow evaporation

$^1\text{H NMR}$ (400 MHz, CDCl_3) δ 7.98 (m, 3H), 7.43 (dd, $J = 8.4, 7.0\text{ Hz}$, 2H), 7.34 – 7.25 (m, 1H), 7.19 – 7.01 (m, 6H), 7.00 – 6.94 (m, 2H), 5.05 (s, 1H), 0.17 (s, 9H).

$^{13}\text{C NMR}$ (100 MHz, CDCl_3) δ 143.74, 143.35, 142.16, 136.07, 130.44, 129.98, 129.18, 128.83, 127.83, 127.75, 127.42, 123.55, 122.83, 122.66, 111.95, 58.88, 0.00

IR (ATR) ν 3055, 2850, 1600, 1486, 1243, 1060, 841, 746 cm^{-1}

HRMS (EI $[\text{M}]^+$) calcd for $\text{C}_{23}\text{H}_{24}\text{N}_2\text{Si}$ 356.1709, found 356.1702



1-(phenyl(trimethylsilyl)methyl)-3-(o-tolyl)-1H-indazole (**2.29**)

Color and State: light yellow liquid

¹H NMR (400 MHz, CDCl₃) δ 7.61 (dt, *J* = 8.1, 1.0 Hz, 1H), 7.58 – 7.52 (m, 1H), 7.33 – 7.28 (m, 1H), 7.27 – 7.21 (m, 2H), 7.16 – 7.09 (m, 4H), 7.06 – 6.95 (m, 4H), 5.07 (s, 1H), 2.48 (s, 3H), 0.12 (s, 9H).

¹³C NMR (101 MHz, CDCl₃) δ 145.01, 142.80, 142.52, 139.02, 134.71, 132.77, 132.38, 130.12, 129.55, 128.03, 127.89, 127.57, 127.48, 125.18, 123.03, 122.41, 111.73, 58.88, 23.16, 0.00

IR (ATR) ν 3061, 2924, 2899, 1611, 1452, 1338, 1224, 1096, 846, 775 cm⁻¹

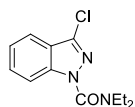
HRMS (EI [M]⁺) calcd for C₂₄H₂₆N₂Si 370.1865, found 370.1870

2.5.6 Representative Experimental Procedure for the N-1 Functionalization of Indazoles

3-Chloro indazole **2.16** (152.58 mg, 1.0 mmol, 1.0 equiv) was dissolved in the minimum amount of anhydrous acetonitrile in a flame-dried round bottom flask under an inert atmosphere. Potassium carbonate (276 mg, 2.0 mmol, 2.0 equiv) was then added in one portion, and the reaction mixture was allowed to stir at 50 °C for *ca.* 24 hours. The reaction mixture was then quenched with an aqueous solution of saturated ammonium chloride and extracted with EtOAc (3 x 10 mL). The combined organic layer was washed with water (2 x 10 mL), brine (1 x 10 mL) and dried with MgSO₄, filtered and concentrated *in vacuo* to afford the crude product. The crude product was purified by flash column chromatography (silica gel, eluting with Et₂O / hexane) to afford 3-chloro-N,N-diethyl-1H-indazole-1-carboxamide **2.52** (229.05 mg, 0.92 mmol, 92%) as a yellow liquid.

2.5.7 Spectra Data for Products of N-1 Functionalization of Indazoles

3-chloro-N,N-diethyl-1H-indazole-1-carboxamide (2.52)



Color and State: Light yellow liquid

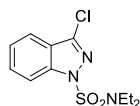
¹H NMR (400 MHz, CDCl₃) δ 8.03 (d, *J* = 8.6 Hz, 1H), 7.61 (d, *J* = 8.1, 1H), 7.45 (m, 1H), 7.25 (m, 1H), 3.54 (q, *J* = 7.0 Hz, 4H), 1.26 (t, ³*J*_{H-H} = 7.0 Hz, 6H).

¹³C NMR (100 MHz, CDCl₃) δ 152.0, 141.9, 137.6, 129.3, 123.5, 122.4, 119.3, 115.0, 43.4, 13.4

IR (ATR) ν 2943, 2939, 1680, 1431, 1339, 1275, 1209, 1066 cm⁻¹

HRMS (EI [M]⁺) calcd for C₁₂H₁₄N₃OCl 251.0825, found 251.0829

3-chloro-N,N-diethyl-1H-indazole-1-sulfonamide (2.50)

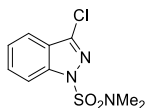


Color and State: Light yellow oil

¹H NMR (400 MHz, CDCl₃) δ 7.98 (d, *J* = 8.6 Hz, 1H), 7.62 (d, *J* = 8.1 Hz, 1H), 7.50 (m, 1H), 7.30 (t, *J* = 7.6 Hz, 1H), 3.39 (q, *J* = 7.2 Hz, 4H), 1.08 (t, *J* = 7.2 Hz, 6H).

¹³C NMR (100 MHz, CDCl₃) δ 141.7, 139.9, 130.0, 124.0, 122.4, 119.8, 113.5, 43.8, 13.7

IR (ATR) ν 2977, 2939, 1392, 1345, 1110, 950, 562 cm⁻¹.



3-chloro-N,N-diethyl-1H-indazole-1-sulfonamide (2.49)

Color and State: colourless solid (mp = 99 - 100 °C)

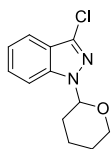
Recrystallization solvent – Et₂O : Hexane (1 : 1)

¹H NMR (300 MHz, CDCl₃) δ 8.03 (d, *J* = 8.5 Hz, 1H), 7.70 (d, *J* = 8.0 Hz, 1H), 7.58 (t, *J* = 7.7 Hz, 1H), 7.38 (t, *J* = 7.5 Hz, 1H), 3.00 (s, 6H).

¹³C NMR (100 MHz, CDCl₃) δ 142.18, 140.46, 130.11, 124.13, 122.23, 119.90, 113.40, 38.94.

IR (ATR) ν 2946, 1611, 1463, 1290, 1241, 1176, 1104, 978 cm⁻¹

HRMS (EI [M]⁺) calcd for C₉H₁₀N₃O₂ClS 259.0182, found 259.0185



3-chloro-1-(tetrahydro-2H-pyran-2-yl)-1H-indazole (2.51)

Color and State: colourless solid (mp = 70 – 71 °C)

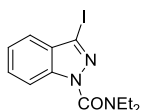
Recrystallization solvent - Et₂O : Hexane (1 : 1)

¹H NMR (400 MHz, CDCl₃) δ 7.60 (dd, *J* = 8.1, 1.1 Hz, 1H), 7.50 (m, 1H), 7.37 (dd, *J* = 8.3, 6.9, 1H), 7.16 (dd, *J* = 7.9, 6.9 Hz, 1H), 5.60 (dd, *J* = 9.2, 2.8 Hz, 1H), 3.95 (m, 1H), 3.66 (m, 1H), 2.48 (m, 1H), 2.08 (m, 1H), 1.99 (m, 1H), 1.76 – 1.51 (m, 3H).

¹³C NMR (100 MHz, CDCl₃) δ 140.79, 134.26, 127.75, 121.89, 119.77, 110.45, 85.35, 67.41, 29.29, 25.04, 22.44

IR (ATR) ν 2963, 2944, 1412, 1212, 1076, 909, 747 cm⁻¹

HRMS (EI [M]⁺) calcd for C₁₂H₁₃N₂OCl 236.0716, found 236.0722



N,N-diethyl-3-iodo-1H-indazole-1-carboxamide (2.15)

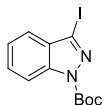
Color and State: colourless liquid

¹H NMR (400 MHz, CDCl₃) δ 7.98 (d, *J* = 8.5 Hz, 1H), 7.44 (m, 1H), 7.39 (m, 1H), 7.23 (m, 1H), 3.52 (q, *J* = 7.0 Hz, 4H), 1.24 (t, *J* = 7.1 Hz, 6H).

¹³C NMR (100 MHz, CDCl₃) δ 151.95, 140.96, 129.15, 129.12, 123.51, 121.31, 114.56, 98.34, 43.52, 13.39.

IR (ATR) ν 2969, 2933, 1455, 1326, 1274, 1051, 853 cm⁻¹

HRMS (EI [M]⁺) calcd for C₁₂H₁₄N₃OI 343.0182, found 343.0189



tert-butyl 3-iodo-1H-indazole-1-carboxylate (2.14)

Color and State: colourless solid (mp = 117 – 118 °C)

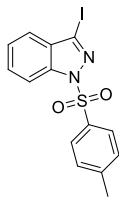
Recrystallization solvent – EtOH : H₂O (20 : 1)

¹H NMR (400 MHz, CDCl₃) δ 8.12 (d, *J* = 8.5 Hz, 1H), 7.59 (t, *J* = 7.8 Hz, 1H), 7.51 (d, *J* = 8.1 Hz, 1H), 7.42 – 7.33 (m, 1H), 1.72 (s, 9H);

¹³C NMR (101 MHz, CDCl₃) δ 148.36, 139.61, 130.19, 129.96, 124.18, 121.99, 114.56, 102.91, 85.51, 28.14.

IR (ATR) ν 2985, 2975, 1724, 1377, 1234, 1143, 1047, 740 cm⁻¹,

HRMS (EI [M]⁺) calcd for C₁₂H₁₃N₂O₂I 344.0022, found 344.0025



3-iodo-1-tosyl-1H-indazole (2.13)

Color and State: colourless solid (mp = 142 – 143 °C)

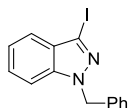
Recrystallization solvent – Acetone slow evaporation

¹H NMR (400 MHz, CDCl₃) δ 8.19 (dd, *J* = 8.5, 0.9 Hz, 1H), 7.96 – 7.84 (m, 2H), 7.64 (t, *J* = 8.4, 1H), 7.51 – 7.46 (m, 1H), 7.40 (m, 1H), 7.32 – 7.23 (m, 2H), 2.39 (s, 3H).

¹³C NMR (100 MHz, CDCl₃) δ 145.69, 140.18, 134.27, 130.29, 130.21, 129.96, 127.70, 124.71, 122.23, 113.18, 104.20, 21.68

IR (ATR) ν 2919, 1383, 1187, 1123, 685, 657, 572, 533 cm⁻¹

HRMS (ESI [M+H]⁺) calcd for C₁₄H₁₂O₂N₂IS 398.9659, found 398.9660



1-benzyl-3-iodo-1H-indazole (2.12)

Color and State: yellow solid (mp = 56 – 57 °C)

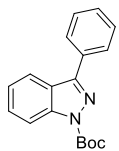
Recrystallization solvent – DCM slow evaporation

¹H NMR (400 MHz, CDCl₃) δ 7.48 – 7.37 (m, 1H), 7.33 (d, *J* = 1.1 Hz, 1H), 7.26 – 7.09 (m, 7H), 5.54 (s, 2H).

¹³C NMR (100 MHz, CDCl₃) δ 140.18, 136.37, 128.79, 128.72, 127.95, 127.56, 127.22, 121.71, 121.48, 109.51, 91.58, 53.61

IR (ATR) ν_{max} 3028, 2921, 1455, 1318, 1246, 1166, 742, 725, 694 cm⁻¹

HRMS (EI [M]⁺) calcd for C₁₄H₁₁N₂I 333.9967, found 333.9961



tert-butyl 3-phenyl-1H-indazole-1-carboxylate (2.36)

Color and State: light yellow solid (mp = 98 – 99 °C)

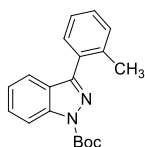
Recrystallization solvent – EtOAc : Hexane (1 : 1)

¹H NMR (400 MHz, CDCl₃) δ 8.24 (d, *J* = 8.3 Hz, 1H), 8.02 (m, 3H), 7.65 – 7.48 (m, 4H), 7.40 (t, *J* = 8.3, 1H), 1.78 (s, 9H).

¹³C NMR (100 MHz, CDCl₃) δ 149.83, 149.43, 141.06, 132.04, 129.28, 128.80, 128.75, 128.33, 124.28, 123.86, 121.46, 114.92, 84.82, 28.24

IR (ATR) ν 2985, 1726, 1340, 1250, 1053, 851, 749, 699 cm⁻¹

HRMS (EI [M]⁺) calcd for C₁₈H₁₈N₂O₂ 294.1368, found 294.1371



tert-butyl 3-(o-tolyl)-1H-indazole-1-carboxylate (2.37)

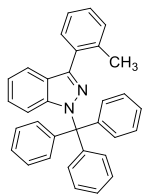
Color and State: colourless solid (mp = 132 – 133 °C)

Recrystallization solvent – EtOAc : Hexane (1 : 1)

¹H NMR (400 MHz, Acetone-*d*₆) δ 8.14 (dd, *J* = 8.5, 0.9 Hz, 1H), 7.57 – 7.47 (m, 2H), 7.42 (d, *J* = 7.2 Hz, 1H), 7.35 – 7.22 (m, 4H), 2.26 (s, 3H), 1.59 (s, 9H).

IR (ATR) ν 2981, 2930, 1737, 1383, 1249, 1151, 760, 743 cm⁻¹

HRMS (EI [M]⁺) calcd for C₁₉H₂₀N₂O₂ 308.1525, found 308.1520



3-(*o*-tolyl)-1-trityl-1H-indazole (2.39)

Color and State: colourless solid (mp = 164 – 165 °C)

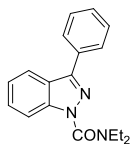
Recrystallization solvent – Et₂O : Pentane (1 : 1)

¹H NMR (400 MHz, CDCl₃) δ 7.76 (d, *J* = 8.0 Hz, 1H), 7.68 – 7.63 (m, 1H), 7.31 (m, 18H), 7.10 (t, *J* = 8.0 Hz, 1H), 7.03 (m, 1H), 6.52 (d, *J* = 8.5, 1H), 2.36 (s, 3H).

¹³C NMR (101 MHz, CDCl₃) δ 143.63, 142.94, 141.90, 137.53, 132.36, 131.03, 130.28, 130.22, 127.74, 127.50, 127.21, 125.51, 125.22, 124.60, 121.12, 120.73, 114.13, 78.57, 21.18.

IR (ATR) ν 3062, 3021, 1606, 1484, 1155, 867, 724, 697 cm⁻¹

HRMS (EI [M]⁺) calcd for C₃₃H₂₆N₂ 450.2096, found 450.2092



***N,N*-diethyl-3-phenyl-1H-indazole-1-carboxamide (2.38)**

Color and State: Yellow solid (mp = 91.2 – 93.1 °C)

Recrystallization solvent – Et₂O : Pentane (1 : 1)

¹H NMR (400 MHz, CDCl₃) δ 8.11 (d, *J* = 8.4 Hz, 1H), 8.02 – 7.85 (m, 3H), 7.55 – 7.33 (m, 4H), 7.26 (t, *J* = 8.0, 1H), 3.60 (q, *J* = 6.9 Hz, 4H), 1.32 (t, *J* = 7.0 Hz, 6H).

¹³C NMR (101 MHz, CDCl₃) δ 153.01, 146.77, 142.42, 132.74, 128.89, 128.84, 128.02, 127.88, 123.23, 122.98, 120.89, 114.89, 43.48, 13.54.

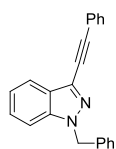
IR (ATR) ν 2974, 2961, 1672, 1415, 1335, 1215, 1054, 854, 754, 695 cm⁻¹

HRMS (EI [M]⁺) calcd for C₁₈H₁₉N₃O 293.1528, found 293.1525

2.5.8 Representative Experimental Procedure for C-3 Sonogashira Coupling Reactions

1-Benzyl-3-iodo-1H-indazole **2.12** (100 mg, 0.30 mmol, 1.0 equiv) was added to a mixture Pd(PPh₃)₄ (17 mg, 5 mol%), copper iodide (6 mg, 10 mol%) and phenylacetylene (0.05 mL, 0.45 mmol, 1.5 equiv) in a flame-dried round bottom flask under an inert atmosphere. Degassed TEA (25 mL) was added and the reaction mixture was stirred at room temperature for *ca.* 12 hours. The reaction mixture was concentrated *in vacuo* and purified by flash column chromatography (silica gel, eluting with Et₂O / hexane) to afford 1-benzyl-3-(phenylethynyl)-1H-indazole **2.76** (83.26 mg, 0.27 mmol, 90%) as a yellow solid.

2.5.9 Spectra Data for Products of C-3 Sonogashira Coupling Reactions



1-benzyl-3-(phenylethynyl)-1H-indazole (**2.76**)

Color and State: yellow solid (91 – 93 °C)

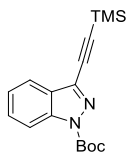
Recrystallization solvent - Et₂O : Hexane (1 : 1)

¹H NMR (400 MHz, Acetone-*d*₆) δ 7.91 (d, *J* = 8.1 Hz, 1H), 7.77 – 7.64 (m, 3H), 7.47 (dd, *J* = 5.0, 2.4 Hz, 4H), 7.43 – 7.16 (m, 6H), 5.74 (s, 2H).

¹³C NMR (100 MHz, Acetone-*d*₆) δ 140.75, 138.00, 132.43, 129.71, 129.57, 129.53, 128.87, 128.65, 128.42, 127.89, 126.68, 123.67, 122.65, 121.05, 111.16, 93.55, 82.01, 53.69

IR (ATR) ν 3058, 3029, 1340, 1254, 1175, 1094, 747, 688 cm⁻¹

HRMS (EI [M]⁺) calcd for C₂₂H₁₆N₂ 308.1313, found 308.1310



tert-butyl 3-((trimethylsilyl)ethynyl)-1H-indazole-1-carboxylate (2.74)

Color and State: colourless solid (96 – 97 °C)

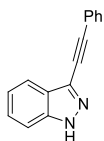
Recrystallization solvent – Et₂O : Hexane (1 : 1)

¹H NMR (400 MHz, CDCl₃) δ 8.02 (d, *J* = 8.5 Hz, 1H), 7.63 (d, *J* = 8.0 Hz, 1H), 7.38 (t, *J* = 8.5, 1H), 7.20 (t, *J* = 8.0, 1H), 1.56 (s, 9H), 0.15 (s, 9H).

¹³C NMR (100 MHz, CDCl₃) δ 149.06, 140.11, 135.07, 129.62, 127.19, 124.36, 121.00, 115.03, 102.48, 94.77, 85.64, 28.42, 0.00.

IR (ATR) ν 2966, 2166, 1736, 1487, 1383, 1367, 1245, 1153, 839, 743 cm⁻¹

HRMS (EI [M]⁺) calcd for C₁₇H₂₂N₂O₂Si 314.1451, found 314.1459



3-(phenylethynyl)-1H-indazole (2.86)

Color and State: yellow solid (mp = 167 – 168 °C)

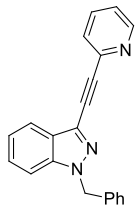
Recrystallization solvent – Et₂O : Hexane (1 : 1)

¹H NMR (400 MHz, Acetone-*d*₆) δ 12.48 (s, 1H), 7.76 (d, *J* = 8.1 Hz, 1H), 7.58 – 7.46 (m, 3H), 7.37 – 7.23 (m, 4H), 7.13 (m, 1H).

¹³C NMR (101 MHz, Acetone-*d*₆) δ 141.45, 132.44, 129.85, 129.66, 129.57, 127.81, 125.59, 123.75, 122.47, 120.69, 111.53, 93.13, 82.39

IR (ATR) ν 3121, 2945, 2906, 2870, 1338, 1253, 1071, 910 cm⁻¹

HRMS (EI [M]⁺) calcd for C₁₅H₁₀N₂ 218.0844, found 218.0840



1-benzyl-3-(pyridin-2-ylethynyl)-1H-indazole (2.79)

Color and State: colorless liquid

¹H NMR (400 MHz, Acetone-*d*₆) δ 8.51 (m, 1H), 7.80 – 7.67 (m, 2H), 7.58 (m, 2H), 7.32 (m, 1H), 7.25 (m, 1H), 7.22 – 7.11 (m, 6H), 5.60 (s, 2H).

¹³C NMR (100 MHz, Acetone-*d*₆) δ 151.18, 143.95, 140.76, 137.85, 137.29, 129.55, 128.70, 128.45, 128.22, 128.16, 128.00, 126.85, 124.22, 122.94, 120.97, 111.30, 93.39, 81.17, 53.84.

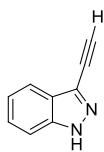
IR (ATR) ν 3057, 3032, 2215, 1580, 1340, 1259, 1178, 697 cm⁻¹

HRMS (EI [M]⁺) calcd for C₂₁H₁₅N₃ 309.1266, found 309.1261

2.5.10 Representative Experimental Procedure for De-silylation Reactions

Tert-butyl 3-((trimethylsilyl)ethynyl)-1H-indazole-1-carboxylate **2.74** (100 mg, 0.32 mmol, 1.0 equiv) was dissolved in ethanol (25 mL) in a round bottom flask attached to a reflux condenser. K₂CO₃ (110 mg, 0.80 mmol, 2.5 equiv) was added in one portion and the resulting mixture was stirred at reflux for 12 hours. The reaction mixture was diluted with EtOAc (25 mL). The organic layer was washed with H₂O (2 × 10 mL), brine (1 × 10 mL), dried over MgSO₄, filtered and concentrated *in vacuo* to afford the crude product. The crude product was purified by flash column chromatography (silica gel, eluting with Et₂O / hexane) to afford 3-ethynyl-1H-indazole **2.77** (15 mg, 0.11 mmol, 34%) as a grey solid.

2.5.11 Spectra Data for Products of De-silylation Reactions



3-ethynyl-1H-indazole carboxamide (2.77)

Color and State: grey solid (mp = 132 – 133 °C)

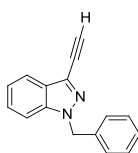
Recrystallization solvent – Et₂O : Hexane (1 : 1)

¹H NMR (400 MHz, CDCl₃) δ 11.68 (s, 1H), 7.85 (d, *J* = 8.2 Hz, 1H), 7.64 (d, *J* = 8.3 Hz, 1H), 7.46 (q, *J* = 8.0, 5.9 Hz, 1H), 7.27 (t, *J* = 7.5 Hz, 1H), 3.45 (s, 1H).

¹³C NMR (100 MHz, CDCl₃) δ 140.22, 128.93, 127.51, 124.77, 122.00, 120.30, 110.51, 81.40, 75.47

IR (ATR) ν 3298, 3153, 2903, 2761, 1624, 1476, 1077, 739 cm⁻¹

HRMS (EI [M]⁺) calcd for C₉H₆N₂ 142.0531, found 142.0534



1-benzyl-3-ethynyl-1H-indazole (2.78)

Color and State: colourless liquid

¹H NMR (400 MHz, Acetone-*d*₆) δ 7.74 (dd, *J* = 8.1, 1.0 Hz, 1H), 7.66 (m, 1H), 7.41 (m, 1H), 7.35 – 7.19 (m, 6H), 5.67 (s, 2H), 3.98 (s, 1H).

¹³C NMR (100 MHz, Acetone-*d*₆) δ 140.60, 137.91, 129.50, 128.63, 128.37, 128.13, 127.85, 126.74, 122.69, 120.76, 111.18, 82.94, 76.33, 53.65

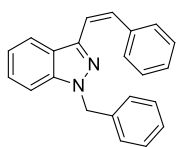
IR (ATR) ν 3283, 3060, 1614, 1491, 1341, 1314, 1101, 743, 698 cm⁻¹

HRMS (EI [M]⁺) calcd for C₁₆H₁₂N₂ 232.1000, found 232.1005

2.5.12 Representative Experimental Procedure for Hydroboration Reactions

1-Benzyl-3-(phenylethynyl)-1*H*-indazole **2.76** (100 mg, 0.32 mmol, 1.0 equiv) was dissolved in anhydrous deuterobenzene (10 mL) in a flame-dried round bottom flask attached to an oven dried reflux condenser under an inert atmosphere. In a separate flame-dried flask under an inert atmosphere was dissolved 9-borabicyclo[3.3.1]nonane (39.05 mg, 0.32 mmol, 1 equiv) in anhydrous deuterobenzene (0.5 mL), which was added drop wise to the flask containing 1-benzyl-3-(phenylethynyl)-1*H*-indazole **2.76** *via* syringe pump (1.0 mL / min). Following the addition of the 9-borabicyclo[3.3.1]nonane, the reaction mixture was stirred at reflux for 72 hours. The reaction mixture was then concentrated *in vacuo* and purified by flash column chromatography (silica gel, eluting with Et₂O / hexane) to afford (Z)-1-benzyl-3-styryl-1*H*-indazole **2.80** (26 mg, 0.08 mmol, 26%) as a light yellow liquid.

2.5.13 Spectra Data for Products of Hydroboration Reactions



(Z)-1-benzyl-3-styryl-1*H*-indazole (2.80)

Color and State: Light yellow liquid

¹H NMR (600 MHz, CDCl₃) δ 7.68 – 7.59 (m, 2H), 7.31 (d, *J* = 8.2 Hz, 1H), 7.07 (m, 11H), 6.89 (t, *J* = 7.5 Hz, 1H), 6.80 (d, *J* = 12.5 Hz, 1H), 5.22 (s, 2H).

¹³C NMR (100 MHz, Acetone-*d*₆) δ 142.06, 141.18, 138.48, 138.31, 132.83, 130.28, 129.42, 128.77, 128.45, 128.34, 127.04, 123.98, 121.79, 121.34, 120.51, 110.51, 71.27, 53.25.

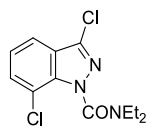
IR (ATR) ν 3057, 3029, 1612, 1452, 1355, 1253, 1182, 695 cm⁻¹

HRMS (ESI [M+H]⁺) calcd for C₂₂H₁₉N₂ 311.15428, found 311.15405

2.5.14 Representative Experimental Procedure for C-7 DoM

2,2,6,6-Tetramethylpiperidine (0.17 mL, 1.0 mmol, 2.5 equiv) was dissolved in anhydrous tetrahydrofuran (2.0 mL) in a flame-dried round bottom flask under an inert atmosphere. This mixture was cooled to 0 °C before drop wise addition of *n*-butyl lithium (0.4 mL, 1.0 mmol, 2.5 equiv, 2.5 M in hexane). This reaction mixture was allowed to stir at 0 °C for *ca.* 20 minutes before it was cooled down to – 78 °C. In a separate flame-dried flask under an inert atmosphere was dissolved 3-chloro-*N,N*-diethyl-1*H*-indazole-1-carboxamide **2.52** (0.10 g, 0.40 mmol, 1.0 equiv) in anhydrous tetrahydrofuran (1.0 mL), before it was added dropwise to the flask containing lithium 2,2,6,6-tetramethylpiperidin-1-ide *via* syringe pump (1.0 mL / min). Following the addition of **2.52**, the reaction mixture was stirred at –78 °C for 1 hour. In a separate flame-dried flask under an inert atmosphere was dissolved hexachloroethane (0.47 g, 2.0 mmol, 5.0 equiv) in tetrahydrofuran (0.3 mL), before it was added *via* drop wise addition to the flask at – 78 °C, ensuring T < – 72 °C. The reaction mixture was then allowed to stir at this temperature for 1 hour, and subsequently warmed-up to room temperature before being quenched with water. The reaction mixture was extracted into EtOAc (3 × 10 mL), washed with water (2 × 10 mL) and brine (1 × 10 mL). The combined organic layers were dried with MgSO₄, filtered and concentrated *in vacuo*. The crude product was purified by flash column chromatography (silica gel, eluting with Et₂O / hexane) to afford 3,7-dichloro-*N,N*-diethyl-1*H*-indazole-1-carboxamide **2.60** (0.81 g, 0.28 mmol, 71%) as a colourless solid.

2.5.15 Spectra Data for Products of C-7 DoM



3,7-dichloro-*N,N*-diethyl-1*H*-indazole-1-carboxamide (2.60)

Color and State: Colourless solid (mp = 80 – 81 °C)

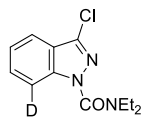
Recrystallization solvent – Et₂O : Hexane (1 : 1)

¹H NMR (400 MHz, CDCl₃) δ 7.52 (d, *J* = 8.2 Hz, 1H), 7.42 (d, *J* = 7.6 Hz, 1H), 7.16 (t, *J* = 7.9 Hz, 1H), 3.52 (q, *J* = 7.1 Hz, 2H), 3.38 (q, *J* = 7.2 Hz, 2H), 1.27 (t, *J* = 7.1 Hz, 3H), 1.15 (t, *J* = 7.2 Hz, 3H).

¹³C NMR (100 MHz, CDCl₃) δ 150.75, 138.67, 137.76, 129.63, 124.57, 123.98, 118.52, 118.03, 43.83, 42.29, 13.96, 12.40

IR (ATR) ν 2979, 1697, 1425, 1365, 1265, 1214, 1161, 1086, 857 cm⁻¹

HRMS (EI [M]⁺) calcd for C₁₂H₁₃N₃OCl₂ 285.0436, found 285.0433



7-deutero-3-chloro-*N,N*-diethyl-1*H*-indazole-1-carboxamide (2.54)

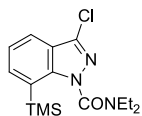
Color and State: Light yellow liquid

¹H NMR (400 MHz, CDCl₃) δ 7.60 (d, *J* = 8.1, 1H), 7.46 (d, *J* = 7.1 Hz, 1H), 7.25 (d, *J* = 8.1, 7.1 Hz, 1H), 3.65 (q, *J* = 7.1 Hz, 4H), 1.25 (t, *J* = 7.1 Hz, 6H).

¹³C NMR (100 MHz, CDCl₃) δ 151.1, 140.9, 136.6, 128.2, 122.5, 121.4, 118.3, 113.7, 42.4, 12.4

IR (ATR) ν 2976, 2925, 1677, 1424, 1340, 1251, 1142, 745 cm⁻¹

HRMS (EI [M]⁺) calcd for C₁₂H₁₃DCIN₃O 252.0888, found 252.0882



7-(trimethylsilyl)-3-chloro-*N,N*-diethyl-1*H*-indazole-1-carboxamide (2.55)

Color and State: Colourless solid (mp = 69 – 70 °C)

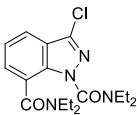
Recrystallization solvent – Et₂O : Hexane (1 : 1)

¹H NMR (300 MHz, CDCl₃) δ 7.80 (d, *J* = 6.9 Hz, 1H), 7.70 (d, *J* = 7.9 Hz, 1H), 7.35 (t, *J* = 7.9 Hz, 6.9 Hz, 1H), 3.67 (m, 4H), 1.4.0 (m, 6H), 0.43 (s, 9H)

¹³C NMR (100 MHz, CDCl₃) δ 153.2, 146.4, 138.6, 137.2, 126.4, 123.2, 122.6, 120.6, 43.7, 41.8, 13.7, 12.8, 0.4

IR (ATR) ν 2944, 1701, 1440, 1249, 1153, 1067, 823, 753 cm⁻¹

HRMS (EI [M]⁺) calcd for C₁₅H₂₂ClN₃OSi 323.1221, found 323.1213



3-chloro-*N1,N1,N7,N7*-tetraethyl-1*H*-indazole-1-dicarboxamide (2.57)

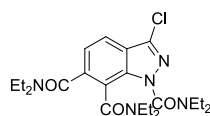
Color and State: light yellow oil

¹H NMR (400 MHz, CDCl₃) δ 7.63 (dd, *J* = 8.0, 1.1 Hz, 1H), 7.32 (dd, *J* = 7.2, 1.1 Hz, 1H), 7.22 (t, *J* = 7.6 Hz, 1H), 3.47 (q, *J* = 7.5, 7.1 Hz, 6H), 3.35 (q, *J* = 7.2 Hz, 2H), 1.23 (m, 9H), 1.13 (t, *J* = 7.1 Hz, 3H).

¹³C NMR (100 MHz, CDCl₃) δ 168.10, 151.74, 138.47, 137.24, 126.36, 123.68, 123.17, 122.54, 120.52, 43.35, 39.05, 13.84, 12.49

IR (ATR) ν 2971, 2935, 1695, 1630, 1428, 1265, 1129 cm⁻¹

HRMS (EI [M]⁺) calcd for C₁₇H₂₃N₄O₂Cl 350.1510, found 350.1506



3-chloro-*N1,N1,N6,N6,N7,N7*-hexaethyl-1*H*-indazole-1-tricarboxamide (2.58)

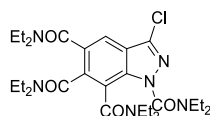
Color and State: light yellow oil

¹H NMR (400 MHz, CDCl₃) δ 7.74 (d, *J* = 8.3 Hz, 1H), 7.23 (d, *J* = 8.3 Hz, 1H), 3.80 (m, 1H), 3.60 – 3.16 (m, 10H), 3.01 (m, 1H), 1.31 (t, *J* = 7.1 Hz, 6H), 1.27 – 1.16 (m, 9H), 0.97 (t, *J* = 7.1 Hz, 3H).

¹³C NMR (100 MHz, CDCl₃) δ 168.51, 165.95, 151.32, 137.70, 136.92, 134.54, 123.00, 121.75, 120.47, 119.56, 44.24, 43.16, 39.15, 38.68, 13.87, 12.95, 12.77, 12.72

IR (ATR) ν 2971, 2875, 1700, 1631, 1429, 1380, 1217, 1132, 1087 cm⁻¹

HRMS (ESI [M+H]⁺) calcd for C₂₂H₃₃O₃N₅Cl 450.22664, found 450.22665



3-chloro-*N1,N1,N5,N5,N6,N6,N7,N7*-octaethyl-1*H*-indazole-1,5,6,7-

tetracarboxamide (2.59)

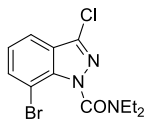
Color and State: light yellow oil

¹H NMR (400 MHz, CDCl₃) δ 7.53 (s, 1H), 3.50 – 3.10 (m, 16H), 1.21-0.97 (m, 24H).

¹³C NMR (100 MHz, CDCl₃) δ 168.58, 166.57, 165.30, 151.20, 137.53, 136.99, 132.31, 131.40, 122.15, 119.75, 117.33, 44.38, 44.01, 43.60, 39.42, 38.82, 38.54, 13.89, 13.01, 12.78, 12.68, 12.53

IR (ATR) ν 2972, 1703, 1634, 1432, 1380, 1269, 1216, 1068 cm⁻¹

HRMS (EI [M]⁺) calcd for C₂₇H₄₁N₆O₄Cl 548.2878, found 548.2889



7-bromo-3-chloro-*N,N*-diethyl-1*H*-indazole-1-carboxamide (2.61)

Color and State: Colourless solid (mp = 68 - 69 °C)

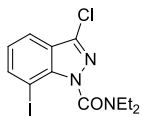
Recrystallization solvent – Et₂O : Hexane (1 : 1)

¹H NMR (400 MHz, CDCl₃) δ 7.60 (m, 2H), 7.10 (t, *J* = 7.8 Hz, 1H), 3.53 (q, *J* = 7.1 Hz, 2H), 3.40 (q, *J* = 7.1 Hz, 2H), 1.29 (t, *J* = 7.1 Hz, 3H), 1.18 (t, *J* = 7.2 Hz, 3H).

¹³C NMR (100 MHz, CDCl₃) δ 150.58, 140.13, 137.70, 133.00, 124.46, 124.24, 119.14, 105.09, 43.84, 42.29, 13.98, 12.39

IR (ATR) ν 3006, 2954, 1697, 1492, 1432, 1262, 1082, 787, 597 cm⁻¹

HRMS (EI [M]⁺) calcd for C₁₂H₁₃N₃OClBr 328.9931, found 328.9932



7-iodo-3-chloro-*N,N*-diethyl-1*H*-indazole-1-carboxamide (2.62)

Color and State: Colourless solid (mp = 76.2 - 77 °C)

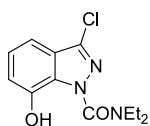
Recrystallization solvent – Et₂O : Hexane (1 : 1)

¹H NMR (400 MHz, CDCl₃) δ 7.90 (d, *J* = 7.4 Hz, 1H), 7.63 (d, *J* = 8.0 Hz, 1H), 6.99 (t, *J* = 7.7 Hz, 1H), 3.55 (q, *J* = 7.2 Hz, 2H), 3.47 (q, *J* = 7.2 Hz, 2H), 1.34 (t, *J* = 7.1 Hz, 3H), 1.24 (t, *J* = 7.1 Hz, 3H);

¹³C NMR (100 MHz, CDCl₃) δ 150.15, 143.26, 140.12, 137.66, 124.60, 123.88, 119.99, 75.22, 43.86, 42.26, 14.15, 12.56

IR (ATR) ν 2971, 1694, 1443, 1381, 1341, 1312, 782, 732 cm⁻¹

HRMS (EI [M]⁺) calcd for C₁₂H₁₃IN₃OCl 376.9792, found 376.9789



7-hydroxy-3-chloro-*N,N*-diethyl-1*H*-indazole-1-carboxamide (2.63)

Color and State: Colourless solid (mp = 42 - 43 °C)

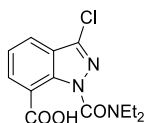
Recrystallization solvent – chloroform slow evaporation

¹H NMR (400 MHz, CDCl₃) δ 10.21 (s, 1H), 7.25 – 7.17 (m, 1H), 7.11 (dd, *J* = 7.8, 1.1 Hz, 1H), 7.01 (dd, *J* = 7.8, 1.1 Hz, 1H), 3.59 (q, *J* = 7.1 Hz, 4H), 1.30 (t, *J* = 7.1 Hz, 6H).

¹³C NMR (100 MHz, CDCl₃) δ 153.67, 143.70, 139.69, 132.05, 126.01, 124.98, 116.38, 110.25, 44.64, 13.11

IR (ATR) ν 3058, 2875, 1648, 1514, 1440, 1316, 1269, 915, 850 cm⁻¹

HRMS (EI [M]⁺) calcd for C₁₂H₁₄N₃O₂Cl 267.0775, found 267.0769



3-chloro-1-(diethylcarbamoyl)-1*H*-indazole-7-carboxylic acid (2.64)

Color and State: Colourless solid (mp = 165-166 °C)

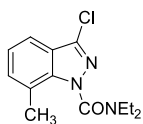
Recrystallization solvent – Et₂O : Hexane (1 : 1)

¹H NMR (400 MHz, CDCl₃) δ 9.06 (s, 1H), 8.16 (dd, *J* = 7.4, 1.1 Hz, 1H), 7.95 (dd, *J* = 8.0, 1.1 Hz, 1H), 7.53 – 7.36 (m, 1H), 3.70 (q, *J* = 7.1 Hz, 2H), 3.59 (q, *J* = 7.1 Hz, 2H), 1.37 (t, *J* = 7.2 Hz, 6H).

¹³C NMR (100 MHz, CDCl₃) δ 169.72, 152.38, 139.68, 138.46, 131.93, 125.12, 124.53, 122.93, 117.10, 43.73, 41.97, 13.52, 12.52

IR (ATR) ν 2968, 2590, 1683, 1592, 1427, 1267, 890, 753 cm⁻¹

HRMS (EI [M]⁺) calcd for C₁₃H₁₄N₃O₃Cl 295.0724, found 295.0719



7-methyl-3-chloro-*N,N*-diethyl-1*H*-indazole-1-carboxamide (2.65)

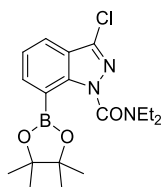
Color and State: Light yellow liquid

¹H NMR (400 MHz, CDCl₃) δ 7.43 (m, 1H), 7.19 (m, 1H), 7.13 (m, 1H), 3.46 (q, *J* = 5.7 Hz, 4H), 2.40 (s, 3H), 1.35 - 1.05 (m, 6H)

¹³C NMR (100 MHz, CDCl₃) δ 152.0, 141.0, 137.7, 130.7, 128.7, 123.5, 123.3, 117.3, 43.8, 42.3, 19.0, 14.1, 12.6

IR (ATR) ν 2972, 2875, 1691, 1461, 1333, 1313, 1272, 1257 cm⁻¹

HRMS (EI [M]⁺) calcd for C₁₃H₁₆N₃OCl 265.0982, found 265.0973



7-Bpin-3-chloro-*N,N*-diethyl-1*H*-indazole-1-carboxamide (2.67)

Color and State: Grey solid (mp = 135 – 136 °C)

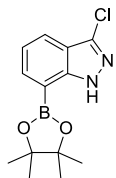
Recrystallization solvent – Et₂O : Hexane (1 : 1)

¹H NMR (400 MHz, CDCl₃) δ 7.71 (dd, *J* = 6.9, 1.1 Hz, 1H), 7.64 (dd, *J* = 8.1, 1.1 Hz, 1H), 7.24 (dd, *J* = 8.1, 6.9 Hz, 1H), 3.62 (s, 4H), 1.32 (s, 12H), 1.23 (t, *J* = 7.1 Hz, 6H).

¹³C NMR (100 MHz, CDCl₃) δ 152.77, 144.57, 138.28, 135.35, 135.13, 123.09, 121.99, 121.37, 84.45, 84.02, 25.14, 24.99

IR (ATR) ν 2927, 2849, 1684, 1592, 1315, 1300, 1264, 1127, 753 cm⁻¹

HRMS (ESI [M+H]⁺) calcd for C₁₈H₂₆O₃N₃BCl 378.1750, found 378.1749



7-Bpin-3-chloro-*N,N*-diethyl-1*H*-indazole-1-carboxamide (2.68)

Color and State: Grey solid (mp = 130-132 °C)

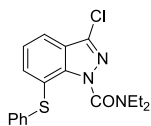
Recrystallization solvent – Et₂O : Hexane (1 : 1)

¹H NMR (400 MHz, CDCl₃) δ 10.54 (s, 1H), 7.79 (d, *J* = 6.9, 1H), 7.75 – 7.71 (m, 1H), 7.16 (dd, *J* = 8.2, 6.9 Hz, 1H), 1.32 (s, 12H).

¹³C NMR (100 MHz, CDCl₃) δ 145.54, 135.35, 134.86, 122.93, 121.29, 119.47, 84.45, 29.70, 24.99

IR (ATR) ν 3337, 2928, 1595, 1430, 1369, 1211, 845, 702 cm⁻¹

HRMS (EI [M]⁺) calcd for C₁₃H₁₆BClN₂O₂ 278.0993, found 278.0988



7-(phenylthio)-3-chloro-*N,N*-diethyl-1*H*-indazole-1-carboxamide (2.69)

Color and State: Colourless solid (mp = 86 - 87 °C)

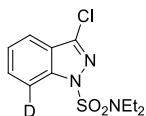
Recrystallization solvent – Et₂O : Hexane (1 : 1)

¹H NMR (400 MHz, CDCl₃) δ 7.48 (d, *J* = 8.1, 1H), 7.25 (d, *J* = 7.5, 1H), 7.20 – 7.08 (m, 6H), 3.44 (q, *J* = 7.1 Hz, 2H), 3.28 (q, *J* = 7.1 Hz, 2H), 1.21 (t, *J* = 7.1 Hz, 3H), 1.11 (t, *J* = 7.1 Hz, 3H).

¹³C NMR (100 MHz, CDCl₃) δ 151.71, 141.21, 137.92, 135.23, 133.14, 131.23, 129.34, 127.50, 124.04, 123.65, 121.26, 118.86, 43.85, 42.21, 13.94, 12.50

IR (ATR) ν 2982, 2870, 1708, 1581, 1431, 1340, 1260, 1213, 1154, 690 cm⁻¹

HRMS (EI [M]⁺) calcd for C₁₈H₁₈N₃OSCl 359.0859, found 359.0850



7-deutero-3-chloro-N,N-diethyl-1H-indazole-1-sulfonamide (2.53)

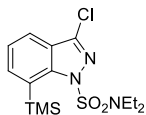
Color and State: colourless liquid

¹H NMR (400 MHz, CDCl₃) δ 7.62 (dd, *J* = 8.1, 1.1 Hz, 1H), 7.50 (dd, *J* = 7.1 Hz, 1H), 7.30 (dd, *J* = 8.1, 7.1 Hz, 1H), 3.39 (q, *J* = 7.19 Hz, 4H), 1.06 (t, *J* = 7.19 Hz, 6H).

¹³C NMR (100 MHz, CDCl₃) δ 141.7, 140.0, 130.0, 124.0, 122.4, 120.0, 113, 43.8, 13.7

IR (ATR) ν 2980, 1383, 1210, 1023, 962, 719, 567 cm⁻¹

HRMS (EI [M]⁺) calcd for C₁₁H₁₃DClN₃O₂S 288.0558, found 288.0549



7-(trimethylsilyl)-3-chloro-N,N-diethyl-1H-indazole-1-sulfonamide (2.66)

Color and State: Grey solid (mp = 68.5 – 70 °C)

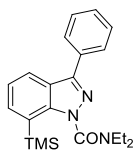
Recrystallization solvent – Et₂O : Hexane (1 : 1)

¹H NMR (400 MHz, CDCl₃) δ 7.78 (dd, *J* = 7.2, 1.2 Hz, 1H), 7.60 (dd, *J* = 7.9, 1.2 Hz, 1H), 7.30 (dd, *J* = 7.9, 7.2 Hz, 1H), 3.22 (q, *J* = 7.2 Hz, 4H), 0.97 (t, *J* = 7.2 Hz, 6H), 0.38 (s, 9H).

¹³C NMR (100 MHz, CDCl₃) δ 146.3, 141.1, 137.1, 126.5, 122.3, 121.5, 118.9, 42.3, 12.0, 0.0

IR (ATR) ν 2977, 2920, 1384, 1339, 1220, 1177, 1098, 856, 723 cm⁻¹

HRMS (EI [M]⁺) calcd for C₁₄H₂₂N₃O₂SClSi 359.0891, found 359.0877



7-(trimethylsilyl)-N,N-diethyl-3-phenyl-1H-indazole-1-carboxamide (2.41)

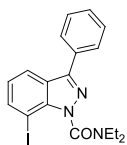
Color and State: colourless solid (mp = 105 – 106 °C)

Recrystallization solvent – Et₂O : Hexane (1 : 1)

¹H NMR (400 MHz, CDCl₃) δ 7.91 (dd, *J* = 8.0, 1.2 Hz, 1H), 7.87 – 7.81 (m, 2H), 7.66 (dd, *J* = 7.0, 1.2 Hz, 1H), 7.45 (m, 2H), 7.42 – 7.36 (m, 1H), 7.24 (dd, *J* = 8.0, 7.0 Hz, 1H), 3.62 (m, 4H), 1.34 (m, 6H), 0.34 (s, 9H).

IR (ATR) ν 2973, 1679, 1433, 1377, 1261, 1153, 825, 746 cm⁻¹

HRMS (EI [M]⁺) calcd for C₂₁H₂₇N₃OSi 365.1923, found 365.1919



7-iodo-N,N-diethyl-3-phenyl-1H-indazole-1-carboxamide (2.42)

Color and State: colourless solid (mp = 75 – 76 °C)

Recrystallization solvent – Et₂O : Hexane (1 : 1)

¹H NMR (400 MHz, Acetone-*d*₆) δ 8.04 – 7.95 (m, 1H), 7.91 – 7.82 (m, 3H), 7.51 – 7.39 (m, 2H), 7.38 – 7.31 (m, 1H), 6.99 (dd, *J* = 8.1, 7.4 Hz, 1H), 3.46 (dq, *J* = 30.2, 7.1 Hz, 4H), 1.22 (dt, *J* = 28.3, 7.1 Hz, 6H).

¹³C NMR (100 MHz, Acetone-*d*₆) δ 151.72, 147.79, 144.36, 139.83, 133.18, 129.88, 129.85, 128.66, 125.29, 124.89, 122.37, 75.86, 44.40, 42.62, 14.59, 12.86.

IR (ATR) ν 2969, 2870, 1695, 1430, 1375, 1261, 1100, 854, 696 cm⁻¹

HRMS (EI [M]⁺) calcd for C₁₈H₁₈IN₃O 419.0495, found 419.0490

Reference

- ¹ Fischer, E. *Justus Liebigs Annalen der Chemie*, **1885**, 227, 305.
- ² Wiley, R. *The Chemistry of Heterocyclic Compounds, Volume 22, Pyrazoles and Reduced and Condensed Pyrazoles*; John Wiley & Sons: New York, NY, **2009**.
- ³ Cankařová, N.; Hlaváč, J.; Krchňák, V. *Org. Prep. Proced. Int.* **2010**, 42, 433.
- ⁴ Schmidt, A. *Adv. Heterocycl. Chem.* **2003**, 85, 67.
- ⁵ Schmidt, A.; Beutler, A.; Snovydyovych, B. *Eur. J. Org. Chem.* **2008**, 4073.
- ⁶ a) Minkin, V. I.; Garnovskii, D. G.; Elguero, J.; Katritzky, A. R.; Denisko, O. V. *Adv. Heterocycl. Chem.* **2000**, 76, 157. b) Catalan, J.; del Valle, J.; Claramunt, R.; Boyer, G.; Laynez, J.; Gomez, J.; Jimenez, P.; Tomas, F.; Elguero, J. *J. Phys. Chem.* **1994**, 98, 10606. c) Catalán, J.; de Paz, J.; Elguero, J. *J. Chem. Soc., Perkin Trans. 2*, **1996**, 57. d) Öğretir, C.; Funda Kaypak, N. *J. Mol. Struct: THEOCHEM.* **2002**, 583, 137. e) Öğretir, C.; Funda Kaypak, N. *J. Mol. Struct: THEOCHEM.* **2002**, 588, 145.
- ⁷ Faure, R.; Vincent, E.; Elguero, J. *Heterocycles*, **1983**, 20, 1713.
- ⁸ Eicher, T.; Hauptmann, S.; Speicher, A. *The chemistry of heterocycles*; Wiley-VCH: Weinheim, **2012**.
- ⁹ Teichert, J.; Oulié, P.; Jacob, K.; Vendier, L.; Etienne, M.; Claramunt, R.; López, C.; Pérez Medina, C.; Alkorta, I.; Elguero, J. *New J. Chem.* **2007**, 31, 936.
- ¹⁰ Smith, D.; Barrett, E. *Acta Crystallogr Sect B*, **1969**, 25, 2355.
- ¹¹ Zimmermann, H.; Geisenfelder, H. *Z. Elektrochem.* **1961**, 65, 368.
- ¹² Dewar, M.; Morita, T. *J. Am. Chem. Soc.* **1969**, 91, 796.
- ¹³ Kamiya, M. *Bull. Chem. Soc. Jpn.* **1970**, 43, 3344.
- ¹⁴ Escande, A.; Lapasset, J.; Faure, R.; Vincent, E.; Elguero, J. *Tetrahedron* **1974**, 30, 2903.
- ¹⁵ Palmer, M.; Findlay, R.; Kennedy, S.; McIntyre, P. *J. Chem. Soc., Perkin Trans.* **1975**, 1, 1695.
- ¹⁶ a) Claramunt, R.; Santa María, M.; Sanz, D.; Alkorta, I.; Elguero, J. *Magn. Reson. Chem.* **2006**, 44, 566. b) Diaz, E.; Maldonado, L.; Obtega, A. *Spectrochim. Acta Part A*, **1970**, 26, 284.
- ¹⁷ Atmani, A.; Aubagnac, J.; Pellegrin, V. *Org. Mass Spectrom.* **1980**, 15, 533.
- ¹⁸ Escande, A.; Lapasset, J. *Acta Crystallogr Sect B*, **1974**, 30, 2009.
- ¹⁹ Cane, E.; Palmieri, P.; Tarroni, R.; Trombetti, A. *J. Chem. Soc. Farad. Trans.* **1993**, 89, 4005.

-
- ²⁰ Velino, B.; Cané, E.; Trombetti, A.; Corbelli, G.; Zerbetto, F.; Caminati, W. *J. Mol. Spectrosc.* **1992**, *155*, 1.
- ²¹ a) Bigotto, A.; Zerbo, C. *Spectrosc. Lett.* **1990**, *23*, 65. b) Pergolese, B.; Bigotto, A. *Spectrochim. Acta Part A*, **2001**, *57*, 1191.
- ²² a) Schutt, H.; Zimmerman, H. *Ber Bunsenges. Phys. Chem.* **1963**, *67*, 54. b) Byrne, J.; Ross, I. *Aust. J. Chem.* **1971**, *24*, 1107. c) Cane, E.; Trombetti, A.; Velino, B.; Caminati, W. *J. Mol. Spectrosc.* **1992**, *155*, 307.
- ²³ Berden, G.; Meerts, W.; Jalviste, E. *J. Chem. Phys.* **1995**, *103*, 9596. b) Jalviste, E.; Temps, F. *J. Chem. Phys.* **1999**, *111*, 3898.
- ²⁴ Palmer, M.; Kennedy, M.; *J. Mol. Struct.*, **1978**, *43*, 203.
- ²⁵ a) Mauret, P.; Fayet, J.; Fabre, M. *Bull. Soc. Chim. Fr.* **1975**, 1675. b) Katritzky, A.; Rees, C. *Comprehensive heterocyclic chemistry*; Pergamon Press: Oxford [Oxfordshire], **1984**.
- ²⁶ Katritzky, A.; Rees, C. *Comprehensive Heterocyclic Chemistry*; Pergamon Press: Oxford [Oxfordshire], **1984**.
- ²⁷ Tiefenthaler, H.; Dorscheln, W.; Goth, H.; Schmid, H. *Helv. Chim. Acta*, **1967**, *50*, 2244
- ²⁸ Grimshaw, J.; Mannus, D. *J. Chem. Soc., Perkin Trans 1* **1977**, 2096.
- ²⁹ Dubois, J.; Labhart, H. *Chimia*, **1969**, *23*, 109.
- ³⁰ Heinzelmann, W.; *Helv. Chim. Acta*, **1978**, *61*, 234.
- ³¹ Palmer, M.; Findlay, R.; Kennedy, S.; McIntyre, P. *J. Chem. Soc., Perkin Trans.* **1975**, *2*, 1695.
- ³² a) Behr, L.; Fusco, R.; Jarboe, C. *Chem. Heterocycl. Compd.*, **1967**, *22*, 1. b) Jaffari, G.; Nunn, A. *J. Chem. Soc., Perkin Trans.* **1973**, *1*, 2371.
- ³³ Luo, G.; Chen, L.; Dubowchik, G. *J. Org. Chem.* **2006**, *71*, 5392.
- ³⁴ a) Habraken, C.; Cohen-Fernandes, P. *J. Org. Chem.* **1971**, *36*, 3084-3086. b) Austin, M. *J. Chem. Soc., Perkin Trans. 2*, **1972**, 632.
- ³⁵ Behr, L.; Fusco, R.; Jarboe, C. *Chem. Heterocycl. Compd.*, **1967**, *22*, 1.
- ³⁶ Boulton, B.; Coller, B. *Aust. J. Chem.*, **1974**, *27*, 2343.
- ³⁷ Cheruvallath, Z.; Tang, M.; McBride, C.; Komandla, M.; Miura, J.; Ton-Nu, T.; Erikson, P.; Feng, J.; Farrell, P.; Lawson, J.; Vanderpool, D.; Wu, Y.; Dougan, D.; Plonowski, A.; Holub, C.; Larson, C. *Bioorg. Med. Chem. Lett.* **2016**, *26*, 2774.
- ³⁸ Li, L.; Liu, F.; Jin, N.; Tang, S.; Chen, Z.; Yang, X.; Ding, J.; Geng, M.; Jiang, L.; Huang, M.; Cao, J. *Bioorg. Med. Chem. Lett.* **2016**, *26*, 2600.

-
- ³⁹ Furlotti, G.; Alisi, M.; Cazzolla, N.; Dragone, P.; Durando, L.; Magarò, G.; Mancini, F.; Mangano, G.; Ombrato, R.; Vitiello, M.; Armirotti, A.; Capurro, V.; Lanfranco, M.; Ottonello, G.; Summa, M.; Reggiani, A. *J. Med. Chem.* **2015**, *58*, 8920.
- ⁴⁰ Fonseca-Berzal, C.; Ibáñez-Escribano, A.; Reviriego, F.; Cumella, J.; Morales, P.; Jagerovic, N.; Nogal-Ruiz, J.; Escario, J.; da Silva, P.; Soeiro, M.; Gómez-Barrio, A.; Arán, V. *Eur. J. Med. Chem.* **2016**, *115*, 295.
- ⁴¹ Sączewski, J.; Hudson, A.; Scheinin, M.; Wasilewska, A.; Sączewski, F.; Rybczyńska, A.; Ferdousi, M.; Laurila, J.; Boblewski, K.; Lehmann, A.; Watts, H.; Ma, D. *Eur. J. Med. Chem.* **2016**, *115*, 406.
- ⁴² Khalaj, A.; Hasselmann, J.; Augello, C.; Moore, S.; Tiwari-Woodruff, S. *J. Steroid Biochem. Mol. Biol.* **2016**, *160*, 43.
- ⁴³ Folkes, A.; Ahmadi, K.; Alderton, W.; Alix, S.; Baker, S.; Box, G.; Chuckowree, I.; Clarke, P.; Depledge, P.; Eccles, S.; Friedman, L.; Hayes, A.; Hancox, T.; Kugendradas, A.; Lensun, L.; Moore, P.; Olivero, A.; Pang, J.; Patel, S.; Pergl-Wilson, G.; Raynaud, F.; Robson, A.; Saghir, N.; Salphati, L.; Sohal, S.; Ultsch, M.; Valenti, M.; Wallweber, H.; Wan, N.; Wiesmann, C.; Workman, P.; Zhyvoloup, A.; Zvelebil, M.; Shuttleworth, S. *J. Med. Chem.* **2008**, *51*, 5522.
- ⁴⁴ Qiang, Y.; Zhang, S.; Xu, S.; Li, W. *J. Colloid Interface Sci.* **2016**, *472*, 52.
- ⁴⁵ Fan, K.; Roberts, J.; Martens, P.; Stenzel, M.; Granville, A. *J. Mater. Chem. B*, **2015**, *3*, 7457.
- ⁴⁶ Kang, Y.; Yoon, T.; Mun, J.; Park, M.; Song, I.; Benayad, A.; Oh, S. *J. Mater. Chem. A*, **2014**, *2*, 14628.
- ⁴⁷ Ahmed, Z.; Iftikhar, K. *Inorg. Chem.* **2015**, *54*, 11209.
- ⁴⁸ Ge, D.; Zhang, X.; Chen, S.; Pu, L.; Yu, X. *Tetrahedron Lett.* **2015**, *56*, 4811.
- ⁴⁹ Bernhammer, J.; Chong, N.; Jothibas, R.; Zhou, B.; Huynh, H. *Organometallics*. **2014**, *33*, 3607.
- ⁵⁰ Wheeler, R.; Baxter, E.; Campbell, I.; Macdonald, S. *Org. Process Res. Dev.* **2011**, *15*, 565.
- ⁵¹ Díaz-Ortiz, A.; De la Hoz, A.; Langa, F. *Green Chem.* **2000**, *2*, 165.
- ⁵² Selvam, K.; Krishnakumar, B.; Velmurugan, R.; Swaminathan, M. *Catal. Commun.* **2009**, *11*, 280.
- ⁵³ a) Schumann, P.; Collot, V.; Hommet, Y.; Gsell, W.; Dauphin, F.; Sopkova, J.; MacKenzie, E.; Duval, D.; Boulouard, M.; Rault, S. *Bioorg. Med. Chem. Lett.* **2001**, *11*, 1153. b) Schmidt, A.; Beutler, A.; Snovydovych, B. *Eur. J. Org. Chem.* **2008**, 4073.
- ⁵⁴ Moore, P. K.; Wallace, P.; Gaffen, Z.; Hart, S. L.; Babbedge, R. C. *Br. J. Pharmacol.* **1993**, *110*, 219.
- ⁵⁵ Bouissane, L.; El Kazzouli, S.; Léonce, S.; Pfeiffer, B.; Rakib, E.; Khouili, M.; Guillaumet, G. *Bioorg. Med. Chem.* **2006**, *14*, 1078.
- ⁵⁶ Bolgunas, S.; Clark, D.; Hanna, W.; Mauvais, P.; Pember, S. *J. Med. Chem.* **2006**, *49*, 4762.

-
- ⁵⁷ Steffan, R.; Matelan, E.; Ashwell, M.; Moore, W.; Solvibile, W.; Trybulski, E.; Chadwick, C.; Chippari, S.; Kenney, T.; Eckert, A.; Borges-Marcucci, L.; Keith, J.; Xu, Z.; Mosyak, L.; Harnish, D. *J. Med. Chem.* **2004**, *47*, 6435.
- ⁵⁸ a) Wroblewski, S.; Chen, P.; Hynes, J.; Lin, S.; Norris, D.; Pandit, C.; Spergel, S.; Wu, H.; Tokarski, J.; Chen, X.; Gillooly, K.; Kiener, P.; McIntyre, K.; Patil-koota, V.; Shuster, D.; Turk, L.; Yang, G.; Leftheris, K. *J. Med. Chem.* **2003**, *46*, 2110. b) Lukin, K.; Hsu, M.; Fernando, D.; Leanna, M. *J. Org. Chem.* **2006**, *71*, 8166. c) Jin, T.; Yamamoto, Y. *Angew. Chem. Int. Ed.* **2007**, *46*, 3323. d) Lebedev, A. Y.; Khartulyari, A. S.; Voskoboynikov, A. Z. *J. Org. Chem.* **2005**, *70*, 596. e) Inamoto, K.; Katsuno, M.; Yoshino, T.; Suzuki, I.; Hiroya, K.; Sakamoto, T. *Chem. Lett.* **2004**, *33*, 1026.
- ⁵⁹ Shoji, Y.; Hari, Y.; Aoyama, T. *Tetrahedron Lett.* **2004**, *45*, 1769.
- ⁶⁰ a) Meyer, V. *Chem. Ber.* **1889**, *22*, 319. (b) Reich, S.; Gaigalian, G. *Chem. Ber.* **1913**, *46*, 2380.
- ⁶¹ Boulouard, M.; Schumann-Bard, P.; Butt-Gueulle, S.; Lohou, E.; Stiebing, S.; Collot, V.; Rault, S. *Bioorg. Med. Chem. Lett.* **2007**, *17*, 3177.
- ⁶² Amherst News,. Family says N.S. pharmaceutical worker named chemical he used before death, 2008.
- ⁶³ a) Gilman, H.; Bebb, R. L. *J. Am. Chem. Soc.* **1939**, *61*, 109. b) Wittig, G.; Pockels, U.; Droge, H. *Chem. Ber.* **1938**, *71B*, 1903.
- ⁶⁴ Puterbaugh, W. H.; Hauser, C. R. *J. Org. Chem.* **1964**, *29*, 853.
- ⁶⁵ Gschwend, H. W.; Hamden, A. *J. Org. Chem.* **1975**, *40*, 2008.
- ⁶⁶ Beak, P.; Brown, R. A. *J. Org. Chem.* **1977**, *42*, 1823.
- ⁶⁷ Meyers, A. I.; Mihelich, E. D. *Tetrahedron* **1975**, *40*, 3158.
- ⁶⁸ Snieckus, V. *Chem. Rev.* **1990**, *90*, 879.
- ⁶⁹ Slocum, D.; Jennings, C. *J. Org. Chem.* **1976**, *41*, 3653.
- ⁷⁰ Beak, P.; Brown, R. *J. Org. Chem.* **1979**, *44*, 4463.
- ⁷¹ Miah, M. A. J. Ph. D. Thesis, University of Waterloo, 1985.
- ⁷² Meyers, A.; Lutomski, K. *J. Org. Chem.* **1979**, *44*, 4464.
- ⁷³ Beak, P.; Kerrick, S.; Gallagher, D. *J. Am. Chem. Soc.* **1993**, *115*, 10628.
- ⁷⁴ Fuoss, R.; Kraus, C. *J. Am. Chem. Soc.* **1933**, *55*, 2387.
- ⁷⁵ Fraser, R.; Bresse, M.; Mansour, T. *J. Am. Chem. Soc.* **1983**, *105*, 7790.
- ⁷⁶ Zhao, Y.; Snieckus, V. *Org. Lett.* **2014**, *16*, 390.
- ⁷⁷ Milburn, R. R.; Snieckus, V. *Angew. Chem. Int. Ed.* **2004**, *43*, 888.

-
- ⁷⁸ Sengupta, S.; Leite, M.; Raslan, D. S.; Quesnelle, C.; Snieckus, V. *J. Org. Chem.* **1992**, *57*, 4066.
- ⁷⁹ Meyers, A. I.; Gabel, R.; Mihelich, E. D. *J. Org. Chem.* **1978**, *43*, 1372.
- ⁸⁰ Beak, P.; Meyers, A. I. *Acc. Chem. Res.* **1985**, *19*, 356.
- ⁸¹ a) Al-Aseer, M.; Beak, P.; Hay, D.; Kempf, D. J.; Mills, S.; Smith, S. G. *J. Am. Chem. Soc.* **1983**, *105*, 2080.
b) Hay, D. R.; Song, Z.; Smith, S. G.; Beak, P. *J. Am. Chem. Soc.* **1988**, *110*, 8145.
- ⁸² Reitz, D.; Beak, P.; Tse, A. *J. Org. Chem.* **1981**, *46*, 4316.
- ⁸³ Olsher, U.; Izatt, R.; Bradshaw, J.; Dalley, N. *Chem. Rev.* **1991**, *91*, 137.
- ⁸⁴ Klumpp, G.; Sinnige, M. *Tetrahedron Lett.* **1986**, *27*, 2247.
- ⁸⁵ Broaddus, C. *J. Org. Chem.* **1970**, *35*, 10.
- ⁸⁶ Jastrzebski, J.; Van Koten, G.; Konijn, M.; Stam, C. *J. Am. Chem. Soc.* **1982**, *104*, 5490.
- ⁸⁷ Reich, H.; Gudmundsson, B. *J. Am. Chem. Soc.* **1996**, *118*, 6074.
- ⁸⁸ a) Pross, A.; Radom, L. *Prog. Phys. Org. Chem.* **1981**, *13*, 1. b) Bachrach, S. M.; Richie, J. P. *J. Am. Chem. Soc.* **1989**, *111*, 3134.
- ⁸⁹ Fraenkel, G.; Hsu, H.; Su, B. M. In Bach, R. O., Ed.; *Lithium Current Applications in Science, Medicine, and Technology*; Wiley: New York, 1985; pp 273.
- ⁹⁰ Seebach, D.; Hassig, R.; Gabriel, J. *Helv. Chim. Acta.* **1983**, *66*, 308.
- ⁹¹ Bauer, W.; Clark, T.; Schleyer, P. *J. Am. Chem. Soc.* **1987**, *109*, 970.
- ⁹² Lewis, H.; Brown, T. *J. Am. Chem. Soc.* **1970**, *92*, 4664.
- ⁹³ Bauer, W.; Schleyer, P. *J. Am. Chem. Soc.* **1989**, *111*, 7191.
- ⁹⁴ a) Hommes, N.; Schleyer, P. *Angew. Chem. Int. Ed.* **1992**, *31*, 755. b) Hommes, N.; Schleyer, P. *Tetrahedron* **1994**, *50*, 5903.
- ⁹⁵ a) Rennels, R.; Maliakal, A. J.; Collum, D. B. *J. Am. Chem. Soc.* **1998**, *120*, 421. b) Hoepker, A. C.; Gupta, L.; Ma, Y.; Faggini, M. F.; Collum, D. B. *J. Am. Chem. Soc.* **2011**, *133*, 7135.
- ⁹⁶ a) Whisler, M.; MacNeil, S.; Snieckus, V.; Beak, P. *Angew. Chem. Int. Ed.* **2004**, *43*, 2206. b) Saa, J. M. *Helv. Chim. Acta* **2002**, *85*, 814
- ⁹⁷ Narasimhan, N. S.; Chandrachud, P. S.; Shete, N. R. *Tetrahedron* **1981**, *37*, 825.
- ⁹⁸ Cartoon, M.; Cheeseman, G. *J. Organomet. Chem.* **1981**, *212*, 1.
- ⁹⁹ Wang, W.; Snieckus, V. *J. Org. Chem.* **1992**, *57*, 424.

-
- ¹⁰⁰ Fu, J.; Zhao, B.; Sharp, M.; Snieckus, V. *Can. J. Chem.* **1994**, *72*, 227.
- ¹⁰¹ James, C.; Snieckus, V. *Tetrahedron Lett.* **1997**, *38*, 8149.
- ¹⁰² Benesch, L.; Bury, P.; Guillaneux, D.; Houldsworth, S.; Wang, X.; Snieckus, V. *Tetrahedron Lett.* **1998**, *39*, 961.
- ¹⁰³ Brandão, M.; de Oliveira, A.; Snieckus, V. *Tetrahedron Lett.* **1993**, *34*, 2437.
- ¹⁰⁴ Chauder, B.; Kalinin, A.; Taylor, N.; Snieckus, V. *Angew. Chem. Int. Ed.* **1999**, *38*, 1435.
- ¹⁰⁵ Wang, X.; Snieckus, V. *Tetrahedron Lett.* **1991**, *32*, 4883.
- ¹⁰⁶ Wang, X.; Snieckus, V. *Tetrahedron Lett.* **1991**, *32*, 4879.
- ¹⁰⁷ Tilly, D.; Magolan, J.; Mortier, J. *Chem. Eur. J.* **2012**, *18*, 3804.
- ¹⁰⁸ Nguyen, T.; Chau, N.; Castanet, A.; Nguyen, K.; Mortier, J. *Org. Lett.* **2005**, *7*, 2445.
- ¹⁰⁹ Katharine, G. Grignard Reagents - Review; Slovak University of Technology: Bratislava, 2014; p. 2.
- ¹¹⁰ a) Hoffmann, R.; Knopff, O.; Kusche, A. *Angew. Chem. Int. Ed.* **2000**, *39*, 1462. b) Schulze, V.; Brönstrup, M.; Böhm, V.; Schwerdtfeger, P.; Schimeczek, M.; Hoffmann, R. *Angew. Chem. Int. Ed.* **1998**, *37*, 824.
- ¹¹¹ Rieke, R. D. *Acc. Chem. Res.*, **1977**, *10*, 301.
- ¹¹² Bartmann, E.; Bogdanovi, B.; Janke, N.; Schlichte, K.; Spliethoff, B.; Treber, J.; Westeppe, U.; Wilczok, U.; Liao, S. *Chem. Ber.* **1990**, *123*, 1517.
- ¹¹³ Bogdanović, B.; Schwickardi, M. *Angew. Chem. Int. Ed.* **2000**, *39*, 4610.
- ¹¹⁴ a) Knochel, P.; Dohle, W.; Gommermann, N.; Kneisel, F.; Kopp, F.; Korn, T.; Sapountzis, I.; Vu, V. *Angew. Chem. Int. Ed.* **2003**, *42*, 4302. b) Prévost, C. *Bull. Soc. Chim. Fr.* **1931**, *49*, 1372.
- ¹¹⁵ a) Hoffmann, R.; Hölzer, B.; Knopff, O.; Harms, K. *Angew. Chem. Int. Ed.* **2000**, *39*, 3072. b) Hoffmann, R. *Chem. Soc. Rev.* **2003**, *32*, 225. c) Chen, Z.; Fu, G.; Xu, X. *Org. Lett.* **2011**, *13*, 2046. d) Rayner, P.; O'Brien, P.; Horan, R. *J. Am. Chem. Soc.* **2013**, *135*, 8071.
- ¹¹⁶ a) Corriu, R.; Masse, J. *J. Chem. Soc., Chem. Commun.* **1972**, 144a. b) Tamao, K.; Sumitani, K.; Kumada, M. *J. Am. Chem. Soc.* **1972**, *94*, 4374.
- ¹¹⁷ Stock, A.; Pohland, E. *Ber. Dtsch. Chem. Ges.* **1926**, *59*, 2210.
- ¹¹⁸ a) Housecroft, C. Sharpe, A. *Inorganic chemistry*; Prentice Hall: Harlow, 2008. b) Niedenzu, K. *Angew. Chem. Int. Ed.* **1964**, *3*, 86.
- ¹¹⁹ Campbell, P. G.; Marwitz, A. J. V.; Liu, S. *Angew. Chem. Int. Ed.* **2012**, *51*, 6074.

-
- ¹²⁰ Bosdet, M.; Piers, W. *Can. J. Chem.* **2009**, *87*, 8.
- ¹²¹ a) Pritchard, R.; Kern, C. *J. Am. Chem. Soc.* **1969**, *91*, 1631. b) Blanksby, S.; Ellison, G. *Acc. Chem. Res.* **2003**, *36*, 255.
- ¹²² a) Thorne, L. *J. Chem. Phys.* **1983**, *78*, 167. b) Grant, D.; Dixon, D. *J. Phys. Chem. A* **2006**, *110*, 12955.
- ¹²³ Liu, L.; Marwitz, A.; Matthews, B.; Liu, S. *Angew. Chem. Int. Ed.* **2009**, *48*, 6817.
- ¹²⁴ a) Campbell, P.; Zakharov, L.; Grant, D.; Dixon, D.; Liu, S. *J. Am. Chem. Soc.* **2010**, *132*, 3289. b) Luo, W.; Zakharov, L.; Liu, S. *J. Am. Chem. Soc.* **2011**, *133*, 13006.
- ¹²⁵ a) Agou, T.; Kobayashi, J.; Kawashima, T. *Org. Lett.* **2006**, *8*, 2241. b) Lu, J.; Ko, S.; Walters, N.; Kang, Y.; Sauriol, F.; Wang, S. *Angew. Chem. Int. Ed.* **2013**, *52*, 4544.
- ¹²⁶ a) Lepeltier, M.; Lukoyanova, O.; Jacobson, A.; Jeeva, S.; Perepichka, D. *Chem. Commun.* **2010**, *46*, 7007. b) Agou, T.; Sekine, M.; Kobayashi, J.; Kawashima, T. *Chem. Commun.* **2009**, 1894.
- ¹²⁷ a) Agou, T.; Sekine, M.; Kobayashi, J.; Kawashima, T. *Chem. Eur. J.* **2009**, *15*, 5056. b) Agou, T.; Sekine, M.; Kobayashi, J.; Kawashima, T. *J. Organomet. Chem.* **2009**, *694*, 3833.
- ¹²⁸ Agou, T.; Kobayashi, J.; Kawashima, T. *Org. Lett.* **2006**, *8*, 2241.
- ¹²⁹ a) Dewar, M.; Kubba, V.; Pettit, R. *J. Chem. Soc.* **1958**, 3073. b) Dewar, M. *Tetrahedron* **1959**, *7*, 213. c) Dewar, M.; Kubba, V. *J. Org. Chem.* **1960**, *25*, 1722. d) Dewar, M.; Kubba, V. *J. Am. Chem. Soc.* **1961**, *83*, 1757. e) Dewar, M.; Maitlis, P. *J. Am. Chem. Soc.* **1961**, *83*, 187. f) Dewar, M. *Tetrahedron* **1961**, *15*, 35.
- ¹³⁰ a) Dewar, M.; Dietz, R. *J. Chem. Soc.* **1959**, 2728. b) Dewar, M.; Dietz, R.; Kubba, V.; Lepley, A. *J. Am. Chem. Soc.* **1961**, *83*, 1754. c) Dewar, M. *Tetrahedron* **1961**, *15*, 26. d) Dewar, M.; Dietz, R. *J. Org. Chem.* **1961**, *26*, 3253. e) Dewar, M.; Hashmall, J.; Kubba, V. *J. Org. Chem.* **1964**, *29*, 1755. f) Dewar, M.; Gleicher, G.; Robinson, B. *J. Am. Chem. Soc.* **1964**, *86*, 5698.
- ¹³¹ Dewar, M.; Marr, P. *J. Am. Chem. Soc.* **1962**, *84*, 3782.
- ¹³² Davies, K.; Dewar, M.; Rona, P. *J. Am. Chem. Soc.* **1967**, *89*, 6294.
- ¹³³ a) Ferles, M.; Polivka, Z. *Collect. Czech. Chem. Commun.* **1968**, *33*, 2121. b) Polivka, Z.; Kubelka, V.; Holubova, N.; Ferles, M. *Collect. Czech. Chem. Commun.* **1970**, *35*, 1131.
- ¹³⁴ Wille, H.; Goubeau, J. *Chem. Ber.* **1974**, *107*, 110.
- ¹³⁵ Marwitz, A.; Matus, M.; Zakharov, L.; Dixon, D.; Liu, S. *Angew. Chem. Int. Ed.* **2009**, *48*, 973.
- ¹³⁶ a) Ashe, A.; Fang, X. *Org. Lett.* **2000**, *2*, 2089. b) Marwitz, A.; Abbey, E.; Jenkins, J.; Zakharov, L.; Liu, S. *Org. Lett.* **2007**, *9*, 4905.
- ¹³⁷ a) Ashe, A.; Fang, X. *Org. Lett.* **2000**, *2*, 2089. b) Ashe, A.; Fang, X.; Kampf, J. *Organometallics* **2001**, *20*, 5413. c) Pan, J.; Kampf, J.; Ashe, A. *J. Organomet. Chem.* **2009**, *694*, 1036.

-
- ¹³⁸ a) Shi, Y.; Yang, D.; Mellerup, S.; Wang, N.; Peng, T.; Wang, S. *Org. Lett.* **2016**, *18*, 1626. b) Yuan, K.; Suzuki, N.; Mellerup, S.; Wang, X.; Yamaguchi, S.; Wang, S. *Org. Lett.* **2016**, *18*, 720.
- ¹³⁹ a) Lepeltier, M.; Lukyanova, O.; Jacobson, A.; Jeeva, S.; Perepichka, D. *Chem. Commun.* **2010**, *46*, 7007. b) Lukyanova, O.; Lepeltier, M.; Laferrière, M.; Perepichka, D. *Macromolecules* **2011**, *44*, 4729.
- ¹⁴⁰ Taniguchi, T.; Yamaguchi, S. *Organometallics* **2010**, *29*, 5732.
- ¹⁴¹ a) Agou, T.; Kobayashi, J.; Kawashima, T. *Org. Lett.* **2006**, *8*, 2241. b) Agou, T.; Kobayashi, J.; Kawashima, T. *Chem. Commun.* **2007**, 3204.
- ¹⁴² Wang, X.; Zhuang, F.; Wang, R.; Wang, X.; Cao, X.; Wang, J.; Pei, J. *J. Am. Chem. Soc.* **2014**, *136*, 3764.
- ¹⁴³ Bosdet, M. J. D.; Piers, W. E.; Sorensen, T. S.; Parvez, M. *Angew. Chem. Int. Ed.* **2007**, *46*, 4940.
- ¹⁴⁴ Hatakeyama, T.; Hashimoto, S.; Seki, S.; Nakamura, M. *J. Am. Chem. Soc.* **2011**, *133*, 18614.
- ¹⁴⁵ Rao, Y.; Wang, S. *Inorg. Chem.* **2011**, *50*, 12263.
- ¹⁴⁶ a) Wu, Q.; Esteghamatian, M.; Hu, N.-X.; Popovic, Z.; Enright, G.; Tao, Y.; D'lorio, M.; Wang, S. *Chem. Mater.* **2000**, *12*, 79. b) Cui, Y.; Liu, Q. D.; Bai, D. R.; Jia, W. L.; Tao, Y.; Wang, S. *Inorg. Chem.* **2005**, *44*, 601. c) Cui, Y.; Wang, S. *J. Org. Chem.* **2006**, *71*, 6485. d) Liu, S.-F.; Seward, C.; Aziz, H.; Hu, N.-X.; Popovic, Z.; Wang, S. *Organometallics* **2000**, *19*, 5709.
- ¹⁴⁷ (a) Hassan, A.; Wang, S. *Chem. Commun.* **1998**, 339, 211. (b) Wu, Q.; Esteghamatian, M.; Hu, N.; Popovic, Z.; Enright, G.; Breeze, S. R.; Wang, S. *Angew. Chem. Int. Ed.* **1999**, *38*, 985. (c) Liu, S. F.; Wu, Q.; Schmider, H. L.; Aziz, H.; Hu, N.; Popovic, Z.; Wang, S. *J. Am. Chem. Soc.* **2000**, *122*, 3671. (d) Liu, Q.; Mudadu, M. S.; Schmider, H.; Thummel, R.; Tao, Y.; Wang, S. *Organometallics* **2002**, *21*, 4743. (e) Liu, Q.; Mudadu, M. S.; Thummel, R.; Tao, Y.; Wang, S. *Adv. Funct. Mater.* **2005**, *15*, 143.
- ¹⁴⁸ a) Wang, S. *Coord. Chem. Rev.* **2001**, *215*, 79. b) Entwistle, C. D.; Marder, T. B. *Angew. Chem. Int. Ed.* **2002**, *41*, 2927. (c) Entwistle, C. D.; Marder, T. B. *Chem. Mater.* **2004**, *16*, 4574. d) Fukazawa, A.; Yamaguchi, S. *Chem. Asian J.* **2009**, *4*, 1386.
- ¹⁴⁹ (a) Liu, S. F.; Wu, Q.; Schmider, H. L.; Aziz, H.; Hu, N.; Popovic, Z.; Wang, S. *J. Am. Chem. Soc.* **2000**, *122*, 3671. (b) Liu, Q.; Mudadu, M. S.; Schmider, H.; Thummel, R.; Tao, Y.; Wang, S. *Organometallics* **2002**, *21*, 4743. (c) Liu, Q.; Mudadu, M. S.; Thummel, R.; Tao, Y.; Wang, S. *Adv. Funct. Mater.* **2005**, *15*, 143.
- ¹⁵⁰ Liu, Q.; Mudadu, M. S.; Thummel, R.; Tao, Y.; Wang, S. *Adv. Funct. Mater.* **2005**, *15*, 143.
- ¹⁵¹ Rao, Y.; Amarne, H.; Zhao, S.; McCormick, T.; Martić, S.; Sun, Y.; Wang, R.; Wang, S. *J. Am. Chem. Soc.* **2008**, *130*, 12898.
- ¹⁵² Amarne, H.; Baik, C.; Wang, R.; Wang, S. *Organometallics* **2011**, *30*, 665.
- ¹⁵³ Amarne, H.; Baik, C.; Murphy, S.; Wang, S. *Chem. Eur. J.* **2010**, *16*, 4750.
- ¹⁵⁴ Hudson, Z.; Ko, S.; Yamaguchi, S.; Wang, S. *Org. Lett.* **2012**, *14*, 5610.

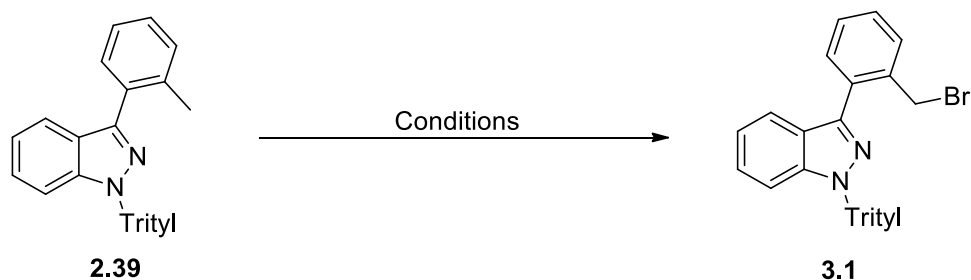
-
- ¹⁵⁵ Rao, Y.; Amarne, H.; Chen, L.; Brown, M.; Mosey, N.; Wang, S. *J. Am. Chem. Soc.* **2013**, *135*, 3407.
- ¹⁵⁶ Baik, C.; Hudson, Z.; Amarne, H.; Wang, S. *J. Am. Chem. Soc.* **2009**, *131*, 14549.
- ¹⁵⁷ M. Kasha, *Discuss. Faraday Soc.* **1950**, *9*, 14.
- ¹⁵⁸ Baik, C.; Murphy, S.; Wang, S. *Angew. Chem. Int. Ed.* **2010**, *49*, 8224.
- ¹⁵⁹ Murphy, S.; Baik, C.; Lu, J.; Wang, S. *Org. Lett.* **2010**, *12*, 5266.
- ¹⁶⁰ Yuan, K.; Suzuki, N.; Mellerup, S.; Wang, X.; Yamaguchi, S.; Wang, S. *Org. Lett.* **2016**, *18*, 720.
- ¹⁶¹ Lu, J.; Ko, S.; Walters, N.; Kang, Y.; Sauriol, F.; Wang, S. *Angew. Chem. Int. Ed.* **2013**, *52*, 4544.
- ¹⁶² a) Lu, J.; Ko, S.; Walters, N.; Kang, Y.; Sauriol, F.; Wang, S. *Angew. Chem. Int. Ed.* **2013**, *52*, 4544. b) Bosdet, M.; Jaska, C.; Piers, W.; Sorensen, T.; Parvez, M. *Org. Lett.* **2007**, *9*, 1395. c) Dewar, M.; Kaneko, C.; Bhattacharjee, M. *J. Am. Chem. Soc.* **1962**, *84*, 4884. d) Dewar, M.; Kubba, V.; Pettit, R. *J. Chem. Soc.* **1958**, 3073.
- ¹⁶³ Ko, S.; Lu, J.; Wang, S. *Org. Lett.* **2014**, *16*, 616.
- ¹⁶⁴ Wang, S.; Yang, D.; Lu, J.; Shimogawa, H.; Gong, S.; Wang, X.; Mellerup, S.; Wakamiya, A.; Chang, Y.; Yang, C.; Lu, Z. *Angew. Chem. Int. Ed.* **2015**, *54*, 15074.
- ¹⁶⁵ Yang, D.; Mellerup, S.; Wang, X.; Lu, J.; Wang, S. *Angew. Chem. Int. Ed.* **2015**, *54*, 5498.
- ¹⁶⁶ Xiao, J.; Jin, C.; Liu, Z.; Guo, S.; Zhang, X.; Zhou, X.; Wu, X. *Org. Biomol. Chem.* **2015**, *13*, 7257.
- ¹⁶⁷ Collot, V.; Dallemagne, P.; Bovy, P.; Rault, S. *Tetrahedron* **1999**, *55*, 6917.
- ¹⁶⁸ Düfert, M.; Billingsley, K.; Buchwald, S. *J. Am. Chem. Soc.* **2013**, *135*, 12877.
- ¹⁶⁹ Ziegler, F.; Fowler, K. *J. Org. Chem.*, **1976**, *41*, 1564.
- ¹⁷⁰ Snieckus, V. *Chem. Rev.* **1990**, *90*, 879.
- ¹⁷¹ Joly, G.; Jacobsen, E. *J. Am. Chem. Soc.* **2004**, *126*, 4102.
- ¹⁷² Haddach, A.; Kelleman, A.; Deaton-Rewolinski, M. *Tetrahedron Lett.* **2002**, *43*, 399.
- ¹⁷³ Dalziel, M.; Hurst, T. Snieckus, V. Unpublished results.
- ¹⁷⁴ Singh, S.; Hurst, T. Snieckus, V. Unpublished results
- ¹⁷⁵ Rogers, H.; Houk, J. *J. Am. Chem. Soc.* **1982**, *104*, 522.
- ¹⁷⁶ Yuan, K.; Suzuki, N.; Mellerup, S.; Wang, X.; Yamaguchi, S.; Wang, S. *Org. Lett.* **2016**, *18*, 720.
- ¹⁷⁷ Brown, H. C.; Scouten, C. G.; Liotta, R. *J. Am. Chem. Soc.* **1979**, *101*, 96.

-
- ¹⁷⁸ Ohmura, T.; Yamamoto, Y.; Miyaura, N. *J. Am. Chem. Soc.* **2000**, *122*, 4990.
- ¹⁷⁹ Sundararaju, B.; Furstner, A. *Angew. Chem. Int. Ed.* **2013**, *52*, 14050.
- ¹⁸⁰ a) Gunanathan, C.; Hölscher, M.; Pan, F.; Leitner, W. *J. Am. Chem. Soc.* **2012**, *134*, 14349. b) Obligacion, J.; Neely, J.; Yazdani, A.; Pappas, I.; Chirik, P. *J. Am. Chem. Soc.* **2015**, *137*, 5855.
- ¹⁸¹ Jorand-Lebrun, C.; Crosignani, S.; Dorbais, J. *PCT Int. Appl.* **2012**, 2012084704.
- ¹⁸² Tromp, R.; van Ameijde, S.; Pütz, C.; Sundermann, C.; Sundermann, B.; von Frijtag Drabbe Künzel, J.; IJzerman, A. *J. Med. Chem.* **2004**, *47*, 5441.
- ¹⁸³ Li-Yuan Bao, R.; Zhao, R.; Shi, L. *Chem. Commun.* **2015**, *51*, 6884.
- ¹⁸⁴ Davies, h. M. L.; Morton, D. *J. Org. Chem.*, **2016**, *81*, 343.

Appendix

The Benzylic methyl group can be readily activated under radical halogenation conditions, and we subjected compound **2.39** to *n*-bromosuccinimide (NBS) in chlorinated solvents under refluxing conditions and the results are reported in **table 1**, free radical initiators such as azobisisobutyronitrile (AIBN) and benzoyl peroxide were also introduced in several experiments for the purpose of optimizing reaction conversions. The best result was obtained by treatment with two equivalents of NBS in refluxing carbon tetrachloride and the desired product **3.1** was isolated in 70 % yield (entry 6).

Table 1 Radical halogenation reactions of compound 2.39.



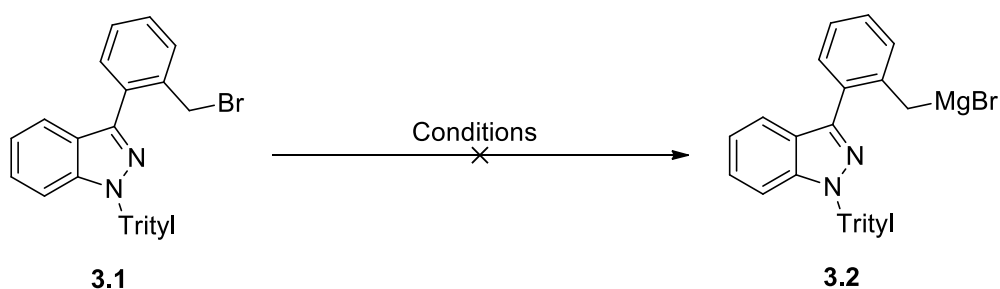
Entry	Conditions	Compound yields(%) ^a
1	NBS (1 equiv), AIBN (0.1 equiv), CHCl ₃ , reflux, 24 h	2.39 recovery (67%)
2	NBS (1 equiv), (PhCO ₂) ₂ , (0.1 equiv) CCl ₄ , reflux, 24 h	3.1 (60%)
3	NBS (1.1 equiv), CCl ₄ , reflux, 24 h	3.1 (20%)
4	NBS (1.1 equiv), AIBN (0.1 equiv), CCl ₄ , RT, 24 h	3.1 (15%)
5	NBS (2 equiv), CCl ₄ , reflux, 4 h	3.1 (55%)
6	NBS (2 equiv), CCl₄, reflux, 4 h	3.1 (70%)

^aYields of isolated products after column chromatography

The classical Grignard reaction was attempted using freshly prepared magnesium turnings with catalytic amounts of iodine sublimed onto metal surfaces, and in the presence of compound **3.1** it was hoped that the Grignard reagent can be generated in refluxing diethyl ether (**Table 2**) Subsequent

experiments also explored knochel-grignard exchange reactions using isopropylmagnesium chloride (*i*-PrMgCl) and isopropylmagnesium bromide (*i*-PrMgBr) to affect magnesium-halogen exchange at the benzylic position of compound **3.1**. However, all of these attempts were unsuccessful in generating the desired Grignard reagent as no further reactions occurred when reactive electrophiles were added into the reaction mixture (**Table 2**).

Table 2 Unsuccessful attempts in the generation of Grignard reagents.

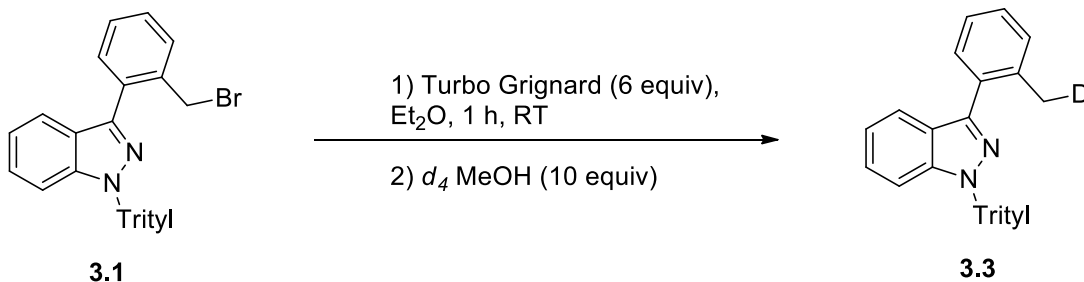


Entry	Conditions
1	1) Mg turnings (2 equiv, crushed), I ₂ (catalytic) 2) SM, Et ₂ O, reflux (5 min) – RT (10 min) 3) Benzaldehyde (5 equiv)
2	1) Mg turnings (2 equiv, crushed), I ₂ (catalytic) 2) SM, Et ₂ O, reflux (30 min) 3) Benzaldehyde (5 equiv)
3	1) <i>i</i> PrMgBr (1 equiv), Et ₂ O, 2 h, RT 2) Benzaldehyde (2 equiv)
4	1) <i>i</i> PrMgCl (2 equiv), Et ₂ O, 2 h, RT 2) Benzaldehyde (2 equiv)

Knochel and colleagues have discovered that the lithium salt additives of *i*-PrMgCl or *i*-PrMgBr in the forms of *i*-PrMgCl·LiCl and *i*-PrMgBr·LiBr can lead to an increase in the rate and overall efficiency of magnesium-halogen exchange reactions with excellent functional group tolerance under mild reaction

conditions. The improvements have lead to the use of the term “turbo Grignard reagents” in describing these compounds. We subjected compound **3.1** to six equivalents of *i*-PrMgCl·LiCl in diethyl ether at room temperature for one hour, and subsequently quenched the reaction mixture with deuterated methanol to afford a crude product mixture that was difficult to purify.

Scheme 1 Grignard reaction of compound 3.1.



We were unable to obtain a satisfactory ¹H NMR spectra of the product after purification to offer evidence in support of compound **3.3**, however, the electron impact MS analysis of the product mixture suggests the presence of a compound whose molecular mass was found to be that of a deuterio substituted for a single hydrogen atom in the molecule (**Figure 1**), which would be expected if the Grignard reagent **3.2** was successfully generated from compound **3.1** before reacting with *d*₄ MeOH to afford the final product **3.3**.

Figure 1 EI-MS analysis of compound 3.3.

